



Diapiric exhumation of Earth's youngest (UHP) eclogites in the gneiss domes of the D'Entrecasteaux Islands, Papua New Guinea

T.A. Little ^{a,*}, B.R. Hacker ^b, S.M. Gordon ^{b,c}, S.L. Baldwin ^d, P.G. Fitzgerald ^d, S. Ellis ^e, M. Korchinski ^a

^a School of Geography Environment & Earth Sciences, Victoria University of Wellington, Wellington 6040, New Zealand

^b Earth Science and Institute for Crustal Studies, University of California, Santa Barbara CA 93106–9630, United States

^c Department of Geological Sciences, University of Nevada, Reno, 1664 N. Virginia, MS 0172, Reno, NV 89557, United States

^d Department of Earth Sciences, Syracuse University, Syracuse, NY 13244–1070, United States

^e GNS Science, P.O. Box 303–68, Lower Hutt, New Zealand

ARTICLE INFO

Article history:

Received 10 November 2010

Received in revised form 31 May 2011

Accepted 9 June 2011

Available online 4 August 2011

Keywords:

UHP rocks

Eclogites

Gneiss domes

Exhumation

Diapirism

Woodlark Rift

ABSTRACT

The Woodlark Rift in Papua New Guinea hosts the world's youngest (2–8 Ma) eclogite-facies rocks and extensional deformation has played a key role in exhuming these (U)HP rocks at rates of >20 mm/yr. During the Eocene Papuan arc-continent collision Australian Plate-derived continental rocks were subducted to (U)HP depths. There they remained for up to 30 m.y. until the Pliocene when asthenospheric circulation ahead of the west-propagating Woodlark spreading ridge introduced heat and fluids. This caused rocks to break away from the paleosubduction channel, recrystallize in the eclogite facies, and rise as Rayleigh–Taylor instabilities. The diapirs ascended adiabatically undergoing partial melting, which lowered their viscosity and increased buoyancy. (U)HP crust ponded near the Moho at ~2–4 Ma, thickening the crust to ~40 km (11 kb). Domal uplifts emerged above sea level, and these are still underlain by an unusually thick crust (>26 km) for a rift that has stretched by factor of ~3 since 6 Ma. After ponding, they acquired a flat-lying foliation during amphibolite-facies retrogression. Vertical shortening accompanied the gravitationally driven outflow of ponded lower crust. The weak material was extended parallel to the rift margin, thinning ductilely by <1/3. The flow was dominated by pure shear ($W_k \sim 0.2$), and was mechanically decoupled from – and orthogonal to – plate motion in the rift. Top-E shear fabrics suggest that this flow was westward, perhaps driven by isostatic stresses towards a strongly thinned rift corridor ahead of the Woodlark spreading ridge. At <2 Ma, the gneisses were upwardly juxtaposed against an ophiolitic upper plate to form nearly symmetric gneiss domes that cooled at >100 °C per m.y. and were mechanically incorporated into the rift's upper crust. Final exposure was by normal faulting and minor erosion. Such exhumation may also apply to other (U)HP terranes where less evidence for Moho ponding is preserved.

© 2011 Elsevier B.V. All rights reserved.

1. Introduction

The recognition that continental crust around the world has been subducted to pressures corresponding to depths of >100 km, and in some cases to >150–250 km (e.g., Kaneko et al., 2000; Zhang et al., 2003), and then returned back to the surface from these ultra-high (UHP) pressures, is a remarkable modern discovery (Andersen et al., 1991; Ernst, 2001; Hacker, 2007). Understanding how rocks from the crust and mantle might be circulated in such a profound manner relates to such fundamental geodynamical processes as the growth of the continents, the evolution of mountain belts, the rheology of the lithosphere, and the driving forces of plate tectonics. Nonetheless,

our current understanding of the processes causing rocks to be taken to UHP conditions and then exhumed is sketchy typically due to the large amount of metamorphic and deformational overprinting that occurs during exhumation.

Most agree that the formation of UHP terranes is associated with subduction of continental margins or microcontinents. After reaching eclogite-facies conditions, deeply subducted terranes are presumed to detach from their denser lithospheric underpinnings and rise within the subduction channel (e.g., Seno, 2008). Many models call upon UHP terrane exhumation during the early stages of collisional orogenesis. Two end-member groups of exhumation behavior have been suggested: 1) the exhumed domains are relatively rigid (e.g., Andersen, 1998; Andersen et al., 1991; Hacker et al., 2010); or 2) they are plume-like and internally strongly ductilely deformed (e.g., Beaumont et al., 2009; Gerya and Stockert, 2006; Warren et al., 2008).

Extrusion wedges are a much-invoked exhumation concept that calls for shearing along the margins of elongate, rigid bodies that are commonly <1–5 km-thick (e.g., Avigad, 1992; Chemenda et al., 1995;

* Corresponding author. Tel.: +64 4 463 6198; fax: +64 4 463 5186.

E-mail addresses: timothy.little@vuw.ac.nz (T.A. Little), hacker@geol.ucsb.edu (B.R. Hacker), staciag@unr.edu (S.M. Gordon), sbaldwin@syr.edu (S.L. Baldwin), pgfitzge@syr.edu (P.G. Fitzgerald), S.Ellis@gns.cri.nz (S. Ellis), megankorchinski@hotmail.com (M. Korchinski).

Epard and Steck, 2008; Ring et al., 2007; Ring and Glodny, 2010; Shaked et al., 2004; Stockhert and Renner, 1998) (e.g., Fig. 1a and b). The recognition of giant UHP terranes (e.g., >60,000 km², Kylander-Clark et al., 2009) have led to exhumation models that invoke reversal of slip on a former subduction zone to extract large slabs of UHP continental crust by a translation-dominated process (Fig. 2a) (Andersen et al., 1991; Frotzheim et al., 2003; Hacker, 2007; Hacker et al., 2000; Webb et al., 2008).

Other exhumational models assume that continentally derived UHP bodies are strongly deformed plumes that have risen buoyantly from mantle depths as diapirs (e.g., Beaumont et al., 2009; Burov et al., 2001; Warren et al., 2008) (Fig. 1c and d). Once they reach the crust, such low-viscosity plumes may pond at the Moho, locally thickening the crust (Walsh and Hacker, 2004). These underplated welts may flow laterally outward and thin in response to isostatic stresses (McKenzie et al., 2000; Walsh and Hacker, 2004), causing a pure shear thinning that can contribute significantly to the exhumation of UHP rocks (e.g., Bond et al., 2007; Dewey et al., 1993; Ring et al., 1999). If so, final exposure must occur by other processes, such as normal faulting or erosion (e.g., Johnston et al., 2007). Alternatively, UHP diapirs may directly penetrate the upper crust, especially in areas of crustal extension or in regions capped by a dense upper layer such as ophiolite (Fig. 2b) (e.g., Martinez et al., 2001). Corner- or forced-return flow geodynamical models (not depicted in Figs. 1 or 2) propose that dynamic pressure gradients are the chief drivers of UHP exhumation (Cloos and Shreve, 1988). Unlike the rigid models, both these and diapir models predict that UHP rocks will be strongly deformed into complexly folded nappes as they rise from the subduction channel and are inserted into the mid to lower crust of the overriding plate (e.g., Gerya and Stockhert, 2006).

Most known UHP terranes are pre-Cenozoic (Ernst, 2001; Ota and Koneko, 2010). For this reason, they are commonly no longer embedded in the geodynamic setting responsible for their burial and unroofing and are likely to have been overprinted by other events; both hinder evaluation of the UHP exhumation process. The Woodlark Rift in SE Papua New Guinea (Fig. 3a, b) contains Earth's youngest known eclogites, some of which are coesite-bearing (Baldwin et al., 2008). The rocks are being “caught in the act” of their exhumation, and the plate motions coeval with their ascent have been studied and are known (Taylor et al., 1999). This setting is a rapidly opening continental rift ahead of an actively spreading ocean basin (Fig. 3b). The eclogites are exposed in the NW D'Entrecasteaux Islands in a NW part of the Woodlark Rift (Fig. 4). Their peak-pressure metamorphism has been dated (ion probe U-Pb ages on zircon, Baldwin et al., 2004; Monteleone et al., 2006) at ~7.9 Ma at the UHP locality; and 4.3–2.1 Ma at other localities. The D'Entrecasteaux Islands eclogite-bearing gneisses occupy the “lower plate” of gneiss domes that are remarkable for their youthful topographic expression. The gneisses display abundant evidence for partial melting and anatectic magmatism that took place during their rapid exhumation (e.g., Hill et al., 1995).

Exhumation of UHP rocks to the surface in most ancient settings has required ≥ 10 m.y. (Ernst, 2001). Typically, such ascent is ascribed to two stages: an initially rapid (10–50 mm/yr), buoyancy-driven ascent through the mantle followed by slower exhumation through the crust (e.g., Epard and Steck, 2008; Glodny et al., 2005; Hacker, 2007; Johnston et al., 2007; Parrish et al., 2006; Rubatto and Hermann, 2001; Walsh and Hacker, 2004). In the Woodlark Rift, the short time lag between peak HP metamorphism and final exposure (as little as ~2 m.y.) suggests that a nearly continuous process – still ongoing – exhumed the eclogites. Hill (1994) argued that the unroofing has been

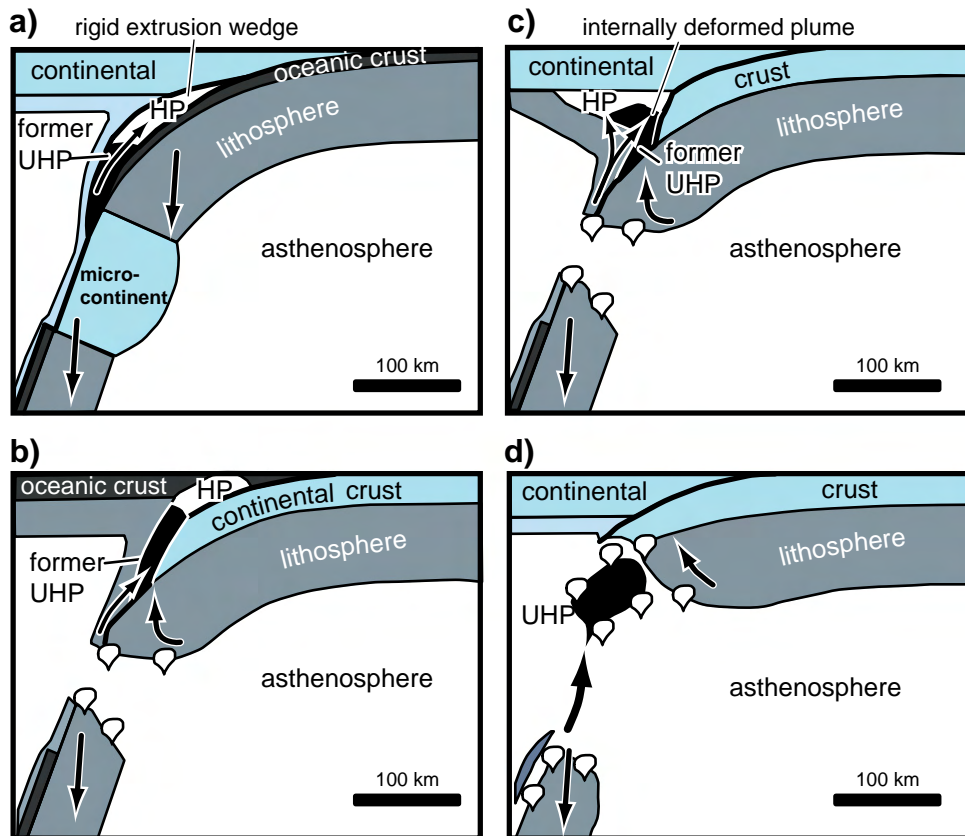


Fig. 1. Cartoons illustrating models for exhumation for global UHP terranes (after Hacker, 2007). a) Subducted UHP microcontinent tears loose from downgoing mostly oceanic plate to rise as rigid extrusion wedge; b) UHP continental crust tears loose as a deeply rooted slab from subducted continental margin, intruding upward into the upper crust of dominantly oceanic upper plate (slab-break-off also illustrated); c) UHP continental crust tears loose from subducted continental margin to form internally deformed crustal blob that rises and ponds at Moho of upper plate (slab-break-off is also illustrated); d) UHP continental crust tears loose from subducted continental margin after slab-break-off of subducted lithosphere (as suggested for central PNG by Cloos et al., 2005).

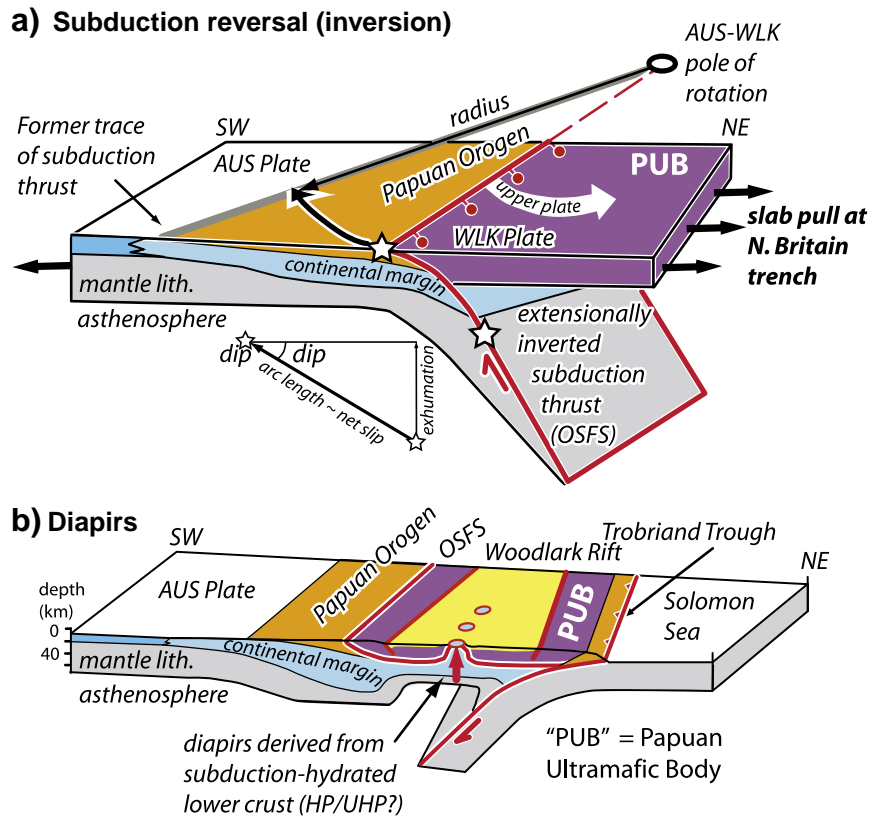


Fig. 2. Two previously suggested models for the exhumation of (U)HP metamorphic rocks in the Woodlark Rift. “AUS” refers to the Australian Plate and “WLK” to the Woodlark Plate. “OSFS” refers to the Owen–Stanley Fault Zone and “PUB” to the Papuan Ultramafic Body. a) The subduction inversion model of Webb et al., 2008. The open stars represent the pre- and post-exhumation positions of UHP rocks; b) the lower crustal diapir model of Martinez et al. (2001). While the latter model invokes buoyancy and crustal flow to form the gneiss domes, it does not address how the (U)HP rocks were exhumed from mantle depths.

accomplished by a brittle-to-ductile continuum of normal-sense slip on a deeply penetrating, low-angle detachment fault/shear zone. In a similar model, Webb et al. (2008) proposed that the UHP rocks have been exhumed in the footwall of an inverted paleo-subduction fault between two pivoting microplates (Fig. 2a). Without referring to the problem of eclogite exhumation, Martinez et al., 2001 argued that the lower crust of the D’Entrecasteaux Islands is intruding upward as diapirs into the denser upper crust of ophiolitic rocks, forming the D’Entrecasteaux Islands gneiss domes (Fig. 2b).

In this paper we apply structural field data and previously published geochronological, thermobarometric, and geophysical data to assess the tectonic processes responsible for the rapid exhumation of these very young eclogites. We argue that (U)HP recrystallization took place tens of millions of years after the arc-continent collision that buried them to mantle depths. Mantle flow, heating, and fluid infiltration linked to the Woodlark continental rifting drove the (U)HP crystallization, and we argue that these processes allowed a previously emplaced eclogitic nappe to heat up and dislodge from its subduction channel to rise as a Rayleigh–Taylor instability. The diapir underwent partial melting during its rapid ascent through the mantle, causing further viscosity reduction and buoyancy. The body ponded at the rift’s Moho to form an overthickened welt of continental crust that was at least ~40 km thick (including an upper crustal ophiolitic unit). There the migmatitic gneisses were retrogressed to the amphibolite facies, and flowed westward under gravity parallel to the rift margin, thinning ductilely by at least 1/3. Finally, the gneisses penetrated the upper crust as symmetric gneiss domes. Surface exposure of the eclogitic rocks resulted from minor erosion and slip on late-stage normal faults that are active today.

Structural data was collected in the Goodenough, Mailolo, and NW Normanby gneiss domes of the northwestern D’Entrecasteaux

Islands during five field seasons. Microstructural observations were also made on >600 oriented samples, each of which was cut into thin-sections both parallel and perpendicular to the lineation. We focus on the following: 1) the contact relationships of the major rock units and deformation zones in the gneiss domes; 2) the spatial distribution and temporal progression of their structures and fabrics; 3) the kinematics of ductile flow and its relationship to eclogite exhumation and gneiss doming; and 4) the relationship of partial melting and diking to metamorphism, exhumation and deformation.

2. Tectonic setting and background

2.1. The Woodlark rift

The Pacific and Australian Plates are converging obliquely at ~110 mm/yr near eastern Papua New Guinea (PNG) (Wallace et al., 2004), and this motion is accommodated across a mosaic of several microplates (Fig. 3a). The Woodlark Rift separates the Woodlark microplate from the Australian Plate. Most workers infer that the rifting is driven by slab pull of the Solomon Sea Plate at the New Britain Trench to the north (Fig. 3a, Wallace et al., 2004; Weissel et al., 1982; Westaway, 2007). GPS geodesy indicates contemporary extensional opening of ~20 mm/yr at the eastern end of the continental rift, whereas, farther to the east, seafloor spreading occurs at up to ~42 mm/yr in the eastern Woodlark Basin (Wallace et al., 2004). In the Pliocene to early Pleistocene (3.6–0.5 Ma), plate motions were ~30% faster and oriented nearly N–S (Goodliffe et al., 1997; Taylor et al., 1999) (Fig. 3b). Focal mechanisms, seismic reflection data, and ODP drilling of a fault at the Moresby Seamount (Fig. 3b) indicate that the rift contains active normal faults, some of which dip as shallowly as 25–30° (Abers, 2001; Taylor and Huchon, 2002). Today, the rift’s

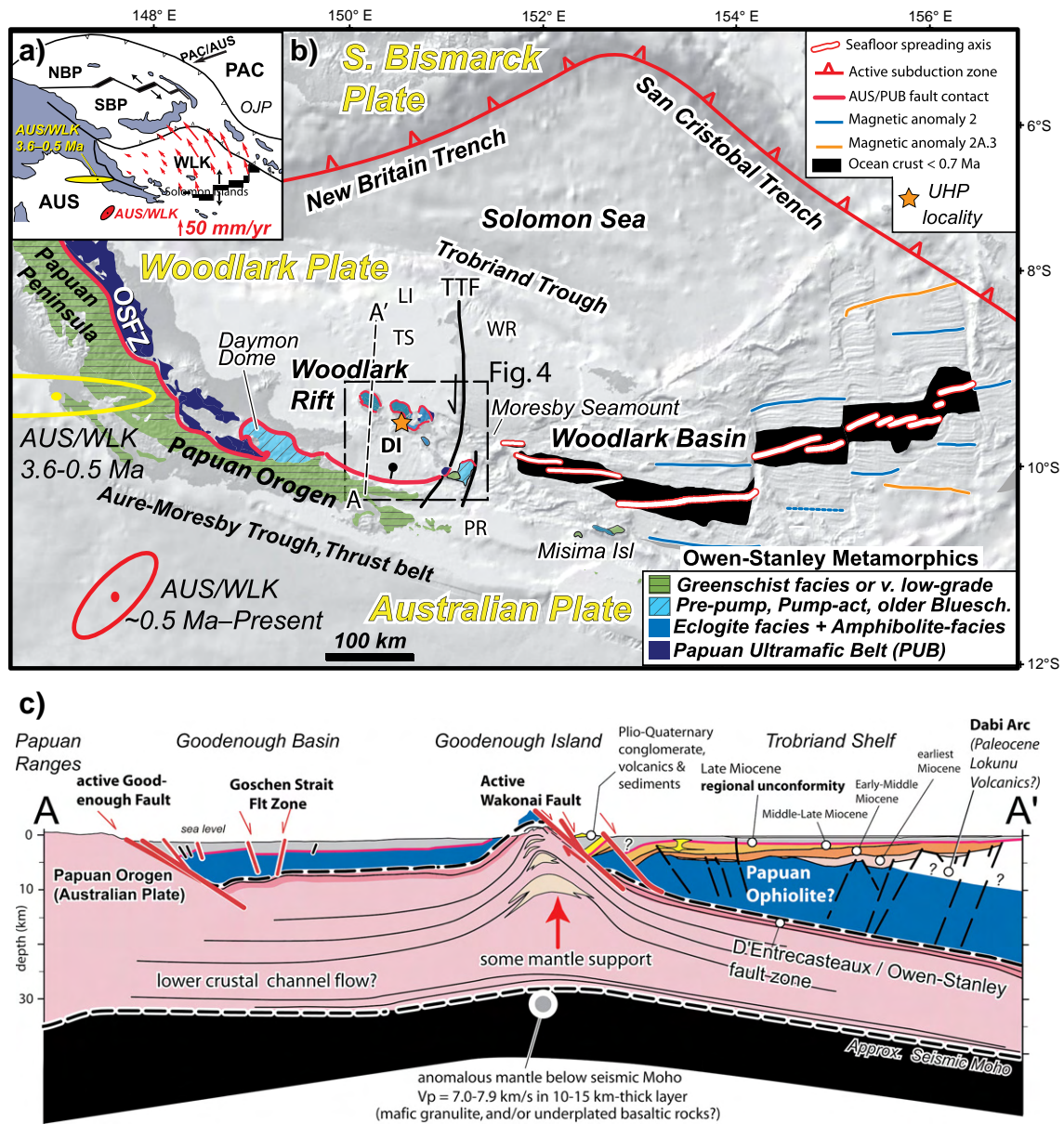


Fig. 3. a) Inset: contemporary plate tectonic map of eastern Papua New Guinea: NBP, North Bismark Plate, SBP, South Bismark Plate, WLK, Woodlark Plate, AUS, Australian Plate, PAC, Pacific Plate; OJP, Ontong-Java Plateau. Bold black arrow shows contemporary velocity of the Pacific Plate relative to the Australian. Small arrows depict contemporary velocities of the Woodlark Plate relative to the Australian (after Wallace et al., 2004); b) Simplified tectonic map of south-eastern Papua New Guinea (modified after Webb et al., 2008), showing key tectonic features and distribution of metamorphic rocks. Background is shaded Digital Elevation Model from GeoMapApp (<http://www.GeoMapApp.org>). Geologic units are much simplified from Davies (1980b) and Daczko et al. (2009). Pole of WLK-AUS rotation for 3.6–0.5 Ma (with error ellipse) is from Taylor et al. (1999); GPS-derived pole of present-day WLK-AUS rotation is from Wallace et al. (2004). Explanation: OSFZ, Owen Stanley fault zone; TTF, Trobriand Transfer Fault; DI, D'Entrecasteaux Islands; WR, Woodlark Rise; PR, Pocklington Rise; TS, Trobriand Shelf; LI, Lusancay Islands; and DD, Dayman Dome. Magnetic anomalies from Taylor et al. (1999). c) Simplified cross-section along profile A–A' (no vertical exaggeration, location shown in Fig. 3b). Moho depths and velocity structure interpretations from Abers et al. (2002) and Ferris et al. (2006). Geology of the Trobriand shelf after Taylor (1999).

most active fault is probably the Goodenough (Owen Stanley) Fault, which may be slipping at rates of 10–20 mm/yr (Figs. 3b, c and 4) (Daczko et al., 2009; Davies, 1980a; Little et al., 2007; Spencer, 2010).

An unconformity cored in drillholes records widespread marine inundation at ~8.4 Ma has been interpreted by some as indicating that Woodlark rifting began in the late Miocene (Fang, 2000; Taylor et al., 1999; Taylor and Huchon, 2002). Since then, the Woodlark spreading ridge has propagated westward >500 km into the rift, splitting the continental crust of SE Papua New Guinea. Near the current tip of the Woodlark spreading ridge, seafloor spreading data require that the crust has been extended by 220 ± 40 km since ~6 Ma, and ~90 km

since 3.6 Ma (Kington and Goodliffe, 2008; Taylor et al., 1999). Despite this large inferred extension, receiver-function and gravity data suggest that there is less crustal thickness variation across the rift than one would predict from the imposed plate motion (Fig. 3c): the crust is ~30–35 km thick beneath the mountainous SW flank of the rift, ~26–29 km thick near its center, and >35 km thick beneath the northern rifted margin (Abers et al., 2002; Ferris et al., 2006). This suggests that the lower crust has had a low enough viscosity to flow out from beneath the rift margins across the ~200 km wide basin over several million years (e.g., McKenzie et al., 2000). The resultant Moho smoothing might explain why subsidence-based estimates of

K-Ar age on andesite, Smith and Compston, 1982). High-K, trachytes and dacites in the nearby Lusancay Islands (Fig. 3a) have been interpreted as adakites derived from the melting of a mafic eclogite source, and have yielded whole-rock K-Ar ages of ~1 Ma (Hasche and Ben-Avraham, 2005; Smith and Compston, 1982). An active, NNE-trending belt of transitional basalt-peralkaline rhyolite volcanism is inferred to be rift-related (Fig. 4, Hegner and Smith; Lackschewitz et al., 2003; Smith, 1976; Stolz et al., 1993).

To summarize, between the late Miocene (~8 Ma) and the mid Pliocene, tectonic events occurred in rapid succession: 1) at ~8.4 Ma Woodlark rifting may have initiated to form the aforementioned unconformity; 2) at ~8 Ma, break-off of subducted Australian oceanic lithosphere beneath the central Highlands of PNG (~200 km west of the Papuan Peninsula) was followed by upwelling of asthenosphere into that lithospheric rupture, and by uplift and widespread magmatism in the PNG Highlands (Cloos et al., 2005); 3) at 7–5 Ma, the Aure fold–thrust belt was rejuvenated along the Aure–Moresby trough, perhaps driving renewed uplift of the Papuan Peninsula (Kugler, 1993; Pigram et al., 1989; Slater et al., 1988; Van Ufford and Cloos, 2005) through the present (Ott et al., 2009); 4) by ~6.3 Ma, calc-alkaline rhyolitic volcanism began in the D'Entrecasteaux Islands (Smith and Compston, 1982); and 5) by ~3 Ma, uplift of the D'Entrecasteaux gneiss domes above sea level resulted in the shedding of conglomerate into surrounding marine basins (Francis et al., 1987; Tjhin, 1976).

2.3. Timing of eclogite-facies metamorphism

Remarkably, the ages of (U)HP recrystallization of the D'Entrecasteaux Island eclogites, as measured by ion-probe U-Pb dating of metamorphic zircons, are late Miocene to Pliocene in age (Fig. 4). The UHP locality on Fergusson Island has yielded an age of 7.9 ± 1.9 Ma (Baldwin et al., 2008; Monteleone et al., 2007). Other HP eclogites have yielded an apparent westward younging trend in metamorphic ages from ~4.3 Ma (NW Fergusson Island, Baldwin et al., 2004) to ~2.9–2.1 Ma (Goodenough Island, Monteleone et al., 2007). The quartzofeldspathic gneisses hosting the eclogites contain abundant evidence of in situ partial melting, and are intruded by ~30–40 vol.% of granodioritic to leucogranitic dikes and plutons (Hill et al., 1995). All the granodioritic melt phases (both in situ leucosome and intrusions) that have thus far been dated by U-Pb on zircon have yielded ages in the range of ~3.5–1.6 Ma; these indicate that anatexis melting of the eclogite-bearing gneisses took place <4.5 Ma, after UHP crystallization and <1–2 m.y. after HP crystallization (Baldwin et al., 1993; Baldwin and Ireland, 1995; Gordon et al., 2009). $^{40}\text{Ar}/^{39}\text{Ar}$ cooling ages on hornblende, white mica, biotite, and feldspar record rapid cooling of the gneisses and granitoids from ~4–1.5 Ma, with western samples yielding younger ages (Baldwin et al., 1993).

2.4. Summary of (U)HP exhumation tectonic context

Several aspects of the tectonic setting of the D'Entrecasteaux Islands eclogites are most important to understanding the exhumation of the UHP rocks: 1) (U)HP recrystallization ages postdate the last known collisional orogeny on the mainland by ~20–30 m.y. but are coeval with sea-floor spreading in the Woodlark Basin; 2) the eclogites were exhumed in a continental rift west of the Woodlark Basin at mean rates of ~20–30 mm/yr (Monteleone et al., 2007); 3) U-Pb ages for the (U)HP recrystallization and $^{40}\text{Ar}/^{39}\text{Ar}$ cooling ages for their subsequent exhumational cooling young in the direction that the rift is propagating; 4) the lower crust of the terrane hosting the eclogites has flowed laterally across the rift on a time scale of several million years and remains unusually thick (>26 km) in the center of the rift despite the large magnitude of crustal extension since ~6 Ma; 5) the eclogite-bearing gneisses preserve evidence for abundant partial melting and felsic magmatism soon after (U)HP

metamorphism and during rapid exhumation; and 6) the eclogitic terrane occurs in a region that has been magmatically active from the early stages of (U)HP metamorphism until today.

3. D'Entrecasteaux Islands gneiss domes

The D'Entrecasteaux Islands occupy a 30 km-wide swath of partially emergent continental crust trending WNW across a central part of the otherwise submerged Woodlark rift (Fig. 3b). A gneiss dome is a structural culmination, cored by high-grade gneissic rock or intrusives, that is mantled by lower-grade rock. Gneiss domes comprise the three largest islands and host the world's youngest (U) HP rocks. From east to west, the D'Entrecasteaux Island gneiss domes are: NW Normanby Dome (on Normanby Island), Oitabu and Mailolo Domes (both on Fergusson Island), and Goodenough Island Dome (Figs. 4 and 5). The domes appear to be spatially periodic at a wavelength of ~30–40 km. Goodenough and Mailolo domes are elongate to the WNW, subparallel to the Woodlark spreading ridge, whereas the Oitabu and NW Normanby dome trend N–S to NNE, respectively. They are typically 20–30 km wide and have length-to-width aspect ratios of ~1.5. The Normanby dome is inferred to extend to SE Fergusson Island beneath the region of active peralkaline rhyolitic volcanism (Fig. 4, Smith, 1976).

The domes are smoothly rounded topographic features with three of the four structures exceeding elevations of 2000 m (Figs. 5, 6, B–B'). They are mantled by slabby foliation dip-slopes that dip <25° on the northern flanks of the domes, are horizontal at their mountainous crests, and are moderately to steeply south dipping on the south flanks. Given the wet climate such strong topographic expression suggests ongoing or recent uplift (Ollier and Pain, 1980). Although it has been suggested that the gneiss domes have not been rising relative to sea level since the Holocene (Mann et al., 2009), extensive coral platforms of probable Holocene age are present at ~1.5 m elevation on the SE coast of Goodenough Island and in the adjacent Barrier Islands (Fig. 5). The uplifted platforms occur on the hanging-wall of adjacent active normal faults, sites that might be expected to be subsiding relative to sea level. The modest elevation of these (undated) platforms and their restricted distribution in the D'Entrecasteaux Islands suggest that the rates of late Quaternary uplift have probably not been great. Farther west, additional evidence for Late Quaternary uplift comes from repeated river incision on the downthrown side of the Wakonai normal fault (Fig. 5). There, the coastal plain has been incised, generating at least four fluvial terraces, with the oldest of these surfaces being perched >80 m above modern river level adjacent to the fault in the NW part of the island. Finally, sixteen apatite fission-track ages from the islands yielded a mean age of $\sim 0.8 \pm 0.1$ Ma (Baldwin et al., 1993), a result indicating significant unroofing of the domes during the Late Quaternary.

4. Geological and structural framework of the D'Entrecasteaux domes

4.1. Upper plate ultramafic nappe

Near their margins, the gneiss domes are overlain by an upper plate of serpentinized ultramafic rocks and local gabbro, which are intruded by mostly undeformed granodioritic plutons (Hill, 1994), the largest of which (Omara granodiorite, Fig. 4) crystallized at 1.98 ± 0.08 Ma (U/Pb age on zircon, Baldwin and Ireland, 1995). The ophiolitic rocks are erosional remnants of a regionally extensive sheet that has been warped upward across the domes (Fig. 4, Davies and Warren, 1988). Davies and Warren (1988) linked the ophiolite to the late Cretaceous Papuan Ultramafic Body (PUB) on the nearby mainland, a correlation that is supported by a U-Pb zircon age of 66.4 ± 1.5 Ma from a diabase recovered at Moresby Seamount (Fig. 4, Monteleone et al., 2001). The ultramafic rocks locally contain a steeply

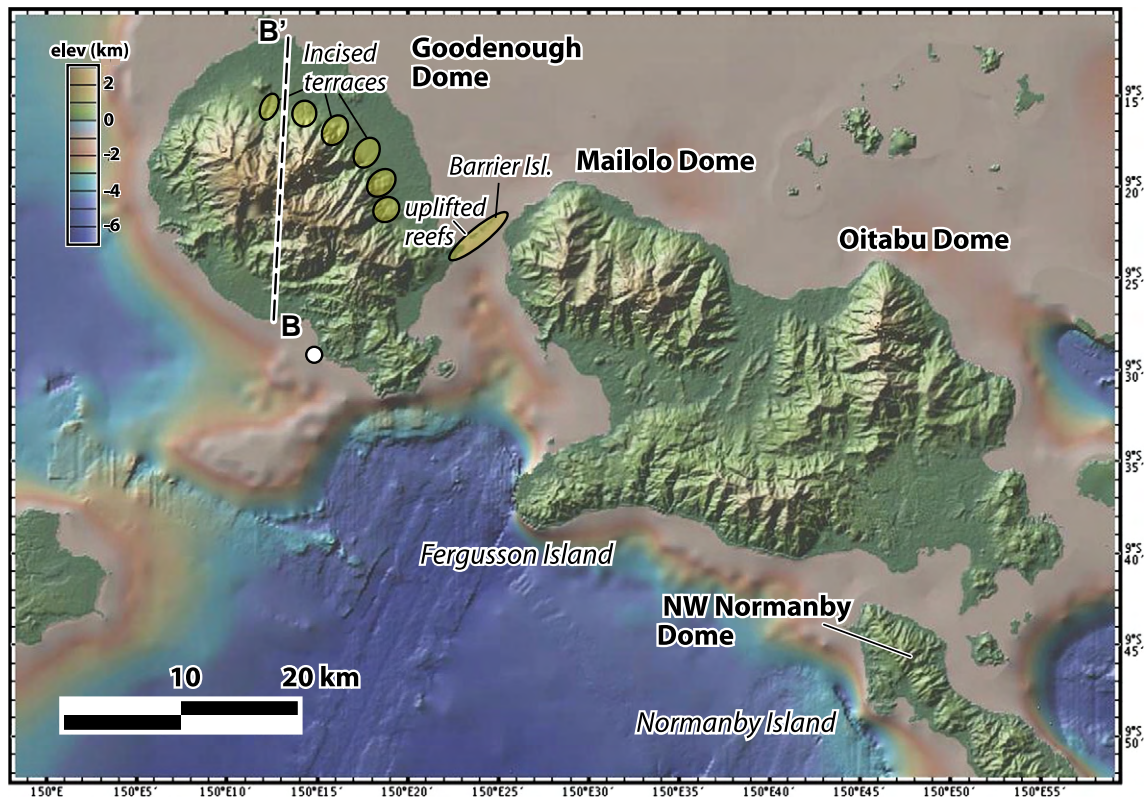


Fig. 5. Digital Elevation Model of a NW part of the D'Entrecasteaux Islands group compiled from gridded topographical and bathymetric data sets lodged at GeoMapApp (<http://www.GeoMapApp.org>). See Fig. 4 for location of map.

dipping decimeter-scale compositional layering or foliation that varies in strike (see mean attitudes plotted on Fig. 4). This observation and the pervasive, dense fractures and faults within the ophiolitic rocks suggest a significant deformation of the upper plate that was largely brittle. The ultramafic rocks are variably veined and altered to antigorite + chrysotile + magnetite + talc + tremolite, and are locally foliated near their base. They are depositionally overlain by flat-lying, unmetamorphosed sediments, including a fossiliferous upper Oligocene to middle Miocene shallow marine limestone on Fergusson Island, and volcanogenic conglomerate and fossiliferous early Miocene limestone on Normanby Island (Davies, 1973; Davies and Warren, 1988). The upper plate thus resided at its current position near sea level before any eclogite-facies metamorphism had affected the subducted continental crustal material that currently lies beneath it and that is exposed in the domes.

4.2. D'Entrecasteaux fault zone

The D'Entrecasteaux fault zone (new name) is the regionally extensive and originally subhorizontal, but now domally warped, tectonic boundary at the base of the upper plate. We interpret this contact to be correlative with the Owen Stanley fault zone along which the Papuan Ultramafic Body was originally obducted in the early Cenozoic (e.g., Davies and Jaques, 1984). Because the lower plate has been subjected to an eclogite-facies metamorphism, whereas upper plate sedimentary rocks of equivalent age are unmetamorphosed (Hill, 1994), the base of the upper plate marks a profound discontinuity in Neogene metamorphism and exhumation level. In north-central Fergusson Island, the D'Entrecasteaux Islands fault zone is intruded by the undeformed Omara granodiorite (Davies, 1973; Hill, 1994) (Fig. 4) with a U-Pb crystallization age of 1.98 ± 0.08 Ma (Baldwin and Ireland, 1995). At the NW tip of Normanby Island,

K-feldspar from deformed granodiorite and schist near the fault zone yielded $^{40}\text{Ar}/^{39}\text{Ar}$ ages of ~ 2 Ma, and an undeformed dolerite dike, ~ 1.8 Ma (Baldwin et al., 1993). These ages suggest that the fault zone has not been active since ~ 2 Ma.

We have observed outcrops of the D'Entrecasteaux fault zone along the SE coast of Fergusson Island and at the NW tip of Normanby Island (Figs. 4, 6, cross-section E–E'). At the latter locality (near the village of Y'o), the D'Entrecasteaux fault zone and its overlying lid of ultramafic rocks have been westwardly overturned on the limb of a marginal, “mushroom-like” fold (Fig. 6, cross-section E–E'). There, an up to ~ 300 m thick body of deformed leucogranite forms the structural top of the lower plate and occurs in fault contact with the upper-plate ultramafics. Mostly massive in texture away from the contact, the leucogranite becomes protomylonitic within ~ 5 m of the boundary. The LS-tectonite fabric in the leucogranite is defined by the shape-preferred orientation (SPO) of weakly deformed, lenticular feldspar porphyroclasts. The rock has local S/C fabrics and white mica fish. Some igneous quartz have been deformed into ribbon grains. Seams of dynamically recrystallized quartz and feldspar anastomose around brittlely deformed feldspar porphyroclasts. Recrystallized quartz is very fine-grained, equigranular, mostly polygonal in shape, and locally defines core-and-mantle structures and oblique grain-shape fabrics. Such microstructures are characteristic of deformation temperatures of ~ 400 – 500 °C (Stipp et al., 2002), where subgrain-rotation recrystallization is a dominant recovery mechanism in quartz (e.g., Regime 2 of Hirth and Tullis, 1992). The leucogranite is cut by three or four high-strain zones, each up to ~ 2 m thick, that consist of biotite phyllonite (schist); and by a 20 cm-thick band of chlorite-bearing quartzofeldspathic ultramylonite. If the foliation is restored to an upright dip, the sense of shear in the ultramylonitic zone is top-SE (see below). An exposure of the D'Entrecasteaux Islands fault zone on the south coast of Fergusson

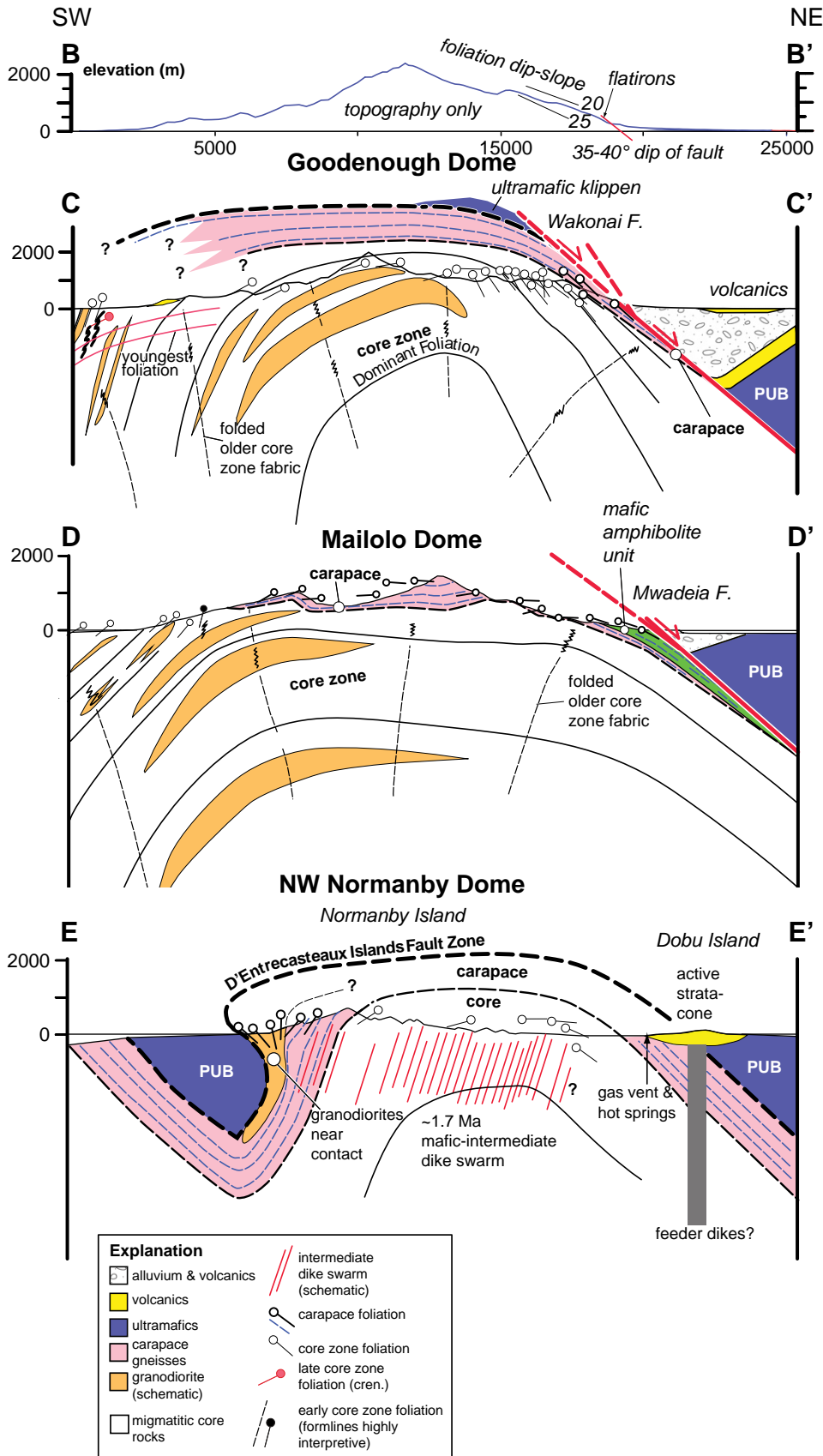


Fig. 6. Cross-sections (no vertical exaggeration) across D'Entrecasteaux Island gneiss domes. B–B', North–South topographic profile across Goodenough Island dome (data from USGS 90 m DEM; see Fig. 5 for location of profile). C–C', NE–SW structural cross-section across Goodenough Island Dome. D–D', NE–SW structural cross-section across Mailolo Dome. E–E', East–West structural cross section of the NW Normanby Dome. See Fig. 4a for location of sections C–C, D–D' and E–E'.

Island contains similar protomylonitic granitoids and shear zones of biotite- and talc-bearing phyllonite that are discordantly intruded by little-deformed dikes of granodiorite and related pegmatite.

Key inferences from the above include: 1) final juxtaposition of the lower plate gneisses against their ophiolitic cover took place during a late phase of the exhumation at ~2 Ma, resulting in a narrow zone of greenschist-facies fabrics that overprint amphibolite-facies fabrics; 2) the D'Entrecasteaux Islands fault zone was active during felsic magmatism (e.g., Omara granodiorite, late granodiorite dikes), and 3) the fault zone was altered during extensive fluid flow to form the phyllonite zones (exposed both on Fergusson and Normanby Islands).

4.3. Active range-front normal faults

The north flanks of the Goodenough, Mailolo, and Oitabu domes are bounded by 30–40° dipping normal faults that are convex toward

the north and that cut late Quaternary–Holocene alluvium in their hanging walls. These NE-dipping active faults locally cut and offset gently dipping erosional remnants of the inactive D'Entrecasteaux Islands fault zone and have down-dropped upper plate rocks on their northern sides (Figs. 4 and 6, C–C'). The range-front faults are marked by a dramatic line of faceted spurs or "flatirons," some reaching elevations of ~800 m (Fig. 7a). On both Goodenough and Mailolo domes, the scarps dip 10–15° steeper than the gneissic foliation in their footwall, and cause prominent knick-points in the longitudinal profile of rivers crossing the range fronts (Fig. 6, B–B'). The range-front faults also coincide with a series of hot springs. In the hanging wall of the Wakonai fault, on Nuamata Island, Neogene volcanic rocks have been tilted southward at up to ~65° (Fig. 4). On the basis of steep, scarp-like bathymetry and topography, Little et al. (2007) interpreted an active, south-dipping normal fault to bound the southern coast of Fergusson Island (Fig. 4). Other faults, many curved,

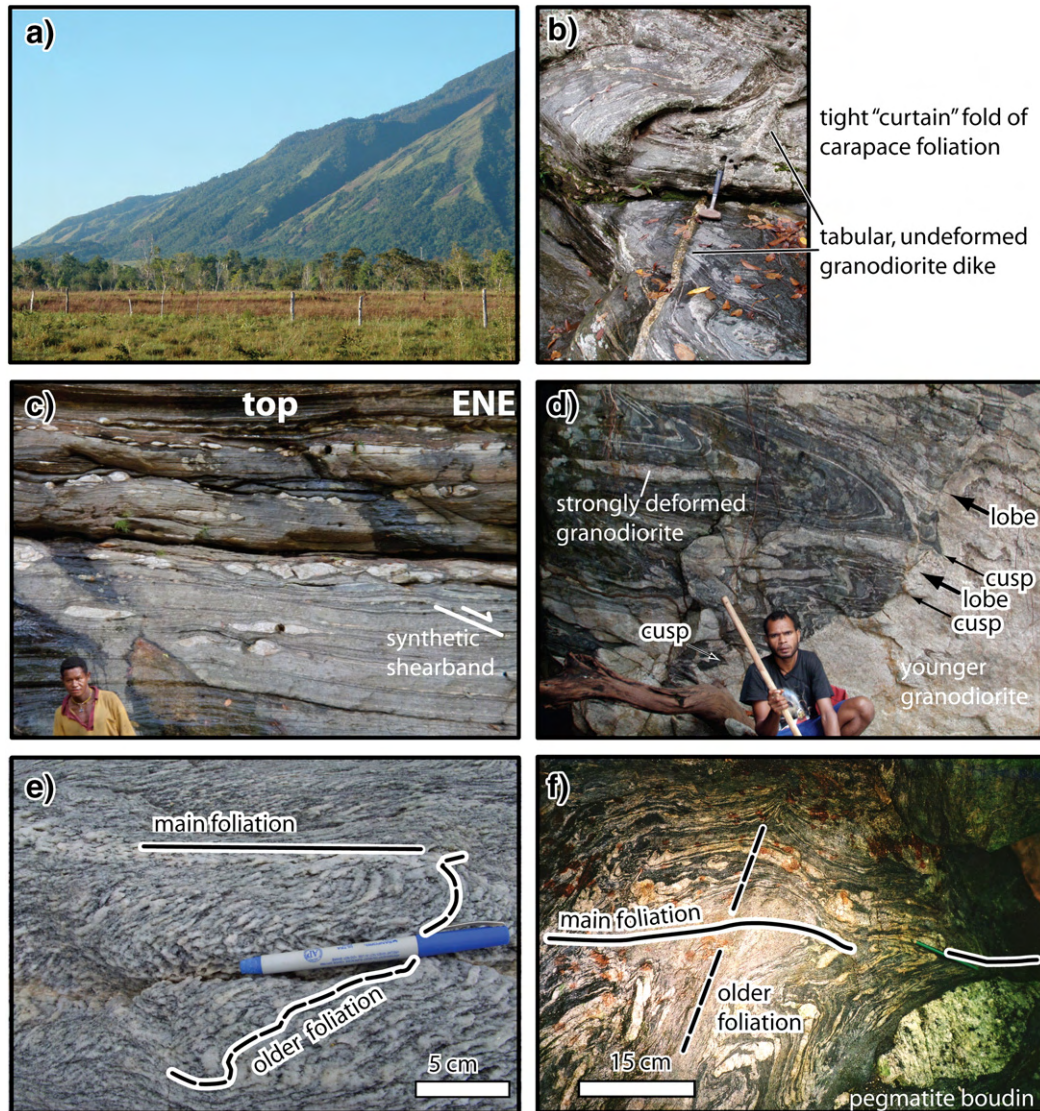


Fig. 7. Photographs of core and carapace structures. a) Faceted spurs on the scarp of the active Wakonai normal fault (photograph, looking south, was taken near the village of Wataluma on the north-central coast of Goodenough Island). The coastal savannah in the foreground (hangingwall) is underlain by alluvial gravels that have been dissected to form at least four fluvial terrace surfaces (only one shown here). b) Thinly laminated foliation of the carapace zone, tightly folded about the stretching lineation and crosscut by undeformed granodiorite dike (lower Mwadeia River gorge, Mailolo Dome). c) Boudinaged (strongly deformed) granodiorite sills in the carapace zone (Wauia River gorge, Mailolo Dome). Note synthetic (Top-ENE) shear band in the matrix outside of the boudin trains. d) Tightly folded, strongly deformed foliation-parallel sheets of granodiorite crosscut by a weakly foliated granodiorite dike with a lobate-cusped margin (same outcrop as photo b, above). The inward-pointing cusps of the fold nullions deforming this contact indicate that the dike was less viscous than its wall rock. e) Crenulated (polyphase) fabric in two-mica leucocratic granodioritic orthogneiss of the core zone (Taleba Bay, SW Goodenough Island). The younger crenulation fabric (parallel to the pen) is the main foliation defining the Goodenough Island dome. f) Dome-and-Basin fold interference pattern in core zone gneiss (inland from Fegani Bay, SW Fergusson Island). The younger E–W striking fabric is the main foliation defining the Mailolo dome. This foliation here dips ~65°S and refolds an older subvertical layering that strikes N–S. Note the stromatic leucosome segregations that partially define the older foliation.

were mapped by Hill (1994) around the poorly exposed southern flanks of Goodenough and Mailolo domes, where they were interpreted to be brittle structures related to the final uplift of the domes. In our work (also that of Davies, 1973) we did not find evidence for these onshore.

Two of the range-front fault zones were observed in outcrop, one on the Wakonai fault, and one on the range-front fault bounding the NE flank of the Oitabu dome. Several meters below the main Wakonai fault, two imbricate splays dip NE at 35–42°. The footwall gneisses have an E–W trending amphibolite-facies stretching lineation that is overprinted by an object lineation defined by brittle elongated feldspars that plunges down-dip to the NE. This younger lineation is associated with a brittle–ductile extensional S/C' shear-band cleavage. The shear-band cleavage in turn is crosscut by the pseudotachylite-bearing slip surfaces that bifurcate into oblique injection veins on the footwall side only (Fig. 13a). We attribute these tensile cracks to dynamic shear rupture propagation (after Di Toro et al., 2005; Griffith et al., 2009). Their asymmetry is consistent with normal-slip during an earthquake rupture that propagated down-dip towards the current exposure. The slip surfaces are locally decorated by down-dip striae. The main range-bounding normal fault on the NE side of Oitabu dome encloses several meters of iron-stained cataclasis and gouge, and dips 35–41° NNE. Slickenlines indicate nearly down-dip, top-NE motion. Below we present evidence that the Goodenough and Mailolo domes have been back-tilted ~20° to the SW. This implies that the range-front normal faults, currently dipping 35–40°, originally dipped at ~55–60°.

The above observations indicate that the range-front faults are major dip-slip normal faults that are still active. They discordantly crosscut the D'Entrecasteaux Islands fault zone and underlying carapace ductile fabrics, and are inferred to be relatively late structures related to the Woodlark Rift rather than detachment faults. Their contribution to exhumation of the (U)HP rocks has been sufficient to exhume pseudotachylite.

4.4. Lower plate metamorphic sequence

The lower plates of the domes in the western D'Entrecasteaux Islands consist chiefly of quartzofeldspathic paragneiss and orthogneiss, but also include minor mafic rock, and uncommon pelites, calcisilicate gneiss and marble (Davies, 1973; Davies and Ives, 1965; Davies and Warren, 1988; Davies and Warren, 1992; Hill and Baldwin, 1993; Little et al., 2007). These protoliths have been inferred to be largely Cretaceous, correlative with the Owen Stanley metamorphics on the Papuan Peninsula, and derived from the underthrust margin of the Australian Plate (Davies, 1980b; Davies and Jaques, 1984; Davies and Warren, 1988). This correlation is supported by isotopic analysis of the gneiss protoliths (Zirakparvar et al., 2010) and by sparse U–Pb ages of inherited zircons in the gneisses (Permian and younger, Baldwin and Ireland, 1995; Waggoner et al., 2008). They are thus a deeply exhumed element of the Papuan collisional orogen.

The N–S striking Trobriand transfer fault divides the Woodlark Rift into two domains of strongly contrasting basement metamorphic grade (Little et al., 2007, Fig. 4). To the west, gneissic rocks beneath the upper plate ophiolitic nappe have experienced (U)HP metamorphism in the late Miocene to Pliocene, followed by amphibolite-facies retrogression. The migmatitic gneisses are intruded by voluminous granodiorites and stretching lineations are mostly E–W, subperpendicular to Pliocene Woodlark–Australia plate motion (see below). The strongly to weakly deformed 'granodiorite' (sensu lato) occurs as tens to hundred km² plutons and dikes and also includes leucogranites. To the east of the Trobriand transfer fault, for example in the Prevost Range metamorphic core complex (Little et al., 2007), only blueschist- and lower greenschist-facies rocks are exposed, one of which has yielded an ⁴⁰Ar/³⁹Ar plateau age (interpreted as a cooling age) of 3.0 Ma ± 0.1 Ma (Monteleone et al., 2006). In this eastern domain,

granodioritic intrusions are absent, and stretching lineations are N–S, sub-parallel to the Pliocene plate motion (Fig. 4).

4.5. Carapace zone (macroscopic description)

The lower plates of the gneiss domes to the west of the Trobriand transfer fault can be divided into an outer carapace and an inner core zone. Following Hill (1994), we define the carapace as the structurally uppermost zone of the lower plate, typically <1.5 km thick, across which the dominant, dome-defining foliation becomes noticeably more planar and thinly laminated relative to structurally deeper rocks (Fig. 7b and c). Only part of the carapace is exposed along the NE flanks of Goodenough, Mailolo and Oitabu domes, because there the zone has been truncated to the north by the range-front normal faults. This offset has caused the D'Entrecasteaux Islands fault zone to be omitted there (e.g., Fig. 6, C–C'). Farther south in the domes, the carapace zone has mostly been removed by erosion except where it is locally preserved as small erosional remnants of the upper plate, for example in the synformal depression between the Mailolo and Oitabu domes. From the NE flank of Mailolo Dome, the lower contact of the carapace projects southward over the crest of the dome as a nearly flat surface (Fig. 6, D–D'), becoming southward dipping at 30–70° along the south coast of Fergusson Island (Fig. 4). This south-dipping flap of the carapace zone continues eastward along the south-central coast of Fergusson Island (Morima Range, Fig. 4). Still farther east, it wraps around the above-mentioned synform before reaching NW Normanby dome (Figs. 4, 6, E–E'). The more complete erosional removal of the carapace zone on the south flanks of the domes relative to the north, and the steeper dip of foliations on the southern flanks relative to the north, leads us to infer that Goodenough and Mailolo domes have been back-tilted to the SW by ~20° (Fig. 6, C–C' and D–D').

Evidence for in situ partial melting is abundant, if not ubiquitous, in the carapace in both felsic and mafic protoliths. These migmatitic rocks are metatextitic, containing 5–15% leucosome. The leucosomes occur as strongly deformed elongate layers subparallel to foliation (stromata), as folded patch-like bodies with diffuse margins, and as dilational infill in strain shadows, veins, and boudin necks (terminology after Sawyer, 2008). In addition to this in situ melt, 1 cm to ~3 m thick dikes of leucocratic or pegmatitic granodiorite, sharply intrude the carapace gneisses. In most outcrops, some of the felsic dikes have been transposed into foliated sheets (or boudins) that are sub-parallel to the foliation (Fig. 7c). Other dikes are typically folded, weakly foliated and discordant to the foliation; locally they have cusped lobate margins (Fig. 7d). The cusps of the fold mullions invariably point towards the dike interior, indicating that the dikes were less viscous than their wall rocks – and possibly still partially molten when folded. Finally, most outcrops also include undeformed dikes, typically leucogranite or aplite, that are a few centimeters thick (Fig. 7b), tabular, unfoliated, and nearly vertical (but vary in strike).

The carapace contains more mafic rocks (amphibolite) as well as pelite and marble than the structurally deeper core rocks (Davies and Warren, 1988). The amphibolite typically occurs as meter-scale boudins that are enclosed within the host quartzofeldspathic gneiss and wrapped by the main foliation. Relict garnets and hornblende–plagioclase symplectites after clinopyroxene indicate an original eclogite-facies assemblage existed in all of the mafic boudins, and that the entire carapace has seen (at least) HP conditions. The amphibolite may have both sedimentary and igneous protoliths. A several km-wide unit of amphibolite can be traced along the range front of Mailolo Dome for >30 km and is interlayered with marble and pelitic gneiss (Figs. 6, D–D'; 11).

4.6. Core zone (macroscopic description)

The part of the lower plate structurally beneath the carapace is called the core zone (after Hill, 1994). Most core zone gneiss has cm–

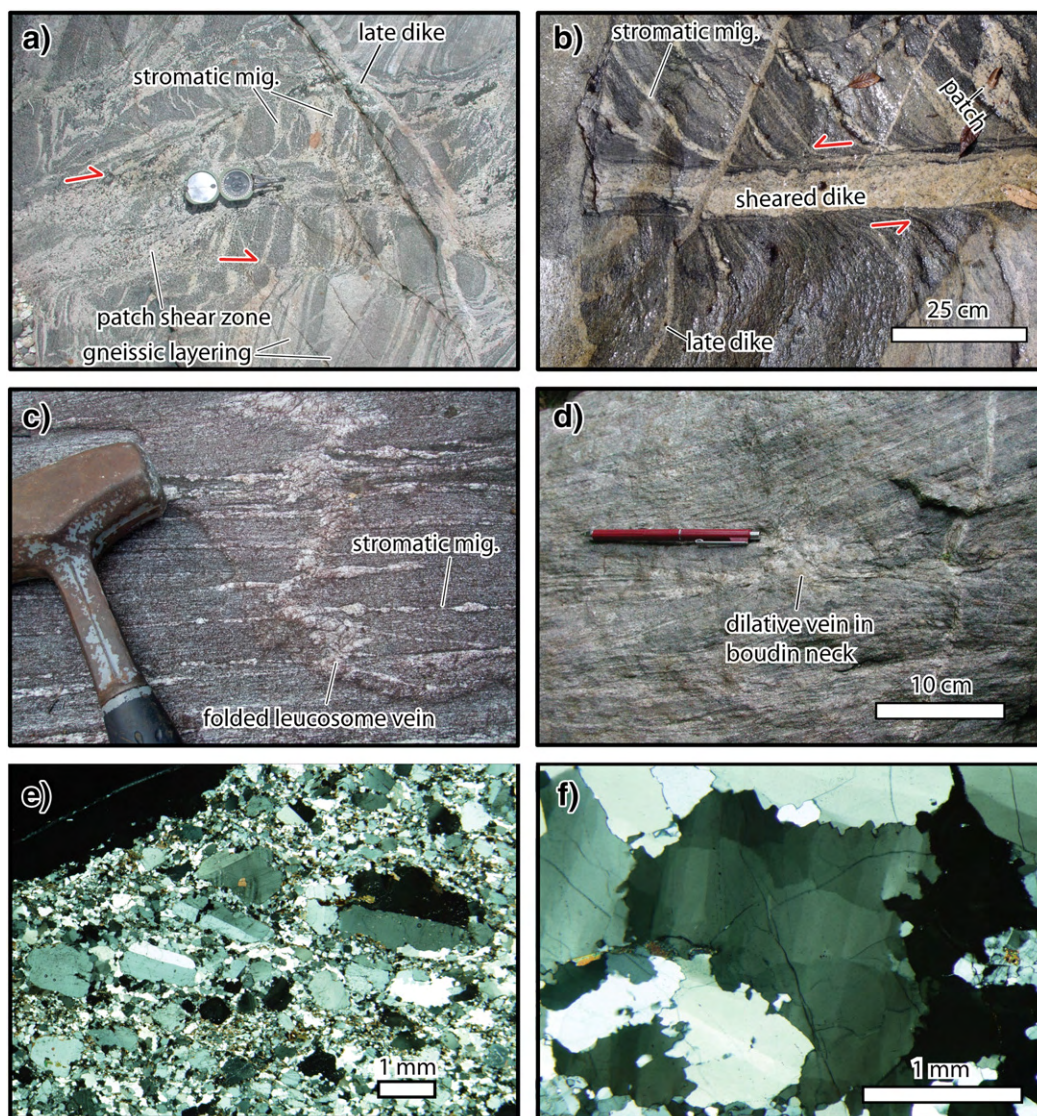


Fig. 8. Photographs of migmatites. a) Quartzofeldspathic gneiss (core zone of Goodenough Dome, Gulawata River), showing stromatic migmatite layers and ductile shear zones (dextral) that pass into sheared leucosome patches. These patches contain syn-magmatic deformational fabrics; b) Quartzofeldspathic gneiss (core zone of Goodenough Dome, Gulawata River), showing early, strongly deformed stromatic and patch migmatite bodies crosscut by granodiorite dike that infilled a ductile shear zone (sinistral). This dike was sheared (note fold mullions on top contact) and is crosscut by a later dike that is steeply dipping and undeformed. c) Strongly deformed stromatic migmatite layers crosscut by less deformed extension vein that was infilled by leucosome and folded (float boulder, Gulawata River). d) Leucosome infilling the neck of a foliation boudinage structure (near Fegani Bay, SW part of Mailolo Dome, core zone). e) Photomicrograph of deformed leucosome from core zone of Goodenough Dome (crossed nicols). Note relict euhedral shape (and growth zoning) of plagioclase crystals and their rotational tilting into the foliation as a result of magmatic or submagmatic flow. f) Photomicrograph of quartz grains in core zone leucogranite, Mailolo Dome (UHP locality, SW Fergusson Island), showing irregular, and strongly bulged to amoeboid grain boundaries and chessboard subgrain structure, indicative of high-temperature, grain-boundary migration dominated recrystallization of quartz (corresponding to regime 3 of Hirth and Tullis's, 1992 scheme).

dm scale compositional layering defined by modal variation in biotite, mica, hornblende and by layer-parallel leucosomes (Fig. 8a). Much of it consists of orthogneiss of tonalitic to granitic composition, and obvious metasedimentary protoliths, such as pelitic gneiss (e.g., kyanite–garnet–phengite–biotite–quartz–plagioclase rock) are rare.

The core zone contains ~5–10% of mafic rock, mostly as meter to decameter scale lenticular blocks of eclogite, amphibolite or garnet–amphibolite; thin-section scale textures (symplectites after omphacite and garnet) consistently demonstrate that all of these mafic blocks have been variably retrogressed from an original eclogite-facies assemblage. This relationship is true throughout all of the domes, wherever mafic protoliths are present, and no “eclogite-in” isograd can be recognized. As noted by Hill (1994), the mafic rocks occur chiefly as dikes, up to 2 m thick, that intrude the quartzofeldspathic gneiss (Fig. 9a). Most of these tabular dikes were later strongly fractured, boudinaged, and partially to completely amphibolitized

(Fig. 9a, b). The foliation in the surrounding quartzofeldspathic gneiss wraps around the mafic boudins, and extends into their retrogressed (hornblende-rich) outer rinds. Most boudins have been so widely separated as a result of extreme finite extension, that they now occur as isolated blocks (Fig. 9c). Some retrogressed eclogites occur as conformable layers up to 10 m thick within the enclosing felsic gneiss; a few (in central Mailolo dome) are homogeneous units >100 m thick. These conformable mafic bodies may have been derived from primary basaltic volcanic rocks.

Most of the core-zone rocks, like the carapace, are migmatitic, containing leucosomes derived from in situ partial melting (Hill et al., 1995). Field measurements at 8 outcrops (using a 1 × 1 m grid) indicate the presence of ~5–15% of still recognizable (i.e., relatively undeformed) leucosome. The leucosomes in these metatexites occur dominantly in boudin necks, as deformed veins with folded or crenulate margins and as strongly deformed, foliation-parallel stromata;

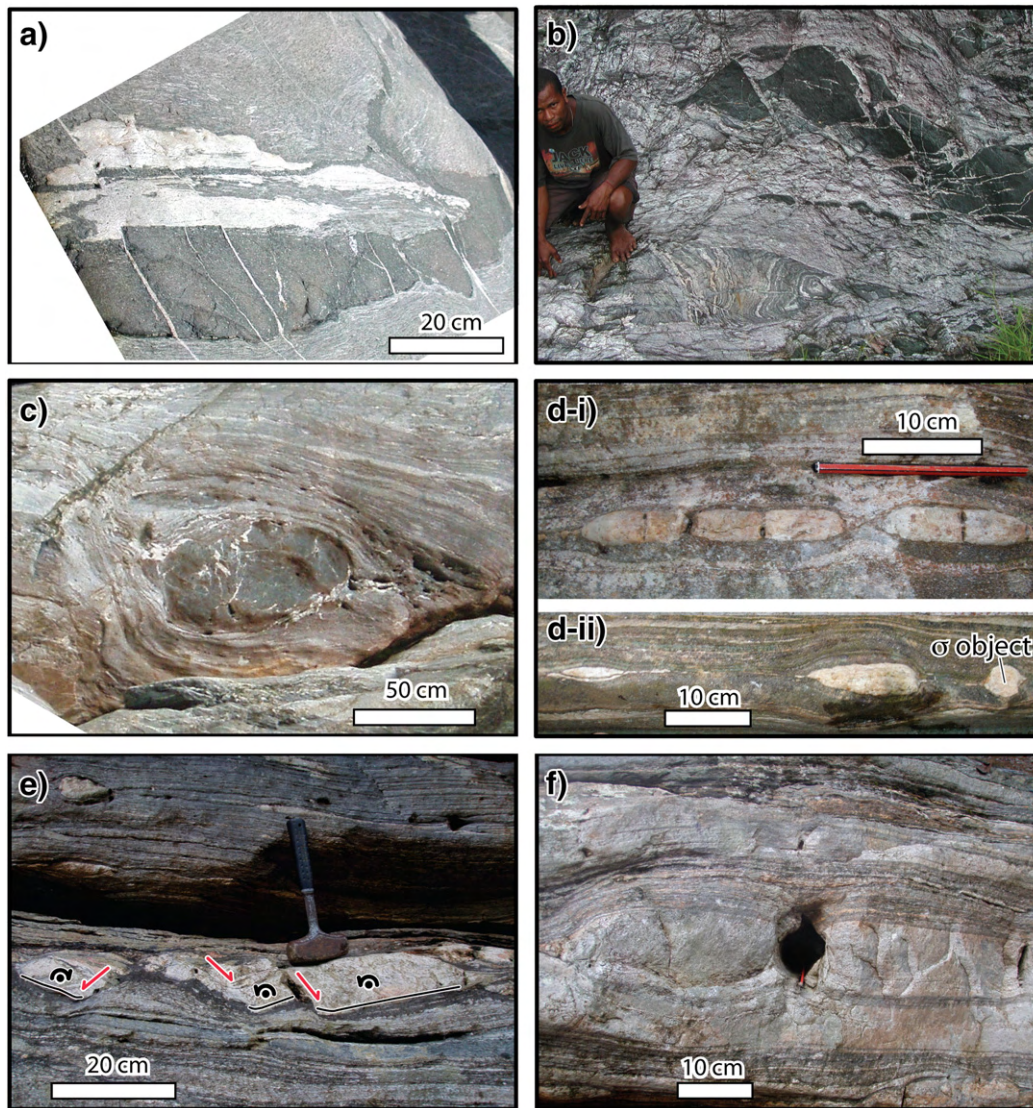


Fig. 9. Photographs of mafic eclogite pods and other boudinage structures. a) Relatively undeformed eclogitized mafic dike (from Gulawata River in the core of the Goodenough Dome), with melt-filled extension fractures and adjacent pods. b) Strongly deformed eclogitized mafic dike (core zone, Gulawata River) invaded by abundant leucosome phase (light-colored); c) Isolated boudin of eclogitized mafic dike rock showing dominant foliation wrapping around the block, melt-filled extension fractures in it, and strain shadows of melt flanking it. d) Boudinage structures in strongly deformed, foliation-parallel granodiorite sheet (carapace zone of the Mailolo Dome, Wauia River) – i, little-separated, symmetrical torn boudins; ii – strongly separated symmetric boudins, one of which has stair-stepping wings reminiscent of a σ -type mantled porphyroclast (top-ENE shear sense). e) Boudins from same outcrop as d, showing boudins that have been conjugately sheared and rotated. f) Boudins from same outcrop as d and e, showing symmetrical open-cavity vein in boudin neck (infilled with drusy quartz).

but there are also minor cm-scale deformed wisps, vein networks, and nebulitic patches with diffuse margins (Fig. 8a, b, c, and d). Many leucosome veins are bordered by melanosomes enriched in coarse-grained hornblende.

Deformation took place during partial melting. Boudin necks, extension veins, strain shadows and other dilation sites contain leucosomes (Figs. 8d, 9a, b, and c). The core of Goodenough Dome contains abundant dm-thick, melt-filled ductile shear zones (Fig. 8a) that are typically N to NE striking, near-vertical, and offset the gneissic layering dextrally. Elongate patches of leucosome fill parts of the shear zones and have been dextrally sheared. The shearing caused igneous hornblende and feldspar crystals in the leucosomes to be rotated parallel to the shear-zone boundaries, an indication of magmatic or submagmatic flow. A later sub-solidus foliation commonly overprints the sheared leucosome.

In addition to one or more types of in situ leucosome, most exposures of core-zone rocks contain abundant dikes of leucocratic

granodiorite or granite. The dikes are cm to m thick, have sharp margins, and may be pegmatitic (Fig. 8b). The volume fraction of intrusions increases with structural depth in all domes. As in the carapace, a typical outcrop includes strongly foliated dikes that are tightly folded, necked or boudinaged (these may be difficult to distinguish from strongly deformed stromatic migmatite). Younger, less-deformed dikes are typically discordant to the foliation. These are weakly foliated, but have locally folded (or fold-mullioned) margins (Fig. 8b). The youngest, least-deformed dikes (often aplitic) are nearly vertical and lack flanking folds (Fig. 8a, b). Some dikes (e.g., Fig. 8b) intruded into pre-existing shear zones where they were later further sheared, suggesting complex feedbacks between ductile dilation (and/or ductile fracturing) in precursor shear zones, later coalescence of dike sheets, and subsequent melt-related weakening to cause continued strain localization in those sheets (e.g., Weinberg and Regenauer-Lieb, 2010). At the deepest exposed levels of Goodenough and Mailolo domes, granodiorite, leucogranite and related

orthogneiss occur in plutonic bodies that are dm to km in width (Figs. 4 and 6, C–C' and D–D'). The summit region of the Goodenough Dome is intruded by a >10 km-wide pluton of strongly foliated leucogranite.

5. Ductile fabrics in the D'Entrecasteaux gneiss domes

5.1. Carapace zone foliation and lineation

Where best exposed along the faulted NE flanks of Goodenough, Mailolo and Oitabu domes, the carapace foliation (S_{3a} of Hill, 1994) dips gently NE (Fig. 10a, b, and c). Farther south, the carapace foliation flattens over the dome crests, (e.g., Mailolo dome, Fig. 6, D–D'). The west side of NW Normanby Dome is remarkable for exposing the D'Entrecasteaux fault zone atop an apparent full section of carapace rocks, and for the overturned dip of both the fault zone and underlying foliation there (Fig. 6, E–E'). This fold resembles the downward-facing antiforms that are a common feature on the margins of natural diapirs (e.g., Jackson and Talbot, 1989).

A stretching lineation on the carapace foliation is everywhere defined by the streaking of deformed quartzofeldspathic aggregates and strain shadows, and by the shape-preferred orientation (SPO) of inequant mineral grains, especially plagioclase. On the NE flanks of Goodenough and Mailolo domes, this stretching lineation generally plunges gently E or ENE, but has a W or WSW plunge farther west where the foliation dips NW (Fig. 11a, b, and c). Although not conclusive, this deflection of the lineation across the dome crests

suggests that the rising dome distorted a pre-existing ENE-trending lineation. In northern Oitabu dome, the carapace stretching lineations plunge NNE, more northerly than the others (Fig. 11d).

The transition between the core and the carapace is gradational over several hundred meters and difficult to map. Across this transition, the intensity and planarity of the dominant foliation and (we infer) the magnitude of solid-state finite strain decreases downward (transition from black to gray foliation pole symbols in Fig. 10b, c, and e). The downward decrease in strain is evident in the thin-laminated carapace foliation being replaced by a cm- to dm-scale gneissic layering, by mafic blocks becoming more elongate and recognizably dike-like, by an increasing amount of migmatite, by an increasing proportion of discordant felsic dikes, and by diminishing transposition of felsic dikes, quartz veins and other folded layers. The attitude of the dominant foliation and lineation does not change across the core-carapace transition. We refer to a single, dome-defining fabric that we recognize, both in core and carapace, as the “dominant foliation.”

Asymmetric folds of the dominant foliation are locally developed at the mesoscopic scale in the carapace (Fig. 7a). Such folds are cylindrical with straight hingelines parallel to the stretching lineation. Other such folds also occur at the micro-scale; for example on NW Normanby dome the stretching lineation coincides with a weak crenulation lineation defined by microfolding of the dominant foliation. We interpret these as “curtain folds” reflecting a constrictive finite strain (after Passchier, 1986), because the deformation apparently caused minor shortening in the plane of the foliation perpendicular to finite extension direction. Rarely, the carapace foliation has been

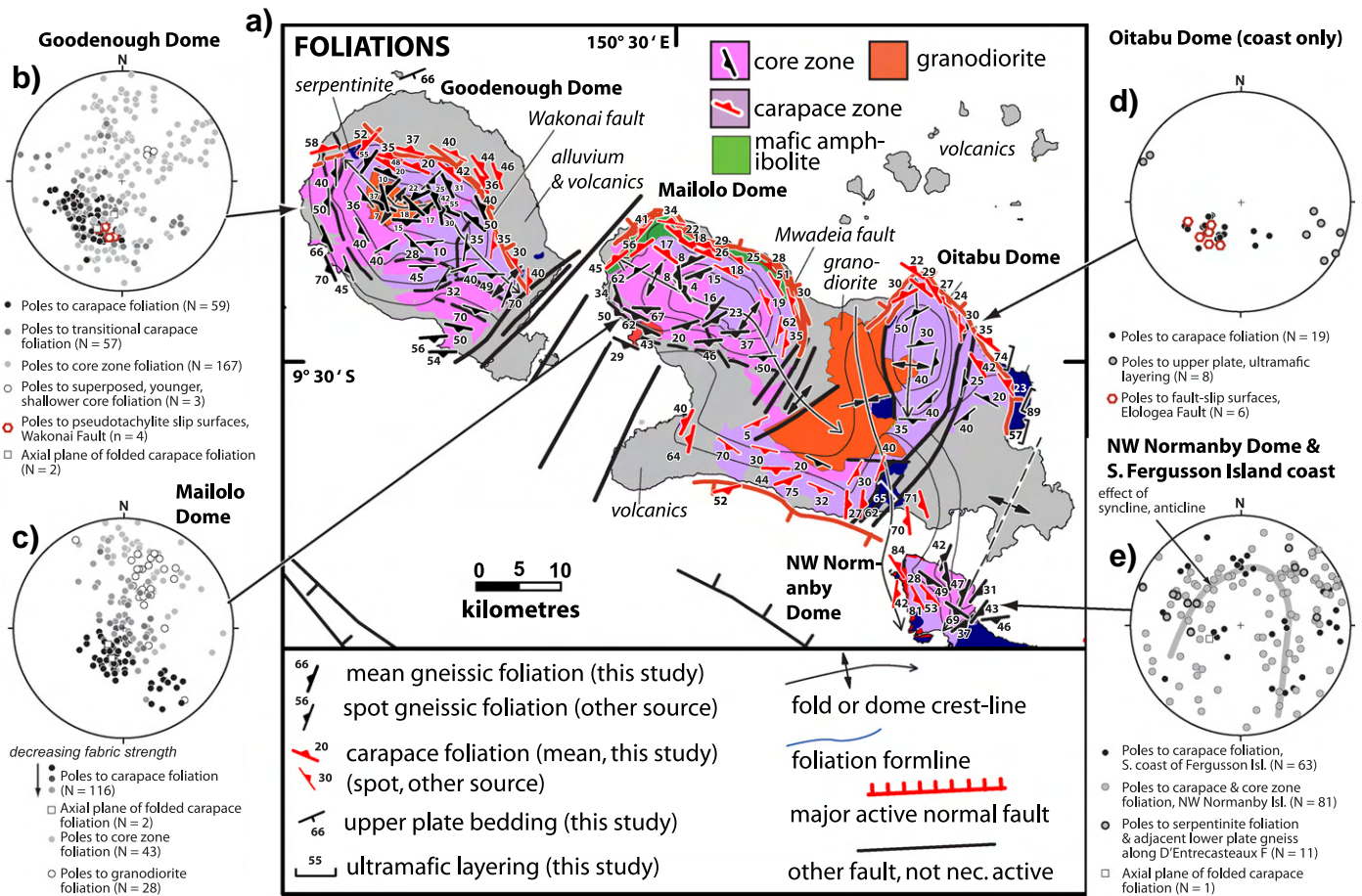


Fig. 10. Foliations in the D'Entrecasteaux Island domes. a) Map of foliation data. Each bold strike and dip symbol represents the vector average of 5–20 foliation attitudes (data from this study); finer strike and dip symbols are taken from Davies (1973) or Hill (1994). b–d) Lower hemisphere, equal-area projection of poles to planar structures in Goodenough, Mailolo, Oitabu, and NW Normanby domes, respectively. Symbol keys plotted below each stereogram. The solid black poles indicate foliations from the structurally highest parts of the carapace, where the fabric is strongest; whereas the pale gray poles denote attitudes from structurally lower parts of the carapace, where the fabric is less intense.

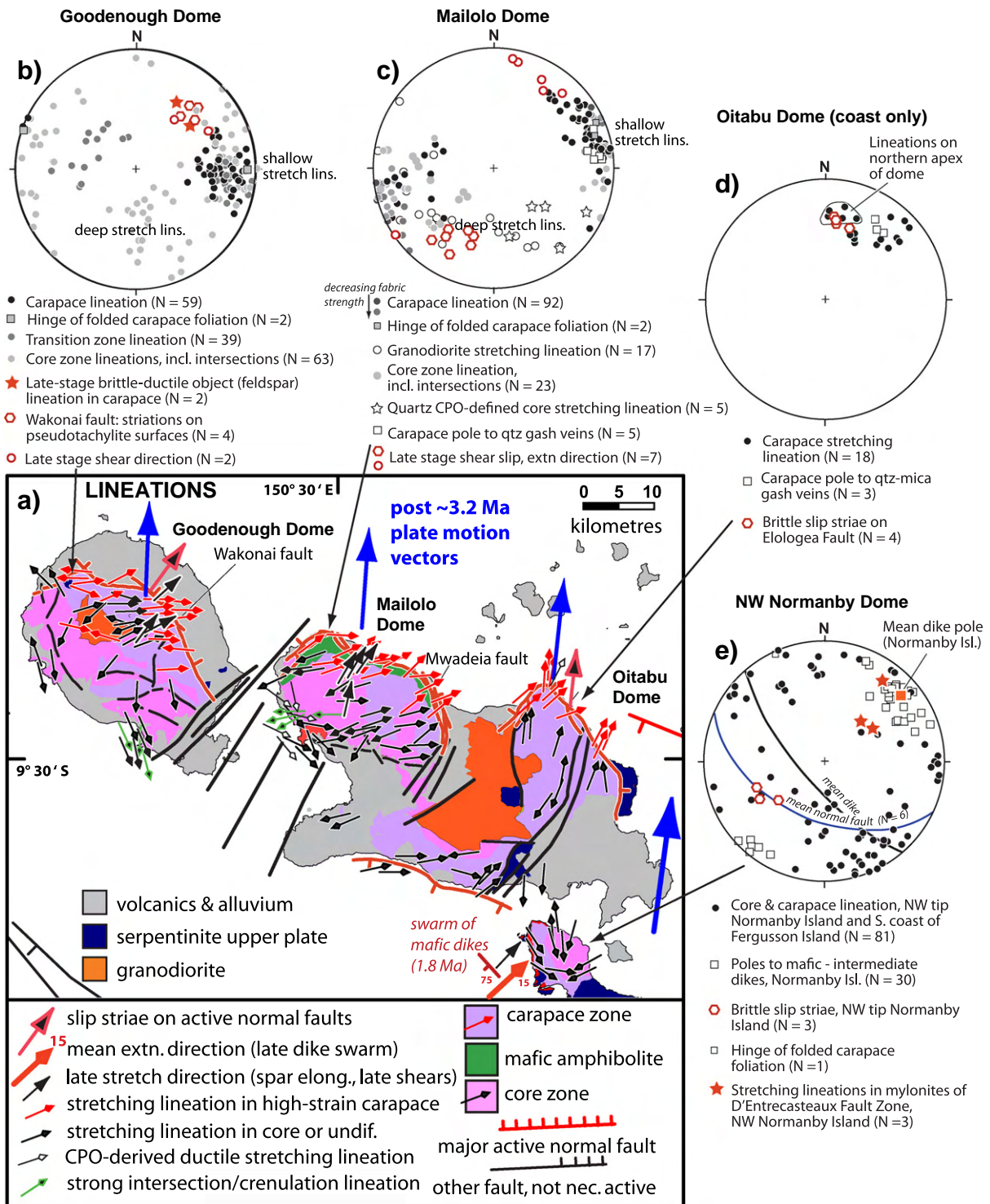


Fig. 11. Lineations in the D'Entrecasteaux Island domes. a) Map of lineation data. Each bold lineation symbol represents the vector average of 5–20 lineation attitudes (data from this study); finer strike and dip symbols are taken from Davies (1973) or Hill (1994). b–d) Lower hemisphere, equal-area projection of linear structures in Goodenough, Mailolo, Oitabu, and NW Normanby domes, respectively. Symbol keys plotted below each stereogram.

folded about hingelines at a high angle to the stretching lineation. In those cases the tight intrafolial folds verge in accordance with adjacent shear indicators (Fig. 12a, inset). We infer these latter folds developed during progressive deformation with flow perturbations in the carapace inducing a rotation of the short limbs of the folds with respect to the local shear plane (e.g., Carreras et al., 2005).

5.2. Carapace microstructures

The dominant fabric in the carapace developed at amphibolite-facies conditions. Microstructures suggest rapid quenching of the grain-boundary microstructure with no static recrystallization. Most quartz grains contain deformation bands. The grains are interlobate

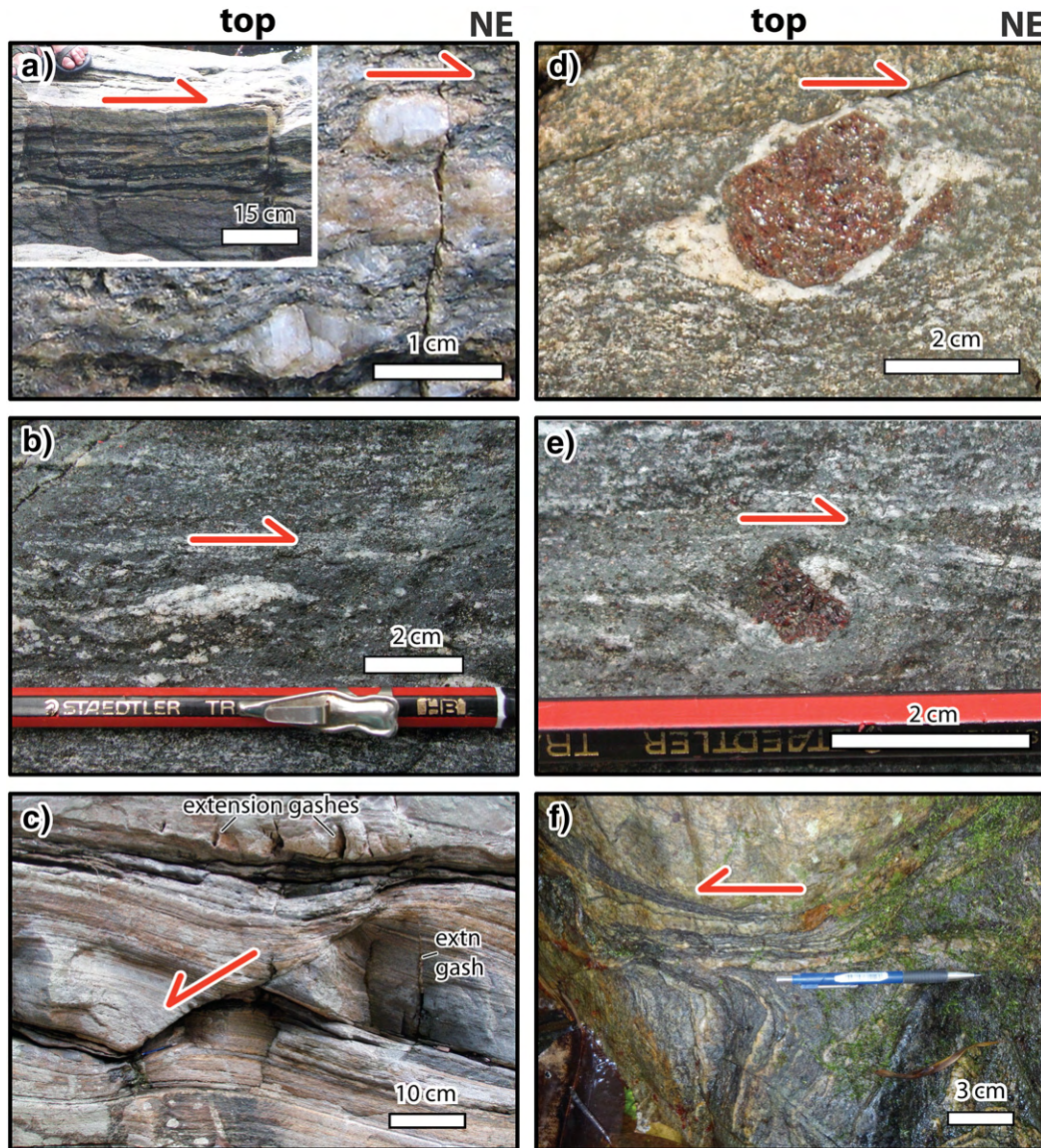


Fig. 12. Evidence for non-coaxial deformation. In all photographs, E or NE is on the right. a) σ -type mantled feldspar porphyroclasts (carapace of Oitabu dome, coastal outcrop). Inset shows asymmetric fold of dominant foliation at the same locality. b) feldspar-rich clot (probably deformed leucosome) with σ -type stair-stepping tails (carapace of Goodenough Dome, Gulawata River); c) Antithetic (C') shear cutting foliation at $\sim 50^\circ$ and extension gashes at $80\text{--}90^\circ$ angle to that foliation in zone of dominantly top NE shear sense (carapace of Mailolo Dome, Wauia River). d) coarse garnet porphyroblast abutted by an asymmetric strain shadow infilled with leucosome (carapace of Goodenough Dome, Gulawata River); e) elongate garnet porphyroblast with σ -type stair-stepping tails, back-rotated against dominant shear sense (top-to-the-NE, same location as d). f) Sheared contact between granodiorite plutonic body and micaceous gneiss (competence contrast).

to amoeboid in shape and inequigranular, although foliation-parallel quartz ribbons (some now recrystallized) may occur in mica-bearing rocks, where they probably reflect extreme deformation, pinning, and enhanced rates of grain-boundary migration parallel to the foliation. The quartz microstructures indicate that recovery in quartz was chiefly accommodated by high-temperature grain-boundary migration recrystallization, probably at temperatures $>500^\circ\text{C}$ (e.g., Regime 3 of Hirth and Tullis, 1992; see also Stipp et al., 2002). The feldspars show undulose extinction, subgrains, deformation twinning, diffuse kink bands, and K-feldspar replacement by myrmekite and flame perthite. The boundaries of feldspar porphyroclasts are highly lobate (especially against quartz) and sharp. Such microstructures are typical of deformation under amphibolite-facies (or greater) conditions ($>600^\circ\text{C}$) and indicate dislocation creep accompanied by subgrain-rotation recrystallization together with high grain-boundary mobility (dissolution-precipitation creep?) (e.g., Altenberger and Wilhelm, 2000; Kruse et al., 2001; Rosenberg and Stunitz, 2003; Tullis, 2002).

Shape preferred orientations (SPO's) of feldspar and hornblende (also quartz aggregates) are conspicuously stronger parallel to the lineation than orthogonal to it, suggesting plane strain or constriction, but not flattening. Quartz grains in the carapace and core zones are $\sim 100\text{--}200\ \mu\text{m}$ in diameter (T. A. Little and B. R. Hacker unpub. EBSD data). In this sense, most of the carapace gneisses have grain sizes typical of gneiss and are not mylonites. Microstructures such as the presence of quartz + feldspar in dilational sites, for example in the strain shadows of garnet porphyroblasts, indicate carapace deformation in the presence of melt (Fig. 12d).

Rare, grain-size reduced mylonitic rocks occur locally in the outermost parts of the carapace, and along the D'Entrecasteaux Islands fault zone (see above), where they occupy decimeter-thick (or thinner) zones of extremely localized, late-stage shearing (D_{3b} shears of Hill, 1994). A single ~ 5 m-wide outcrop in the Gulawata River gorge on Goodenough Island exposes three bands of greenschist-facies mylonitic rocks, each 15–20 cm thick. These bands consist of chlorite-

carbonate-rich phyllonitic schist that concordantly overprint (retrogress) the amphibolite-facies foliation in their gneissic walls. Along the south coast of Fergusson Island and on NW Normanby Island, some gneisses that outcrop within ~200 m of the D'Entrecasteaux fault zone include seams of very fine-grained, dynamically recrystallized quartz and feldspar. The mm- to cm-thick seams anastomose through the otherwise coarse-grained amphibolite-facies gneiss, wrapping around quartz ribbons, feldspar porphyroclasts, and white-mica fish to define a protomylonitic S/C fabric.

5.3. Core zone foliation and lineation

The dominant foliation dips outward from the core of each dome. Beneath the carapaces that flank the north sides of Goodenough and Mailolo domes, the core-zone foliation dips NE or NW at 25–30°, parallel to the foliation in the carapace (Fig. 6, C–C' and D–D'). Farther southward and inward into these domes, the foliation flattens and reverses dip over the crest of the domes (Fig. 10a, b, c). On the southern dome flanks, the foliation dips southward at 40–70° (Fig. 11a). This is 10–30° steeper than the foliation on the north flank of the same domes, a relationship that supports a model of back-tilting of the domes to the SW by ~20° (Fig. 6, C–C' and D–D').

The deep gorges and steep topography on the NE flank of the Goodenough Island dome expose abrupt horizontal and vertical transitions in the dip of the core-zone foliation. Inward towards the center of the dome, the foliation steepens in dip from ~25 to ~50° to the NE, whereas structurally upward the foliation shallows abruptly to become subhorizontal at the crest of the island. The inferred pattern of foliation trajectories resembles a set of nested parabolas, with the inner ones being more tightly curved than the outer (Fig. 6, C–C'). Such deformation patterns are also typical of deformed, originally

horizontal layering in natural and model diapirs (Cruden, 1988, 1990; Dixon, 1975; Jackson and Talbot, 1989; Talbot and Jackson, 1987).

In contrast to the planar morphology of the foliation in the carapace, the dominant foliation in the core anastomoses at the 1–10 m scale. Especially in Goodenough and Mailolo domes, the dominant foliation in the core is typically irregular or swirled at the outcrop scale because of i) the large volume of magmatic material, both in situ and intruded – including melt-filled shear zones (Fig. 8a, b), ii) the presence of lithologic contacts (competence boundaries) across which the foliation refracts, and iii) abundant layer and foliation boudinage (e.g., Arslan et al., 2008; Goscombe et al., 2004) (Fig. 8d). The bulk deformation has yielded a rock in which competent material (mafic or granodioritic gneiss) occurs as lenses or boudins bounded by sheared interfaces and wrapped by less-competent, more strongly foliated rock (quartzofeldspathic or micaceous gneiss) (Fig. 12f). Regionally, the pattern of shear across these variably inclined interfaces between the stiffer bodies is bivergent, similar to the conjugate pattern of synthetic (C') and antithetic (C'') shearing in the carapace. These observations suggest that bulk deformation in the core was to some extent irrotational (see below), and reminiscent of the deformation-partitioning models of Dewey et al. (1993); Andersen et al. (1994); Hudleston (1999) Engvik and Andersen (2000) and Foreman et al. (2005).

Stretching lineations in the core have a complex 3D pattern. On the NE flanks of Goodenough and Mailolo domes, stretching lineations in upper parts of the cores of these domes plunge gently E or ENE, parallel to lineations in the carapace (Fig. 11a, b, c). Within the core, the stretching lineations rotate anticlockwise with increased structural depth exposed to the SW, becoming, in turn, SW-, S-, and SE-trending with increasing proximity to the SW coast of both islands (Fig. 11, also Table 1). On Goodenough Island, where our data are most

Table 1
Summary of Mean Extension Directions in the D'Entrecasteau Domes.

Structural depth	Trend	Plunge	N	Structure
<i>Mailolo Dome</i>				
Post-dominant fabric				
Shallow	30	14	7	Late-stage C'' oblique extensional shears (mean extension direction)
Dominant fabric				
Shallowest	74	12	23	Structurally highest carapace lineation
Shallow	72	1	69	Mean carapace stretching lineation
	138	15	12	Mean Core zone stretching lineation (granodiorite pluton)
Deep	135	35	5	Mean core zone stretching lineation (from quartz CPO's)
<i>Goodenough Island Dome</i>				
Post-dominant fabric				
Shallow	44	35	4	Wakonai rangefront fault mean brittle slip striation (pseudotachylite)
Shallow	39	37	2	Wakonai rangefront brittle–ductile stretching lineation (S–C fabrics)
Various levels	49	38	7	Late-stage C'' oblique extensional shears (extension direction)
Dominant fabric				
Shallowest	88	27	60	Mean carapace stretching lineation (NE flank of Goodenough)
Deeper	84	9	22	Mean upper core zone stretching lineation (lower part of Gulawata River gorge)
Deeper	68	13	22	Mean core zone stretching lineation (upper part of Gulawata River gorge)
Deeper	181	28	11	Mean core zone stretching lineation (south-central Goodenough, data from Hill, 1994)
Deepest	166	45	28	Mean core zone stretching lineation (southwest coast)
<i>Oitabu Dome (N. flank only)</i>				
Post-dominant fabric				
Shallow	10	33	4	Oitabu Dome Rangefront fault mean brittle slip striation
Dominant fabric				
Shallow	32	28	18	Oitabu Dome mean carapace stretching lineation
<i>NW Normanby Dome</i>				
Post-dominant fabric				
Shallowest	41	36	2	Stretching lineation in D'Entrecasteaux Fault zone brittle–ductile mylonites
Various levels	49	15	30	Mean late dike pole (extension direction)
Dominant fabric				
Shallow	86	1	14	Mean carapace stretching lineation, south-central coast, Fergusson Island (west of synform)
Shallow and deep	155	5	55	Mean carapace and core lineation, NW Normanby Island (west limb of antiform)
Shallow and deep	285	54	13	Mean carapace and core lineation, NW Normanby Island (east limb of antiform)

densely spaced, the inward anticlockwise deflection of lineations includes a reversion to E–W trends locally near the topographic crest of the island, presumably because of that site's structurally high position and proximity to the eroded carapace (Fig. 6, C–C'). We are unsure whether this SW-ward anticlockwise deflection in lineation trend reflects a purely vertical gradient in finite strain (i.e., a function of increased structural depth inward into the core), or one that may be in part horizontal (horizontal distance to the SW), or one that may be in part the effect of an unrecognized mixture of different-aged lineations in different places.

5.4. Core zone microstructures

The amphibolite-facies fabric in the core shows little or no evidence for static recrystallization, implying rapid cooling and quenching of the microstructures. Quartz grains are amoeboid in shape, with deeply interpenetrating bulges, re-entrants, and island grains (Fig. 8f). They are inequigranular, with some very coarse grains. They have sweeping undulose extinction or, more commonly, deformation bands. The latter commonly occur in apparent orthogonal sets to define a chessboard subgrain structure (Fig. 8f). The microstructures indicate that recovery in quartz was accommodated chiefly by high-temperature grain-boundary migration recrystallization (e.g., Regime 3 of Hirth and Tullis, 1992; Kruhl and Peternell, 2002; Stipp et al., 2002), and suggest combined activity of basal $\langle a \rangle$ and prism $\langle c \rangle$ slip in quartz (Kruhl, 1998). Feldspar microstructures in the core-zone rocks resemble those in the carapace, and indicate dislocation creep accommodated by subgrain-rotation recrystallization with highly mobile grain boundaries. Feldspar grains have a strong shape preferred orientation. This SPO is consistently much stronger parallel to the lineation than orthogonal to it, suggesting flow involving either plane strain or constriction. Biotite occurs in seams that anastomose around rhombic- or lens-shaped feldspar grains. Asymmetric shear sense indicators, such as phengite fish, are rare. Melt accumulation phase in dilational sites, such as strain shadows, and the rotational tiling of euhedral igneous feldspar and hornblende in leucosomes suggest melt-present deformation (Fig. 8e).

6. Fabric superposition in the gneiss domes

6.1. Foliations that pre- and post-date the dominant foliation

As recognized by Hill (1994), the foliation in the core of Goodenough and Mailolo domes was superposed across older gneissic fabrics (including what Hill called "S₁") that are best preserved at deep structural levels. The older and younger fabrics both formed at amphibolite-facies conditions in conjunction with partial melting and leucosome segregation (Hill et al., 1995, this study). The fabric superposition is expressed by the tight folding or crenulation of an older gneissic layering during the development of the dominant foliation (Fig. 7e); also by a crenulation lineation developed parallel to the intersection between the two foliations and by mesoscopic fold interference patterns (Fig. 7f). In most cases, the intersection lineation is parallel to stretching lineations defined, for example, by elongate feldspar augen or strain shadows in nearby deformed granodiorite plutons. The enveloping surface of the (now crenulated) older foliation typically lies at a high angle ($>60^\circ$) to the younger, dominant foliation (Fig. 7e, f). Because the dominant foliation is regionally subhorizontal (removing the effect of later doming), this relationship implies that the older foliation was originally moderately to steeply dipping prior to crenulation. In the carapace zone of NW Normanby and Mailolo domes, this near-orthogonal superposition of fabrics is supported by the geometry of garnet inclusion trails in metapelitic rocks. There, the garnet porphyroblasts contain planar inclusion trails (relict internal foliation) that are everywhere inclined at a steep (70–90°) angle to the younger dominant foliation. The latter wraps around

the garnets externally and truncates the older internal foliation (Fig. 13f). After doming, some relatively steeply dipping ($>60^\circ$) panels of the dominant foliation were further crenulated by younger, shallow-dipping foliations. The latter are the youngest ductile fabrics found in the core of the domes. For example, on the SW coast of Goodenough Island, the dominant foliation dips 60–70° SW, and it has locally been crenulated by a younger foliation, the axial surfaces of which dip SW at 15–30°. Steeply dipping, undeformed granodiorite dikes crosscut this youngest foliation. Other examples of flat-lying crenulation fabrics superposed across steeply dipping parts of the dominant foliation were observed on the NE flank of Goodenough dome and the SW limb of NW Normanby dome.

6.2. Relationship of early foliation to (U)HP metamorphism and exhumation

The above-mentioned two foliations in the gneiss developed after recrystallization of the eclogite-facies assemblages, as both of the fabrics wrap around the amphibolite-facies rinds of mafic boudins and both penetrate retrogressed parts of the mafic dikes. Similarly, their intersection lineation is imprinted not only into the felsic host gneiss, but also the retrogressed rinds of the mafic blocks. Most eclogite blocks are massive, but some preserve weak eclogite-facies foliations. In our opinion, any pre-eclogite-facies fabrics that may once have been present are (generally) no longer preserved. By contrast, Hill (1994) interpreted her S₁ to predate the eclogite-facies metamorphism. Finally, our observations indicate that the crenulated, earlier foliation occurs not only in the strongly layered "host" gneisses but also in the large, leucocratic granodiorite plutons that intrude those gneisses. Because such granodiorites are younger than 4 Ma, this observation supports the view that the older (now crenulated) fabric formed during exhumation of the eclogite-bearing gneiss.

6.3. Summary of ductile fabric development

In summary, the relationships between gneissic and igneous fabrics in the carapace and core zones suggest the following deformation sequence. There are no (obvious) pre-eclogite-facies foliations preserved. Eclogite-facies mineral assemblages are locally preserved in some mafic boudin cores, but structures related to this event are weak to absent. Subsequent to the late Miocene–Pliocene (U)HP metamorphism, at least two ductile fabrics formed at amphibolite-facies conditions prior to ~2 Ma (U–Pb zircon age of little-deformed Omara granodiorite and $^{40}\text{Ar}/^{39}\text{Ar}$ cooling ages of youngest white micas, Baldwin and Ireland, 1995; Baldwin et al., 1993). At the exposed structural levels, which are little eroded and near the head of the domes, the dominant fabric is domal and crenulates an older foliation that is more steeply dipping. The older fabric is best preserved at the deepest exposed structural levels of the domes, and is inferred to have been originally near vertical. Both fabrics developed during partial melting and intrusion of granitoid dikes. Prior to doming, the younger dominant foliation was subhorizontal and regionally extensive, accommodating vertical shortening and horizontal E–W ductile extension with either plane strain or slight constriction. This flow is most strongly expressed in the planar fabrics of the carapace, but also pervaded the rocks that would become core of the gneiss domes. Later upwelling bent dominant foliation to form the domes. This upwelling was followed by rapid cooling that quenched-in the high-temperature microstructures in the gneisses. Finally, shallow-dipping crenulation fabrics locally overprinted the dipping flanks of the dome.

7. Kinematics of ductile flow during amphibolite-facies overprint

7.1. Directions of ductile shear and kinematic vorticity number estimation

Ductile flow dominated the deformation after the eclogitic gneisses had been exhumed to lower crustal depths, and this led to

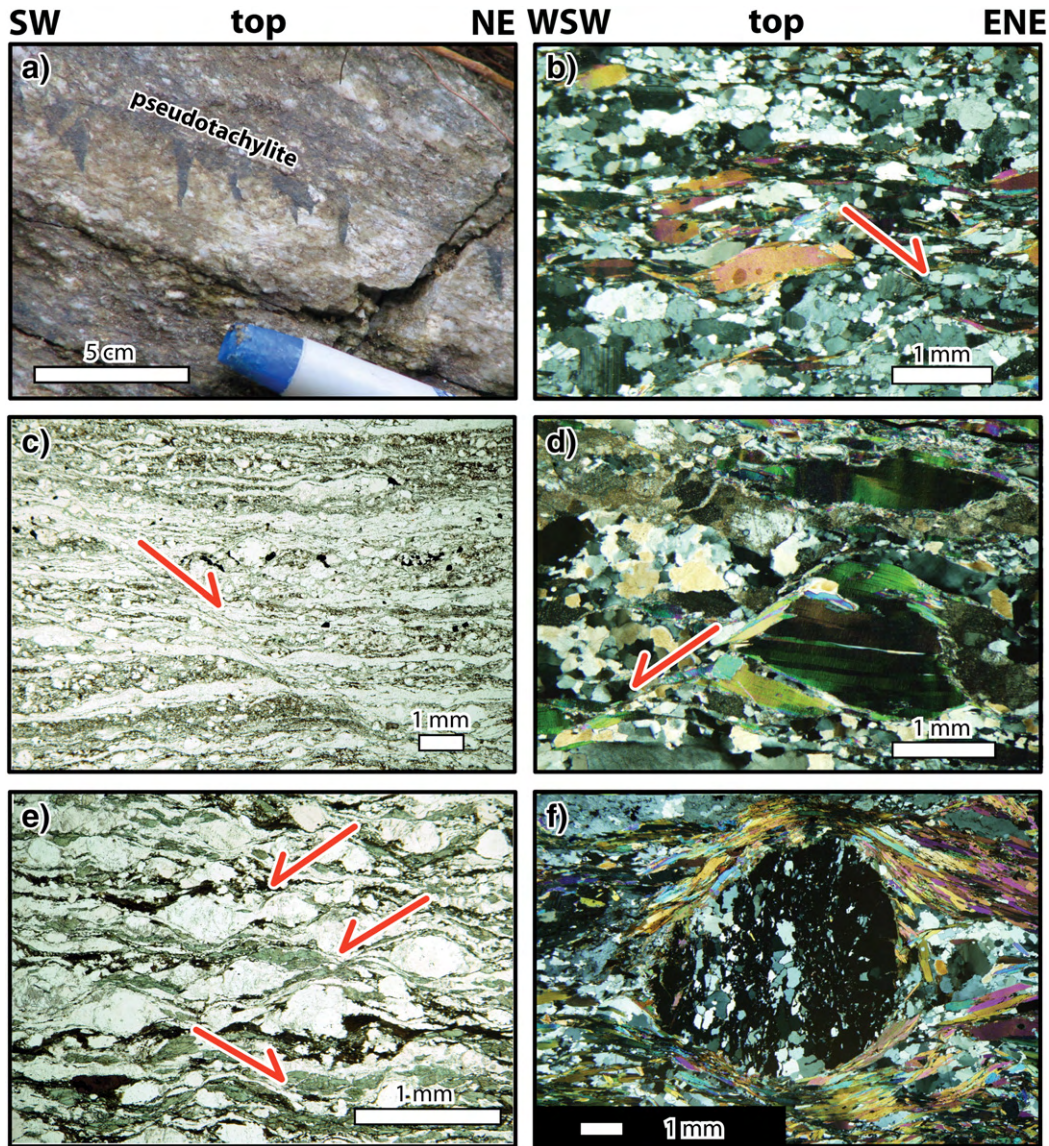


Fig. 13. Selected Microstructures (mostly shear-sense indicators). In all photographs, the foliation is shown horizontal, and the E or NE direction on the right. a) Pseudotachylite adjacent to Wakonai range front fault, NE Goodenough Island, showing slip surface and obliquely inclined injection veins indicating top-NE slip; b) C'-type phengite fish (carapace of Goodenough Dome, gorge to the NW of Gulawata River); c) C'-type extensional shear band (carapace of Oitabu dome, coastal outcrop); d) C''-type (antithetic) extensional shear band (same locality as b); e) Conjugate (C' and C'') extensional shear bands (same locality as c); f) Garnet porphyroblast showing overgrown early foliation (preserved as inclusion trails) at a high angle to the dominant (dome defining) foliation (NW Normanby dome, near village of Yo'o).

the development of their dominant foliation and lineation. Prior to doming, the dominant foliation was subhorizontal, and the flow was dominated by vertical thinning and E–W extension. The apparently continuous, sweeping and dominantly E–W lineations across the lower plate of the domes (Fig. 11a) suggests a complex and 3D finite strain field within a coherent body that is larger and older than any individual dome. Whatever the cause of this complexity, it seems fair to say that it contrasts with what one would expect in a simple shear-dominated metamorphic core complex. Uplift of the domes resulted in the warping of this regionally widespread LS-tectonite fabric about dome axes that were discordant to the earlier stretching lineations.

A key observation is that the dominant E–W trend of the stretching lineations across Goodenough and Mailolo domes (at least in the upper structural levels) is at a high angle to the plate motion direction across the Woodlark Rift (Fig. 11a). Such discordance indicates that the ductile flow was largely decoupled from Woodlark–Australia plate motion and was probably gravity driven. Interplate tractions from the side or bottom did not drive the dominantly E–W flow within the

body of (U)HP continental crust that became the D'Entrecasteaux Islands.

Ductile shear-sense indicators are relatively common in the carapaces of Goodenough, Mailolo, Oitabu and NW Normanby domes (Fig. 14a). These include phengite fish (Fig. 13b), feldspar-rich aggregates or porphyroclasts with stair-stepping tails that define σ objects (Fig. 12a, b) and boudins deformed into σ -objects (Fig. 9d-ii). Phengite fish are mostly C'-parallel (Fig. 13b), but may include lenticular morphologies (classification scheme of ten Grotenhuis et al., 2003). Late-stage asymmetric folds with hingelines at a high angle to the stretching lineation are inferred to verge in the shear direction (Fig. 14a). The dm-thick shear zones at competence boundaries (e.g., Fig. 12f) have sigmoidal foliations indicative of shear sense.

In the D'Entrecasteaux Island gneiss domes, mesoscopic to micro-copic extensional (C') shear bands are an abundant shear indicator in the carapace and carapace-core transition zone ("D_{3c}" structures of Hill, 1994), but not in the core zone. At a given locality, extensional shear bands may verge in either direction parallel to the lineation

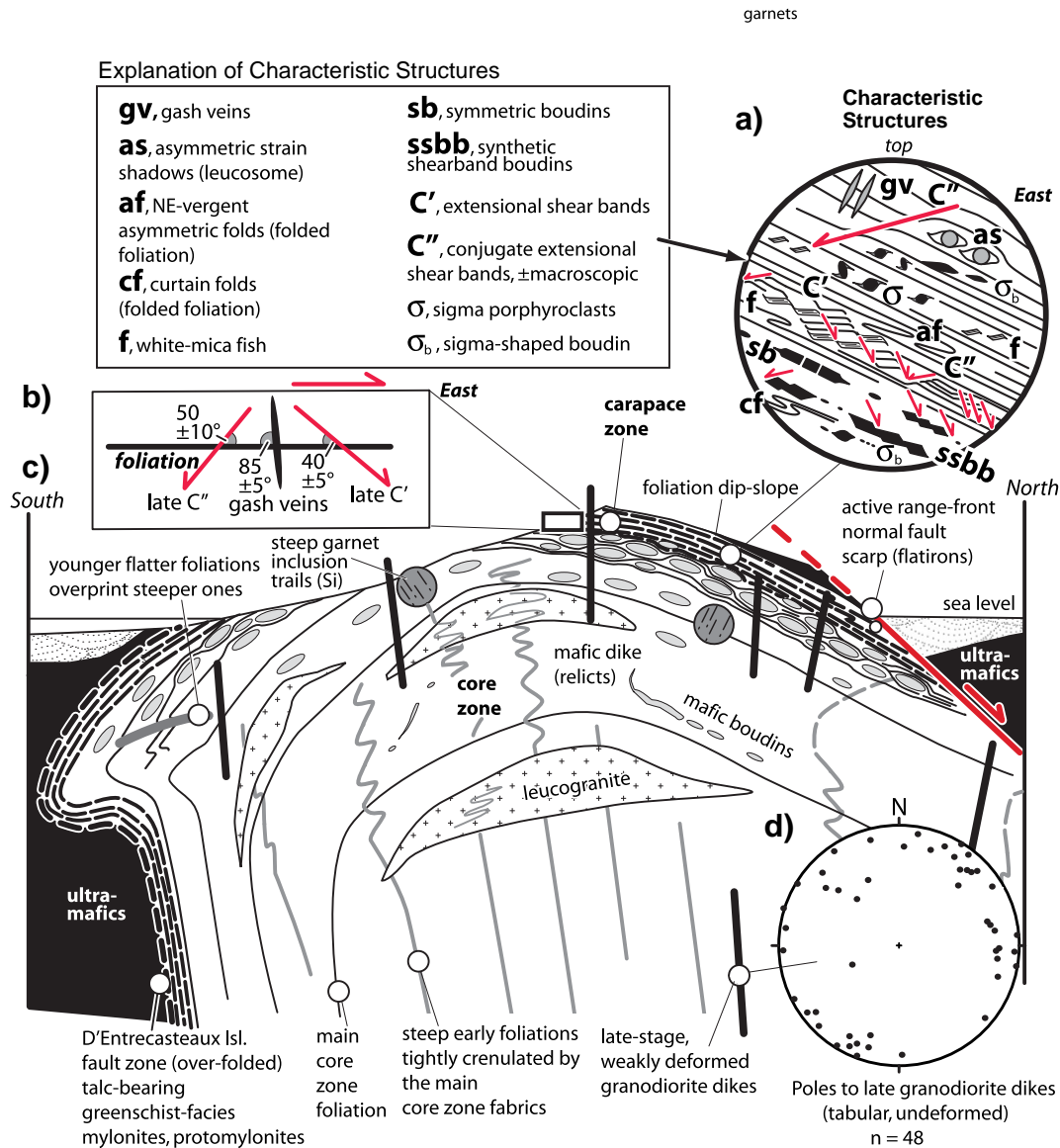


Fig. 14. Representative structural features of the D'Entrecasteaux Islands gneiss domes: a) Summary of meso- and micro-scale structures found in the carapace zone of the domes (the statistically dominant sense of shear is top-to-the-East. Abbreviations are explained in the adjacent key); b) Summary of measured orientations of extensional shear bands and extension gashes (as seen in lineation-parallel section perpendicular to the dominant foliation); c) cartoon cross-section showing key fabric relationships in the domes; and d) lower-hemisphere equal area projection of poles to late-stage, undeformed granodiorite dikes.

(Fig. 13b, c, and d) or occur in conjugate sets (Fig. 13e). Steeply dipping, undeformed granodiorite dikes were observed to intrusively crosscut brittle-looking, dm-long shear bands in outcrop, indicating that granitoid magmatism outlasted the latest stages of ductile deformation.

A majority of shear indicators and LPOs measured by EBSD record top-E motion, but there are many reversals in shear-sense to yield a statistically divergent pattern (Fig. 15; Little et al., 2010 and unpub. data). For example, the carapace in a lower part of the Gulawata River contains abundant top-W indicators (mica fish, S/C fabrics), but is flanked above and below by top-E shear fabrics. Such reversals in shear sense occur on the scale of a few tens to hundreds of meters. We infer that the local sense of the shear was controlled in part by the attitude of relatively stiff units, with shearing being localized along the margins of lenticular bodies. In rocks that have conjugate extensional shear (C') bands, reversals in shear sense occur on the scale of millimeters. Except for late-stage brittle structures (see below), the statistically dominant shear sense is everywhere top-E, even on the W and SW flanks of the domes. In other words, the sense

of shear is not top-towards-the center of each dome, nor does it obviously reverse across the dome crests. The regional top-E pattern supports our previously stated interpretation that the dominant fabric largely predates dome growth, rather than being related to ductile upflow into those structures. We infer that regional ductile flow in the lower crust occurred on a scale larger than any of the individual domes.

The variability of shear sense and the abundance of conjugate extensional shear bands suggest that the flow in the carapace was not completely by simple shear ($W_k = 1$), but that the deformation included an irrotational (pure shear) component causing E–W elongation and ductile thinning of the zone (i.e., it was a thinning-lengthening shear zone in the sense of Tikoff and Fossen, 1999 with a $W_k < 1$). Information regarding the kinematic-vorticity number of the flow comes from: 1) apparent back-rotation of mantled porphyroclasts in the carapace; 2) obliquity of late, incremental extension gashes to the foliation in the carapace; and 3) dihedral angles of the synthetic (C') and antithetic (C'') shear bands. All estimates are based on an assumption of steady-state deformation.

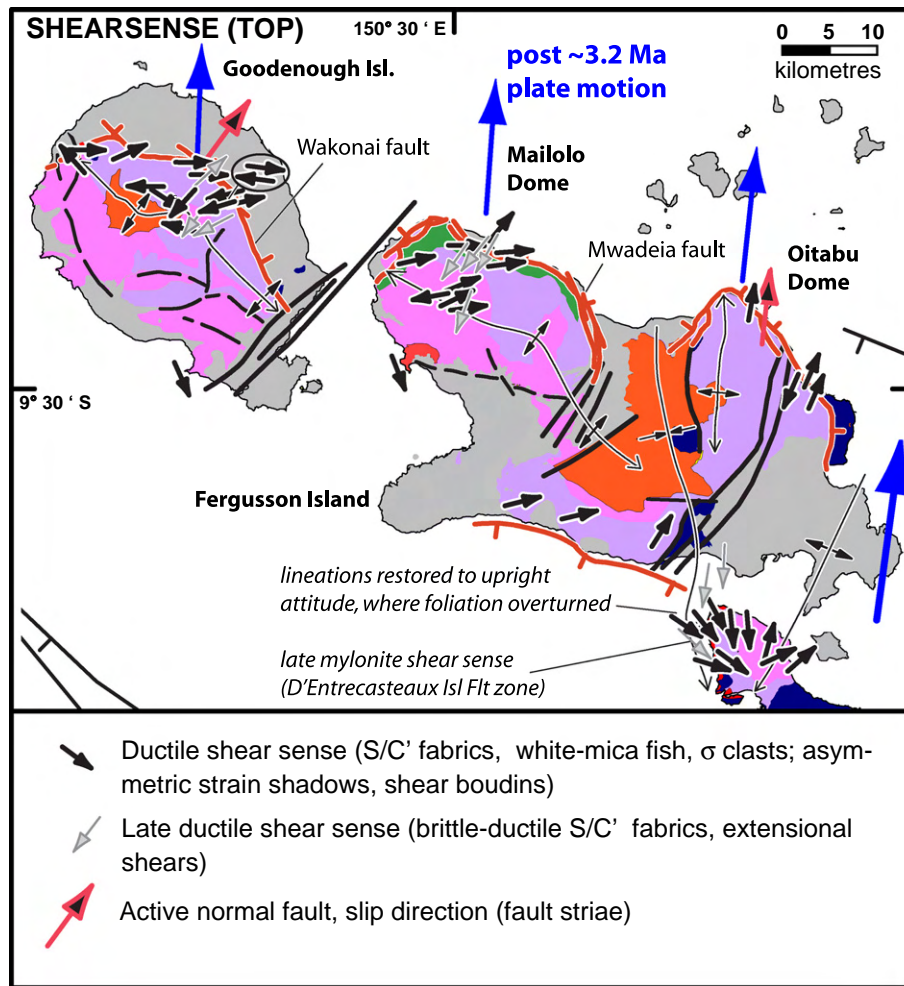


Fig. 15. Map of ductile shear-sense directions based on outcrop and microstructural observations. See key for explanation of symbols.

Large (up to 3 cm diameter) garnet porphyroclasts occur in the carapace of the Goodenough Island dome in a large outcrop in the lowermost Gulawata River gorge, where the local sense of shear is top-to-the east (Fig. 12b and d). The garnets are mantled by strain shadows of deformed quartzofeldspathic leucosomes. Of the 28 coarse garnets that we observed, 24 have tails that define a symmetrical, in-plane geometry. These have aspect ratios between 1.0 and 1.5 and span a $\sim 180^\circ$ range of axial orientations with respect to the foliation (Fig. 16). Four garnets with aspect ratios > 1.4 have asymmetric, stair-stepping tails consistent with top-E shear. Of these σ -type grains, three have an apparently “forward-rotated” geometry (Fig. 12d), but one is “back-inclined” at $\sim 35^\circ$ to the foliation (Fig. 12e). This last garnet is the most elongate (aspect ratio of ~ 1.6), a relationship that suggests that it (alone of the ones we observed) may have reached a stable position in the flow. If so, both the minimum axial ratio technique of Passchier (1987) and the porphyroclast hyperbolic distribution method (Forte and Bailey, 2007; Simpson and De Paor, 1993) yield a kinematic-vorticity number (W_k) estimate of ~ 0.4 . This is at best a crude estimate because of the mostly near-equant grain shapes, the small sample size (only one, more-elongate back-rotated grain), and because the outcrop plane was not exactly parallel to lineation; it is, however, robust evidence for $W_k < 1$ (i.e., sub-simple shear deformation).

In the carapace of both the Mailolo and Oitabu domes, further evidence for $W_k < 1$ includes the large dihedral angle between weakly deformed, late, incremental quartz-phengite gash veins and the foliation (Figs. 12c, 14b). In both locations, the veins intersect the foliation exactly orthogonal to the dominant stretching lineation,

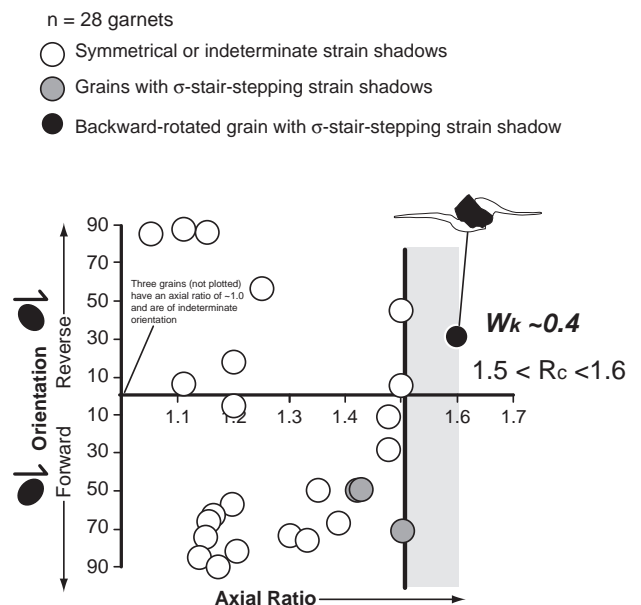


Fig. 16. Geometry of porphyroclastic garnet grains from the lower Gulawata River gorge, NE Goodenough Island (carapace zone). a) Graph of axial ratio (plotted on horizontal axis) vs. axial orientation (relative to foliation, plotted on vertical axis) of 26 garnet grains with attached strain shadow tails. Solid dot refers to the back-rotated σ -type grain depicted in Fig. 13e, and from which the minimum axial ratio technique of Passchier (1986) can be used to infer a sectional kinematic vorticity number, W_k , of ~ 0.4 .

suggesting that these structures are cogenetic. If the veins are taken as a recorder of the minimum instantaneous stretching direction (ISA), the observed $85 \pm 5^\circ$ obliquity (average of 11 vein–foliation pairs at three outcrops) between the veins and the foliation indicates top-NE shearing in agreement with other microstructures. Assuming plane strain, our dihedral angle measurements imply a W_k of ~ 0.17 (minimum 0, maximum 0.34) (e.g., Tikoff and Fossen, 1995).

Analysis of the dihedral angles between the synthetic and antithetic shear bands can yield another estimate for kinematic vorticity number (e.g., Kurz and Northrup, 2008). Grasmann et al. (2003) numerically modeled extensional shear bands as a type of flanking structure in 2D flows of varying kinematic vorticity number, and concluded that conjugate shear bands form in pure shear dominated flows with $W_k < 0.6$, and that these structures will rotate as a function of increasing finite deformation. At the outcrop scale in the carapace zones of the gneiss domes, throughgoing (dm-long) synthetic (C') shear bands intersect the foliation at a mean angle of $40 \pm 5^\circ$ (average of 12 measurements at 4 sites, 1σ); this is an unusually high angle for C' structures in ductile shear zones, which are more typically inclined at $\sim 25^\circ$ (e.g., Blenkinsop and Treloar, 1995). At the thin-section scale, synthetic (C') shear bands typically cut the foliation at a smaller mean angle (average of $28^\circ \pm 10^\circ$ for 90 measurements at 24 sites), but make a similar maximum angle of $\sim 45^\circ$ (e.g., Fig. 13b, c). Outcrop-scale (dm-long) antithetic (C'') shear bands intersect the foliation at an angle of $50 \pm 10^\circ$ to the foliation ($n = 14$ at 6 sites), dipping the opposite direction to the synthetic ones, and cut relatively stiff units with dm offsets (Fig. 12c). Thin-section scale antithetic (C'') shears cut the foliation at a mean angle of $32 \pm 9^\circ$ ($n = 29$ at 9 sites); but make a similar maximum angle of $\sim 50^\circ$ (Figs. 13c, d). The deflection of the dominant, amphibolite-facies foliation across the extensional shear bands, and the locally brittle character of their offsets (especially the dm-long, outcrop scale shears) indicates that the higher-angle shears (both synthetic and antithetic) were active at a late stage of the exhumation. We interpret highest-angle shears to preserve an attitude similar to that at which the shear bands nucleated, whereas the other shears (most obvious in thin-section) have rotated to lower angles as a result of finite deformation (Fig. 14a, b). The highest-angle synthetic (C') and antithetic (C'') shear bands are orthogonal to one another (dihedral angle of $90 \pm 10^\circ$), with the synthetic C' bands making a $\sim 10^\circ$ smaller acute angle to the foliation than do the C'' bands (Fig. 14b).

If conjugate shear bands form parallel to planes of maximum instantaneous shear-strain rate, then they are predicted to nucleate in orthogonal sets, with their bisectors coinciding with eigenvectors of the flow, with the angle between these eigenvectors being a function of the kinematic vorticity number (Bobyarchick, 1986; Kurz and Northrup, 2008; Simpson and De Paor, 1993). Others view conjugate ductile shear bands as initiating at a fixed $90\text{--}110^\circ$ angle to the contractional ISA axis (Carreras et al., 2010; Mancktelow, 2002; Zheng et al., 2004; Zheng et al., 2009). Either way, with reference to the D'Entrecasteaux gneiss domes, a W_k value of 0.17 ± 0.17 is calculated from the observed shear attitudes. This estimate assumes that the shears are late-stage structures that have not rotated relative to the foliation as a result of finite deformation. We note that this estimate agrees with our previously stated W_k estimate based on the late-incremental gash vein orientations (which also makes this assumption).

7.2. Estimate of foliation-orthogonal ductile thinning

We derived a minimum estimate of finite ductile thinning perpendicular to the dominant foliation from an analysis of boudins in the carapace of the Mailolo Dome in the Waia River (Fig. 4). At this site numerous foliation-parallel (i.e., sill-like) granodiorite dikes, up to 15 cm thick, have been boudinaged (Fig. 7c). Many boudins are symmetric torn boudins (Fig. 9d, f) (nomenclature of Goscombe et al.,

2004). Other asymmetric–dilatational boudins are bounded by shears at $50\text{--}75^\circ$ to the foliation (Fig. 9e). As is consistent with the calculated low kinematic vorticity number, these shears have slipped in both a synthetic and antithetic sense relative to the dominant top-NE shear sense indicated by σ -shaped deformed boudins (Fig. 9d-ii) and synthetic (C') shear bands outside the boudins (Fig. 7c). Using photomosaics, we undertook a graphical reconstruction (after Ferguson, 1981) to restore each granodiorite boudin (assumed rigid) into contact with its neighbors along ten different layer-parallel transects. From this analysis, we calculated a mean foliation-parallel apparent stretch, $(1 + e)$, of 2.2 ± 0.5 . This apparent stretch was then used to calculate a bulk layer-parallel stretch value using the analog- and numerical modeling-based technique of Mandal et al. (2007), assuming pure shear. We regard our foliation-parallel bulk finite stretch calculation, 3.6 ± 0.75 , to be a minimum estimate because the boudins were not rigid and the analysis only considers deformation post-dating intrusion of the sills. The stretch value, if representative at a crustal scale, implies a corresponding vertical contractile stretch (thinning factor) of ~ 0.3 , implying that perhaps a third of the exhumation of the eclogites may have been a result of ductile thinning. Because relict coesite has so far been confirmed at only one locality in the D'Entrecasteaux Islands (Baldwin et al., 2008), and some or all of the other eclogites may also have experienced UHP conditions, we currently cannot recognize a spatial boundary between HP and UHP eclogitic rocks (if indeed one exists); thus it is unknown to what extent this crustal thinning may have brought original UHP rocks into proximity with any higher level HP rocks.

8. Doming and late-stage deformation

The shedding of metamorphic-derived conglomerate into the offshore region to the north of Goodenough Island indicates that domes had become emergent by ~ 3 Ma (Davies and Warren, 1988; Francis et al., 1987; Tjhin, 1976). The growth of the domes resulted in folding of the regionally developed foliation, lineation, and shear fabrics. On the NW flanks of the domes, rotation of the lineations about the discordant, WNW–ENE trending crests of the domes resulted in deflection of the generally E-plunging lineations to local W or SW plunges. The dominant shear sense of the ductile fabrics is top-E on all flanks of all the domes (Fig. 15). These relationships suggest that the doming caused upwarping of a pre-existing amphibolite-facies fabric that was widespread and subhorizontal.

A marked rotation of the dominant lineation and foliation around dome-defining fold structures provides further evidence that the dominant fabric developed prior to amplification of the mainly ESE-trending gneiss domes. Along the south-central coast of Fergusson Island, the foliation is deflected anticlockwise to N–S strikes inside the SSE-plunging synform that lies between Oitabu and Mailolo domes (Fig. 10a, e), and the lineation becomes north-trending (Fig. 11a, e). Farther east, the lineation wraps around the SSW-plunging hinge of the NW Normanby dome to resume its original E–W trend (Figs. 10a, 11a). In addition to such first-order (dome-scale) folds of the older LS-tectonite fabric, we identify an almost radial pattern of smaller, second-order folds of the foliation that plunge away from the crest-lines of the main domes at a high angle (Fig. 4). These may have formed as a result of a constriction of the foliation during upward doming.

The doming predated intrusion of the latest, undeformed felsic dikes, as these steep dikes cut an already domed foliation. In most outcrops in Goodenough, Mailolo, and Oitabu domes, the youngest granodiorite dikes are tabular, steeply dipping, and undeformed. The dikes dip steeply regardless of the dip of the host-rock foliation, but strike in all directions (Fig. 14d). On NW Normanby Dome, a swarm of 1–3 m thick basaltic–andesitic dikes with chilled margins intrude leucocratic orthogneiss in the core and carapace of that NNE-elongate structure. The undeformed dikes dip steeply NNE or SSW despite large

variations in the attitude of the gneissic foliation wrapping around the SSW-plunging NW Normanby structure (Fig. 12a, e). One of these basaltic-andesitic dikes yielded a whole-rock $^{40}\text{Ar}/^{39}\text{Ar}$ total-fusion age of ~ 1.8 Ma (Baldwin et al., 1993). A late-stage, vertical dike on the SW flank of Goodenough Island dome yielded an ion-probe U-Pb age on zircon of ~ 1.98 Ma (S. Baldwin, unpub. data). From these data, and the 1.98 ± 0.08 Ma U-Pb zircon age of the Omara granodiorite (Baldwin and Ireland, 1995), we infer that the doming was complete by 1.8–2.0 Ma.

During the doming, the lower plate (U)HP terrane was emplaced into its current high-level position against the low-grade, ophiolitic upper plate. If any greenschist–blueschist facies rocks were originally present beneath the ophiolite, similar to those cropping out today to the east in the Prevost Range of SE Normanby Island (Little et al., 2007), they were apparently excised before or as a result of this emplacement. The rising UHP gneissic terrane may have impinged against the upper plate as a result of the density contrast between the still hot, migmatitic gneisses and the overlying, cooler ultramafic rocks. This upper plate may have been relatively strong, forming a mechanical lid. Extension (necking) of that dense lid may have caused a local isostatic reduction in vertical normal stress, thus driving final ascent of the domes into that extended region. Rather than deforming ductilely, the lid may have been largely pushed out of the way, pervasively faulting and detaching along its sole in response to the rising of hot (U)HP rocks beneath it.

Final doming was associated with development of the greenschist–facies mylonitic fabrics along the D'Entrecasteaux Islands fault zone, and the localized downward penetration of late-stage (greenschist–facies, strongly grain-size reduced) shear zones into the carapace rocks. Ductile dome emplacement was followed by rapid cooling, resulting in quenching of the high-temperature microstructures in the gneisses (e.g., amoeboid and chessboard structures in quartz). On the south coast of Fergusson Island, some $^{40}\text{Ar}/^{39}\text{Ar}$ ages on white mica are as old as ~ 4 –3 Ma (S. Baldwin, unpub. data). Farther west on Goodenough Island, $^{40}\text{Ar}/^{39}\text{Ar}$ cooling ages on white mica and biotite are both in the range of 2–1.5 Ma (Baldwin et al., 1993; Waggoner et al., 2008). This age westward progression matches the propagation direction of the Woodlark spreading ridge. By 1.5–0.5 and 1.8–0.3 Ma, these two gneiss domes had cooled at shallow levels of the upper crust as indicated by fission-track ages and (U-Th)/He ages in apatite, respectively – ages that again display westwardly younging spatial trends (Fitzgerald et al., 2008).

Woodlark–Australia plate motions for the period 3.2 Ma to ~ 0.5 Ma were north–northeastward (Goodliffe et al., 1997; Taylor et al., 1999) (Fig. 11a). The discordance between this direction and stretching lineations in the gneisses records a decoupling between the rift motions and the gravity-driven flow that took place in the (U)HP terrane. Following rapid cooling, however, the gneiss domes were no longer able to flow and were mechanically incorporated into the upper crust of the Woodlark rift. Progressive anticlockwise deflection of late-stage extension direction indicators away from the E–W trend of the older ductile stretching lineation direction, and towards the N–S direction of the Woodlark–Australia plate motion record this transition. Structures indicative of late-stage extension directions include (summarized in Table 1): 1) fault-like or brittle extensional faults or shear bands that cut and offset the dominant foliation on Goodenough and Mailolo dome (mostly top-to-the-SSW, Fig. 11a, b, and c); 2) brittle–ductile object lineations, defined by brittle elongation of feldspar grains or aggregates (NE-trending while discordantly overprinting the dominant E–W trending stretching lineation in the carapace of NE Goodenough Island, Fig. 11a, b); 3) the attitude of the intermediate–mafic dike swarm on NW Normanby Island (pole trends 049° , plunging 15° N), 4) slip on associated SW-dipping normal faults (Fig. 11a, e); and 5) slip striae on the major active normal faults bounding the north flanks of Goodenough and Oitabu dome (NE to NNE trending, subparallel to Pliocene plate-

motion direction, Fig. 11a, b, and d). In summary, the indicators of late-stage, ductile–brittle extension suggest anticlockwise rotation of the crustal extension direction towards the coeval plate motion. As the gneisses cooled, solidified and became mechanically incorporated into the strong upper crust, their deformation was increasingly coupled to inter-plate tractions.

9. Discussion

9.1. (U)HP exhumation path, part I: rapid ascent from mantle to lower crust

Geochronological and thermobarometric data (Baldwin et al., 2004, 2008; Davies and Warren, 1992; Hill and Baldwin, 1993) indicate that the coesite-bearing eclogites ascended from mantle depths to the lower crust in ~ 3 m.y., whereas the HP eclogites reached that level in < 1 –2 m.y. (Fig. 17). The data require a rapid, near-isothermal ascent at ≥ 20 –30 mm/yr. At the UHP locality on SW Mailolo dome, thermobarometric data and U-Pb ages of zircon indicate that the rocks were at > 90 km depths at ~ 7 –8 Ma, whereas retrogressive amphibolite-facies metamorphism took place in the lower crust at ~ 4 –5 Ma followed by pegmatite intrusion at ~ 3.4 Ma (Baldwin et al., 2008; Gordon et al., 2009, 2010; Monteleone et al., 2007). Thermobarometry and U-Pb ages on zircon indicate that other eclogites (lacking preserved coesite) resided at > 60 km depth at ~ 4 –2 Ma, and that they were intruded by deformed granodiorites at 2.1–1.7 Ma (Baldwin et al., 2004; Baldwin et al., 2008; Baldwin

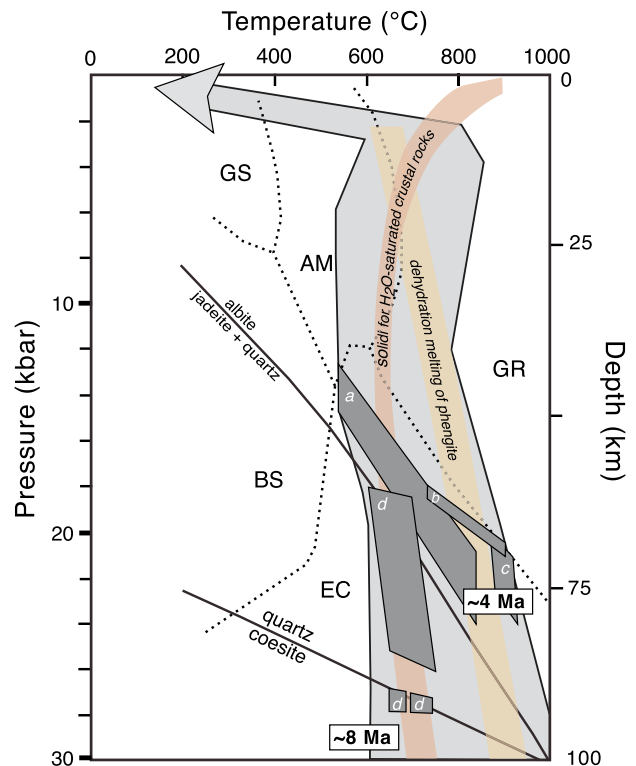


Fig. 17. Summary of thermobarometry for D'Entrecasteaux eclogites. a) P-T conditions for eclogites; Davis and Warren, 1988; b) P-T conditions for retrogressed core zone gneisses; Hill and Baldwin, 1993; c) P-T conditions for retrogressed eclogite; Baldwin et al., 2004; d) thermobarometry for coesite eclogite; Baldwin et al., 2008. Exhumation path based on compilation of P-T data for eclogites, carapace zone gneisses, and retrogressed core zone gneisses after Hill and Baldwin 1993. U-Pb zircon ages on eclogites from the Mailolo dome of Fergusson Island indicated (Baldwin et al., 2004; Monteleone et al., 2007). Note that a single P-T-t-D path is not implied for the compiled data. Abbreviations for metamorphic facies are blueschist (BS), greenschist (GS), amphibolite (AM), eclogite (EC), granulite (GR). Solidus for water-saturated crustal rocks and dehydration melting of phengite after Hacker, 2006.

and Ireland, 1995; Gordon et al., 2009; Monteleone et al., 2007). Although the pattern is complex in detail and variable along strike, most $^{40}\text{Ar}/^{39}\text{Ar}$ cooling ages fall in range of 3–2 Ma (hornblende), 3.5–1.5 Ma (white mica), and 1.7–1.5 Ma (biotite) (Baldwin et al., 1993). By 1.5 (Fitzgerald et al., 2008) Ma the rocks were exhumed to shallow crustal levels to accumulate (U-Th)/He and fission-track ages on apatite (that is, to temperatures of $<120^\circ$ and $<80^\circ$ C, respectively).

We infer that structural processes accomplishing this initial rapid ascent of the eclogites through mantle depths are largely not recorded in the rock structures because of later amphibolite-facies retrogression and overprinting (at temperatures of $\geq 570^\circ$ C and pressures of 7–11 kb, Baldwin et al., 2004; Davies and Warren, 1988; Davies and Warren, 1992; Hill and Baldwin, 1993). The oldest recognized fabric in the gneiss domes is a foliation, locally preserved in their cores, that is younger than the eclogite-facies metamorphism, and associated with migmatization. Boudins preserving eclogite-facies minerals are now separated by up to tens of meters, implying large finite deformation subsequent to the (U)HP metamorphism, and their strain shadows are filled with leucosome, implying anatexis during their deformation. The oldest preserved foliation was later folded (transposed) about one or more younger, and more shallow-dipping (but still amphibolite-facies) fabrics. Warping of the dominant foliation occurred during formation of the gneiss domes.

Whereas Hill (1994) suggested that the eclogites were exhumed from mantle depths as a result of progressive slip on a deeply penetrating fault and related shear zones, our data does not support such a detachment model. Large-magnitude slip on a detachment fault should be expressed by a gradient in exhumation level parallel to the slip direction, with deeper levels (higher-grade rocks) exposed nearest the breakaway (in Hill's model these were located along the north flanks of the domes). We find no evidence for such an asymmetric metamorphic-field gradient in the lower plate gneisses. Eclogite-facies mineral assemblages (or related symplectites) are preserved in mafic blocks at all structural levels in the lower plates of all the domes, as is migmatitic leucosome. In other words, no "eclogite-in" or "melt-in" isograds are present. Instead, the gneiss domes are approximately symmetrical (albeit now slightly back-tilted) structures with both flanks mantled by a high-strain carapace and erosional remnants of a once extensive, ophiolitic upper plate. Microstructures and field observations indicate an inward increase in deformational temperature and melt and pluton percentage towards the core of the domes. In addition, the detachment-fault model would require slip-rates well in excess of the plate velocity to accomplish exhumation at ~ 2 cm/yr rates (e.g., a >4 cm/yr slip-rate would be required on a normal fault dipping 30°). Stretching lineations in the gneisses are approximately orthogonal to the plate motion direction, rather than parallel, as would be expected in a case of prolonged simple shearing along a plate-boundary. Finally, such a detachment-related exhumation process, especially along a low-angle fault, is predicted to yield significant cooling of the footwall due to conductive loss of heat into the hangingwall (e.g., Fayon et al., 2004). This prediction is incompatible with the early, near-isothermal decompression history that has been documented for the (U)HP terrane (Baldwin et al., 2008).

The above observations support a model in which the largely quartzofeldspathic, eclogite-bearing terrane ascended rapidly through mantle depths as one or more diapirs. The diapirs consisted of partially molten continental crust and were significantly less dense than the surrounding mantle. Anatexis of the gneisses was likely the result of dehydration-melting during the near-isothermal decompression (e.g., Whitney et al., 2004). This melting timeframe contrasts with an earlier model in which rifting-related asthenospheric upwelling is suggested to have first led to magmatic underplating of basaltic rocks at the base of the crust, then to partial melting of the overlying continental crust, and finally to (still later)

pulses of crustal extension and core-complex formation (Hill et al., 1992, 1995).

9.2. (U)HP exhumation path, part II: ductile flow and thinning in the lower crust

After exhumation from mantle depths, the hot, low viscosity bodies may have stalled in their ascent path at the base of the continental crust (e.g., Walsh and Hacker, 2004), which may thicken to depths of circa 40 km (based on metamorphic pressures of ~ 11 kb, Hill and Baldwin, 1993; Baldwin et al., 2004). Here they were completely overprinted by flat-lying dominant foliation, pervasively retrogressed in the amphibolite-facies, and subject to further anatexis and granodiorite intrusion. Microstructures in the core zone rocks confirm that high-temperature ($>650^\circ$ C) deformation (e.g., chessboard subgrain-structure in quartz) took place in the presence of a melt phase (leucosomes). Gravitationally-driven, outward spreading of the ponded body of hot, weak (U)HP crust accommodated vertical shortening and E–W subhorizontal extension sub-parallel to the rift margin. The flow was mechanically decoupled from the N–S Woodlark Rift plate motion. The bulk ductile deformation included significant irrotational, pure-shear thinning. This was accommodated by motion on bivergent shear zones at many scales, including conjugate extensional shear bands, and is supported by our W_k estimates of ~ 0.2 in the carapace. If the crust was ~ 40 km thick (consistent with thermobarometric estimates for the amphibolite-facies metamorphism of up to ~ 11 kb, and thicker than the current ~ 35 km crustal thickness beneath the Papuan Peninsula), then our boudin-based minimum thinning factor ($1 + e$) estimate of ~ 0.3 suggests that >25 km of exhumation of the (U)HP terrane may have been the result of pervasive ductile thinning within that crust during its lateral outflow, and that the crust may have continued to be underplated from below as it thinned.

The highest-strain solid-state deformation fabrics were imprinted into the carapace rocks during top-E flow. This polarity records a westward underflow of the eclogite-bearing crust parallel to the rift axis. Perhaps heterogeneous extension during rifting led to rift-parallel gradient in upper plate thickness and therefore, lithostatic pressure. For example, a locally reduced thickness of the high-density Papuan Ultramafic Body (PUB) in a stretched corridor ahead of the Woodlark spreading center, might have focused any rising diapirs to flow towards that extensional neck (e.g., Tirel et al., 2008). In apparent agreement with our observed flow direction, axial underflow of ductile lower crust away from the tip of a spreading center, and toward the adjacent continental rift has been predicted by geodynamic models of rift propagators (Van Wijk and Blackman, 2005). We note, however, that at the time of their ductile deformation, the D'Entrecasteaux Islands were located >300 km to the west of the Woodlark spreading ridge (Taylor et al., 1999). As an alternative explanation for the regional top-E shear sense, perhaps the NE dipping Papuan Ultramafic Body (Davies, 1980a; Davies and Jaques, 1984) upwardly confined any diapirs impacting against that upper crustal lid to flow up dip of its basal contact.

In detail, the ductile-stretching direction deflects from E–W trends at higher levels to NW–SE at greater depth. Such depth-dependent (or at least spatially variable) changes in stretching lineation trend also characterize other migmatitic gneiss domes, for example in the Kigluaik Mountains, Alaska (Amato and Miller, 2004; Calvert et al., 1999; Miller et al., 1992); the Nigde Massif, Central Anatolia, Turkey (Gautier et al., 2008; Whitney and Dilek, 1997a, b); and the Naxos migmatite dome in Greece (Kruckenberg et al., 2011). Such deflections have been interpreted as recording an along-strike inflow of a weak lower crust in isostatic compensation for localized extension in the upper crust (Amato and Miller, 2004; Gautier et al., 2008). In the Woodlark rift, a rift-parallel inward flow of crust might provide an explanation to the riddle of why subsidence- and crustal thickness-

based estimates of crustal extension across the Woodlark rift (Kington and Goodliffe, 2008) fall ~50% short of thinning predictions based on seafloor spreading-derived plate motions.

9.3. (U)HP exhumation path, part III: gneiss dome formation and final exposure

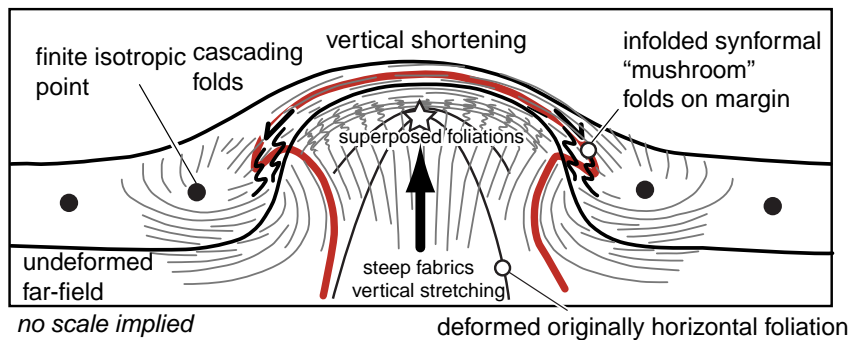
The geochronological and structural data indicate that any stalling of the (U)HP terrane in the lower crust was temporary, and that the gneiss domes were later emplaced into the upper crust. The final stage of ascent of the (U)HP terrane resulted in its juxtaposition against the ophiolitic rocks of the upper plate along the D'Entrecasteaux Islands fault zone. The uniformly eclogite-facies grade of the lower plate rocks indicates that their final emplacement against the weakly metamorphosed upper plate nappe was accommodated by the removal (or penetration through) any originally intervening lower grade rocks. Gneiss dome emplacement was probably accompanied by slip on the retrogressive, greenschist-facies mylonitic shear zones that border the D'Entrecasteaux Islands fault zone. Dome uplift was apparently complete before the youngest dikes were intruded at ~1.8 Ma. A narrow range in $^{40}\text{Ar}/^{39}\text{Ar}$ ages of white mica and biotite and other low temperature thermochronometers records rapid cooling of the gneisses subsequent to the doming. We infer that the rapid cooling caused a quenching of high-temperature microstructures in the gneisses, and was a prerequisite to transmission of N–S Woodlark Rift tensional stresses into the rocks.

Diverse processes can lead to gneiss doming, including diapirism (Rayleigh–Taylor instabilities) and isostatic unloading related to normal faulting or erosion (Beaumont et al., 2001; Burg et al., 2004; Lee et al., 2004; Teyssier and Whitney, 2002; Tirel et al., 2008; Whitney et al., 2004; Zeitler et al., 2001). In the case of migmatitic gneiss domes,

magmatism and partial melting are inferred to be key agents of crustal weakening and buoyancy contributing to their uplift (Bittner and Schmeling, 1995; Siddoway et al., 2004; Teyssier and Whitney, 2002; Vanderhaeghe, 2004). Detachment-bounded gneiss domes are also called metamorphic core complexes (MCCs) (Yin, 2004). MCCs typically record peak pressures of <12 kb, presumably because their detachments sole into the middle crust (Wernicke, 1992). By contrast, thermobarometric studies indicate a much deeper origin for the lower plates of the D'Entrecasteaux Islands gneiss domes, where the eclogitic gneisses reached peak temperatures of 650–900 °C and pressures of ≥ 27 kb (UHP rocks) or ≥ 14 kb (HP rocks); and this was followed by near isothermal decompression to 7–11 kb (~25–40 km); where the rocks were retrogressed in the amphibolite facies (Baldwin et al., 2004; Baldwin et al., 2008; Davies and Warren, 1988; Davies and Warren, 1992; Hill and Baldwin, 1993; Monteleone et al., 2007)

The features of the D'Entrecasteaux gneiss domes (Fig. 18a) that resemble analog and numerical models of diapirs (Burg et al., 2004; Cruden, 1988, 1990; Dixon, 1975; Jackson and Talbot, 1989; Ramberg, 1972, 1981; Talbot and Jackson, 1987) include: 1) the inward increase in structural depth towards the dome cores; 2) the overturned, “mushroom-like” shape of folds marginal to the NW Normanby dome (in diapirs this reflects an outward flow of rocks away from its rising central stem followed by an inward return flow); 3) the ~30 km spacing between the gneiss domes, consistent with Raleigh–Taylor instabilities (these may have had a characteristic wavelength related to thickness and/or viscosity of the rising crustal mass and/or the crustal layers it penetrated); 4) the variation in the finite stretching directions within the domes, implying a 3D flow; 5) the abrupt upward transition from ~50° outward-dipping foliations on both dome flanks to flat-lying foliations at the dome crest; 6) the local superposition of gently dipping, late-stage crenulation foliations

a) Diapir



b) Symmetrical (Pure Shear) Gneiss Dome

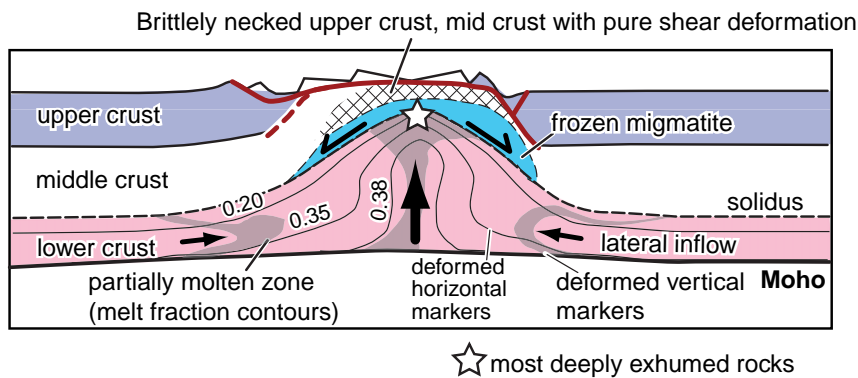


Fig. 18. Cartoons illustrating characteristic structures of a) diapirs (after Dixon, 1975; Burg et al., 2004) and b) symmetrical gneiss domes (after Gessner et al., 2007; Rey et al., 2009). Note that a classical diapir may rise in response to buoyancy forces only, whereas migmatitic gneiss domes are commonly thought to respond to both buoyancy and isostatic forces. Modeling of the latter (e.g., Rey et al., 2009) suggests that symmetrical, pure shear-dominant gneiss domes will be most likely to form where extensional strain-rates are high, in which case partial melt zones may be advected upward and freeze to form migmatitic gneisses.

across older foliations on the dome flanks (in diapirs such overprinting results from steep fabrics being advected into the zone of vertical shortening near the diapir's head); 7) the radial pattern of outwardly plunging, secondary folds around the Goodenough and Mailolo domes, and 8) an approximately radial strike distribution of late-stage, undeformed, and steep granodiorite dikes. Some features commonly attributed to diapirs that are not present in the D'Entrecasteaux Islands domes are radial stretching lineations, oblate finite strains near the top of the dome; and cascading folds that verge circumferentially away from dome centers. In fact, many gneiss domes lack such radial structures, presumably because they were emplaced into actively deforming zones (e.g., [Teyssier et al., 2005](#); [Vanderhaeghe, 2004](#); [Whitney et al., 2004](#)). For example, the well-exposed migmatitic gneiss dome on Naxos, Greece shares several key features with the D'Entrecasteaux domes. These include strongly deformed outer carapace zone with solid-state, LS-tectonite fabrics; syn-deformational partial melting, local overturning of foliations on the dome flanks (i.e., mushroom-like folds); tight "pinched synclines" that intervene between much broader antiformal culminations; lineation attitudes that vary in 3D within individual domes; and the mechanical uncoupling of the rising gneiss in the domes (or sub-domes) from the surrounding regional tectonic framework ([Kruckenberg et al., 2011](#)).

Whereas the active normal faults that bound the northern flanks of the Goodenough, Mailolo, and Oitabu domes played a role in exhuming the eclogite-bearing gneisses through the upper crust, these faults cut the dominant ductile fabrics in the domes, and are late, brittle structures. [Hill \(1994\)](#) interpreted the D'Entrecasteaux gneiss domes as metamorphic core complexes bounded by long-lived, north-dipping, ductile-to-brittle shear zones. We have argued against this scenario, but acknowledge that there may be a continuum between gneiss domes that are detachment-related and those which are diapiric – a result of the variable degree to which gravitational forces compete with localized slip on shear zones and normal faults. Geodynamic modeling has shown that a high viscosity (or low melt content) in the lower crust or a high degree of strain softening can lead to the development of asymmetric gneiss domes (metamorphic core complexes) in an extensional setting ([Buck and Lavier, 2001](#); [Gessner et al., 2007](#); [Rey et al., 2009](#); [Tirel et al., 2008](#)). On the other hand, a high melt content (or low viscosity) promotes symmetrical doming, a predominance of pure shear thinning, and diapir-like flow kinematics ([Fig. 18b](#), [Gessner et al., 2007](#); [Rey et al., 2009](#); [Tirel et al., 2008](#)). The D'Entrecasteaux gneiss domes appear to most closely resemble the latter. Moreover, we infer that they contained a large enough melt fraction (e.g., >7%, the Melt Connectivity Transition of [Rosenberg and Handy, 2005](#)) to have greatly reduced their effective viscosity, a rheological situation that would promoted rapid ascent of the domes.

9.4. Possible plate tectonic models

The D'Entrecasteaux Islands eclogite-facies rocks are notable for the short time span between their peak metamorphism and surface exposure (as short as 2–4 Myr). Such brevity implies that there may have been a nearly continuous exhumation process ([Fig. 19](#)). Any successful model must explain not only why the rocks occur in a rift, but also: i) how the HP/UHP rocks were able to reach the surface at cm/yr rates; ii) why peak metamorphism took place in the late Miocene to Pliocene, a time when there was no known subduction (but when the Woodlark rift was active); iii) why this metamorphism, and subsequent cooling, young westward in the propagation direction of the Woodlark spreading ridge; and iv) why (U)HP recrystallization was delayed more than 20 m.y. after the main phase of the Papuan arc-continent collision on the mainland ([Davies, 1990](#); [Davies and Jaques, 1984](#); [Rogerson et al., 1987](#); [Van Ufford and Cloos, 2005](#)). How could the rocks have remained in a subduction channel at UHP depths for 20 to 30 m.y. without being metamorphosed to eclogite facies? During the collision, the Owen–Stanley metamorphic rocks on the mainland were underthrust northward and accreted at relatively

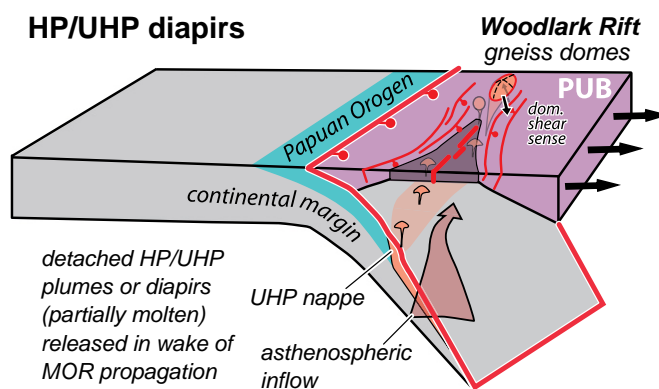


Fig. 19. Cartoon illustrating proposed geodynamical context of the D'Entrecasteaux Islands (U)HP gneiss domes. See text for further discussion.

shallow levels beneath the Papuan Ultramafic Body. Despite being similarly derived from the Australian continental margin, these rocks did not remain metastable, but reacted to form low-grade (blueschist, pumpellyite-actinolite, lower greenschist) mineral assemblages as a result of their attempted subduction in the Paleogene ([Daczko et al., 2009](#)). A key question is what was the metamorphic history experienced by the higher-grade rocks, presumably down-dip of them, that would ultimately form the late Neogene (U)HP rocks in the D'Entrecasteaux region to the north?

Several scenarios can be explored to explain the metamorphic history, and hence tectonic derivation, of rocks that ultimately became these late Neogene (U)HP rocks. One invokes the lodging of a large nappe of Australian Plate-derived continental crust into the subduction channel during the Papuan arc-continent collision, followed by its long-term residence in that channel (since at least the late Oligocene) during which it remained metastable with respect to the ambient eclogite-facies conditions. Woodlark rifting began in the late Miocene, resulting in asthenospheric flow ahead of the west-propagating Woodlark seafloor-spreading ridge, with a possible arrival in the D'Entrecasteaux region soon thereafter. Mantle upwelling may have heated the previously subducted crust, and/or fluxed it with fluids, resulting in crystallization of eclogite-facies assemblages in the late Miocene to Pliocene. Subsequent partial melting of the nappe may have generated one or more diapirs. Once detached from their Australian Plate lithospheric substrate, these diapirs rose through the mantle at cm/yr rates (Phase 1 of the exhumation, above), at which time they underwent decompression melting.

Continental crust subducted to mantle depths can preserve unreacted, pre-subduction mineral assemblages, as demonstrated in the Western Gneiss Region and Bergen Arcs of the Norwegian Caledonides ([Austrheim, 1987](#); [Austrheim and Mørk, 1988](#); [Engvik et al., 2000](#); [Krabbendam et al., 2000](#); [Peterman et al., 2009](#)); the European Alps ([Pennacchioni, 1996](#)) and China ([Zhang and Liou, 1997](#)). However, there are problems with the above scenario. The metastability is most likely if the subducted crust is initially dry, and remains so. For PNG this seems unlikely, because the protoliths, including basaltic rocks and some pelites and marbles, are inferred to consist chiefly of Mesozoic continental margin sediments and volcanic rocks. Moreover, to avoid conductive heating and melting during its long residence, the nappe must have been very large (e.g., >25 km in dimension, based on simple thermal diffusion calculation; see also [Root et al., 2005](#) and [Kylander-Clark et al., 2009](#)). If southward subduction of Solomon Sea lithosphere at the Trobriand trough ([Fig. 3b](#)) during the Miocene was refrigerating the relict Papuan paleo-subduction zone in the upper plate of the Trobriand subduction zone, then it must also be explained why fluids driven off the subducted Solomon Sea lithosphere not drive reaction of the rocks to eclogite-facies assemblages?

Our second and preferred model is similar to the first, but posits that the deeply subducted continental protoliths experienced a polymetamorphic (U)HP history that began with the Papuan arc-continent collision (e.g., like the Western Gneiss Region, [Kylander-Clark et al., 2009](#); [Hacker et al., 2010](#)). We infer that the Paleogene collision and subduction may have caused an early phase of eclogite-facies metamorphism, and that this was followed by long-term residence of one or more nappes in the paleosubduction channel. Finally, the Woodlark rifting and reheating caused widespread Late Neogene (U)HP metamorphic recrystallization in the nappe that strongly overprinted the older (U)HP assemblages. If so, relict high-pressure Paleogene metamorphic mineral assemblages should be present locally, a scenario for which there now emerging evidence ([Zirakparvar et al., 2009](#), and manuscript in review).

A third, albeit more speculative model acknowledges that [Cloos et al. \(2005\)](#) have argued for break-off of subducting Australian oceanic lithosphere beneath the central Highlands of PNG, at ~8 Ma, followed by upwelling of asthenosphere into that lithospheric rupture ([Fig. 1d](#)). This event approximately coincides with the timing of UHP crystallization on Fergusson Island. Could an adjoining segment of Australian Plate lithosphere ~300 km to the east (in the area of the present-day D'Entrecasteaux Islands) have similarly been broken off or otherwise removed at about this same time? If so, the descending lithosphere could have included an adhering body of Australian Plate-derived continental crust that was temporarily dragged down into the mantle before detaching itself from its oceanic lithosphere substrate and rising diapirically (i.e., hybrid of the models in [Fig. 1c](#) and [d](#)). Recent geodynamic modeling of convective removal of mantle lithosphere indicates that entrainment of continental crust with convectively removed mantle is at least possible ([Stern et al., 2010](#)). One boundary condition favoring this is a vertical discontinuity across which there is an abrupt lithospheric thickness contrast (relative lithospheric thinning of >30% on one side). As a result, shallow asthenospheric mantle is laterally juxtaposed against lithospheric upper mantle ([Stern et al., 2010](#), and manuscript in preparation). Such an unstable edge discontinuity conceivably may have existed on the flanks of the Woodlark Rift in the late Neogene, where it abutted against the orogenic lithosphere of the pre-existing Papuan Orogenic belt. A low viscosity lower crust is also required (as we have argued existed in the Woodlark Basin). Although this model is quite speculative, it cannot yet be ruled out. The model would not require prolonged residence of the UHP protoliths in the Papuan paleo-subduction zone; it predicts very young UHP crystallization followed immediately by exhumation; it could explain the large crustal omission across the D'Entrecasteaux fault zone (convective removal of crust?); and it might help to explain why the Woodlark rift contains migmatitic UHP-bearing gneiss domes and extrudes peralkaline (and K-rich) volcanics.

Finally we note that extrusion wedge and other fault-dominated exhumation models for UHP exhumation ([Fig. 1a, b](#)) provide a poor fit to the Papua New Guinean (PNG) eclogite terrane. Firstly, exhumation of the PNG rocks was not synchronous with collision or convergence; second, the exhumed bodies were pervasively deformed rather than rigid; and third, there is no record of any unidirectional or up-dip shearing on the margins of the UHP body. For similar reasons, large-scale slab eduction or subduction reversal models ([Fig. 2a](#)) do not fit the data well. Instead, we infer that some variant of the deformed UHP diapir model, including a phase of ponding and extension in the lower crust, is most applicable to the PNG terrane ([Fig. 1c](#), e.g., [Walsh and Hacker, 2004](#); [Warren et al., 2008](#); [Beaumont et al., 2009](#)).

9.5. Comparison of PNG eclogitic terrane to the western gneiss region of Norway

Our preferred model (the second, above) provides an explanation for westward-younging of (U)HP metamorphism at depth beneath a

continental rift that was also propagating westward. If correct, would such a scenario be peculiar to the world's youngest eclogite-facies terrane in Papua New Guinea, or might it also apply to other UHP terranes? For example, although the Western Gneiss Region (WGR) of Norway is a much larger UHP terrane, it similarly resided at eclogite-facies depths for >20 Myr ([Kylander-Clark et al., 2009](#)). And, although the WGR is inferred to be chiefly a single, thick, regionally coherent slab of continental crust, the distribution of eclogite-facies pressures suggests more chaotic deformation in the highest-pressure rocks ([Hacker et al., 2010](#)). Both terranes are characterized by mostly flat foliations preserving evidence for significant vertical ductile thinning at amphibolite-facies conditions with low kinematic vorticity number (W_k). In both cases, the ductile flow included a coaxial component that increases structurally downward; yield mixed (or domainal) shear sense indicators, and are dominated by a finite strain that was plane or constrictional, and not oblate ([Andersen et al., 1994](#); [Andersen and Jamtveit, 1990](#); [Barth et al., 2010](#); [Dewey et al., 1993](#); [Hacker et al., 2010](#); [Labrousse et al., 2002](#); [Marques et al., 2007](#)). [Engvik and Andersen \(2000\)](#) present data supporting pure-shear dominated ductile flow beginning during HP metamorphism in the WGR; however, as in the D'Entrecasteaux Islands, most of the preserved ductile fabrics in the WGR were imprinted during subsequent amphibolite-facies retrogression (e.g., [Johnston et al., 2007](#)). Both terranes (in PNG and western Norway) share an early isothermal decompression history through mantle depths, and both were ultimately exhumed in zones of continental extension, with normal faulting playing a role in the exhumation during the late stages only (e.g., [Andersen and Jamtveit, 1990](#)). Domal structures that expose high-strain zones of migmatitic UHP and HP eclogitic gneisses are present in some of the UHP domains of western Norway, where, as in this study, partial melting is inferred to have been synchronous with exhumation, when it enhanced the buoyancy and lowered the viscosity of the rocks ([Labrousse et al., 2004, 2002](#)). In his now classic papers, Hans Ramberg interpreted domal culminations in the Caledonides to be at least partly diapiric in origin ([Ramberg, 1980, 1981](#)). Perhaps the processes causing the early and most dramatic phase of exhumation of the UHP terranes from mantle to crust were similar in both regions, even if the style and scale of their final extensional exposure at the surface were not. If so, the youthful and rapidly exhumed PNG terrane may provide a clearer window into that otherwise enigmatic process.

10. Conclusions

The short time between metamorphism of HP eclogites and their surface exposure in the Woodlark Rift (e.g., 2–4 Ma) argues for a near continuity of buoyancy-driven exhumation processes between the mantle and the surface, and for extension playing a key role. Structural and microstructural data, together with previously published thermobarometric and geochronological data, imply that the world's youngest (U)HP rocks in the D'Entrecasteaux Islands of Papua New Guinea were exhumed as diapirs from depths of >100–60 km to the surface of the Woodlark Rift at mean rates of >20 mm/yr. Any tectonic model must explain why the world's youngest eclogite-facies rocks experienced HP to UHP metamorphism at a time of active continental rifting and why the metamorphic and cooling ages young to the west – the same direction that the Woodlark rift is propagating. Evidence for rapid and near-isothermal ascent from mantle depths, abundant syndeformational partial melting, and a symmetrical dome structure, all argue for diapirism as the chief processes for exhumation through mantle depths. The abundance of a partial melt phase and intrusive felsic magmatic rocks throughout the (U)HP terrane (we estimate 40% by volume in the core zone rocks) lead us to conclude that a melt phase was present at fractions exceeding the Melt Connectivity Transition (~7%), and that this melt led to a low effective

viscosity of the terrane (Rosenberg and Handy, 2005), while also enhancing its positive buoyancy.

The eclogite bodies of SE Papua New Guinea were derived from a subducted part of the Australian margin that had remained lodged in the Papuan Orogen's subduction channel for >20 Ma after the end of arc-continent collision. The rocks were heated as a result of asthenospheric inflow ahead of the west-propagating Woodlark spreading ridge, causing them to weaken and detach from their mantle underpinnings. We infer that an early rapid phase of near-isothermal decompression through mantle depths was accomplished by the ascent of diapirs of partially molten (U)HP continental crust. After rising through the mantle to the base of the crust, they pooled near the Moho, accumulating in a welt of weak, partially molten lower crustal rocks. This over-thickened body spread outward under gravity, thinning by a vertical stretching factor of ~1/3. The flow formed a flat-lying amphibolite-facies LS tectonite fabric, and included a strong contribution of pure shear (W_k estimate of ~0.2). The finite extension direction related to this flow was E–W, and was decoupled from the coeval N–S Woodlark–Australia plate motion in the upper crust of the rift. The dominance of top-E shear fabrics suggest an overall westward extrusion of the (U)HP gneissic terrane, perhaps in response to isostatic stresses decreasing towards a crustal neck ahead of the west-propagating Woodlark spreading ridge, or because of the body's confinement beneath the NE-dipping ultramafic lid. Dome growth was followed by rapid cooling at >100°m.y. Dip-slip normal-faulting and minor erosion resulted in final exposure of the domes, which still appear to be rising relative to sea level today.

Acknowledgments

This work was supported by Marsden Fund grant 08-VUW-020 (Little, L. M. Wallace, and S. Ellis), NSF grants EAR 0208334 (Baldwin, Fitzgerald) and EAR 0709054 (Baldwin, Fitzgerald, and L. E. Webb), and NSF grant EAR-0607775 (Hacker). The paper has been improved as a result of the thoughtful and comprehensive review of T. B. Andersen and the editorial efforts of F. Storti. Laura Webb, Alec Waggoner (dec.), and Brian Montealeone contributed to fieldwork and to discussions of topics related to this paper. Laura Wallace helped with field logistics during the 2009 and 2010 field seasons, and shared many of her tectonic insights. Stewart Bush prepared hundreds of thin-sections and polished sections.

References

- Abers, G.A., 2001. Evidence for seismogenic normal faults at shallow depths in continental rifts. In: Wilson, R.C.L., Whitmarsh, R.B., Taylor, B., Froitzham, N. (Eds.), Non-volcanic Rifting of Continental Margins: The Geological Society of London Special Publication, 187, pp. 305–318. London.
- Abers, G.A., Roecker, S.W., 1991. Deep structure of an arc-continent collision: earthquake relocation and inversion for upper mantle P and S wave velocities beneath Papua New Guinea. *Journal of Geophysical Research* 96, 6379–6401.
- Abers, G.A., Ferris, A., Craig, M., Davies, H., Lerner-Lam, A., Mutter, J.C., Taylor, B., 2002. Mantle compensation of active metamorphic core complexes at Woodlark rift in Papua New Guinea. *Nature* 418, 862–865.
- Altenberger, U., Wilhelm, S., 2000. Ductile deformation of K-feldspar in dry eclogite facies shear zones in the Bergen Arcs, Norway. *Tectonophysics* 320, 107–121.
- Amato, J.M., Miller, E.L., 2004. Geologic map and summary of evolution of the Kigluak Mountains gneiss dome, Seward Peninsula, Alaska. In: Whitney, D.L., Teysier, C., Siddoway, C.S. (Eds.), Gneiss Domes in Orogeny: Geological Society of America Special Paper, 380, pp. 295–306.
- Andersen, T.B., 1998. Extensional tectonics in the Caledonides of southern Norway, an overview. *Tectonophysics* 285, 333–351.
- Andersen, T.B., Jamtveit, B., 1990. Uplift of deep crust during orogenic extensional collapse: a model based on field studies in the Sogn–Sunnfjord region of western Norway. *Tectonics* 9, 1097–1111.
- Andersen, T.B., Jamtveit, B., Dewey, J.F., Swensson, E., 1991. Subduction and eduction of continental crust: major mechanisms during continent-continent collision and orogenic extensional collapse: a model based on the south Norwegian Caledonides. *Terra Nova* 3, 303–310.
- Andersen, T.B., Osmundsen, P.T., Jolivet, L., 1994. Deep crustal fabrics and a model for the extensional collapse of the southwest Norwegian Caledonides. *Journal of Structural Geology* 16, 1191–1203.
- Arslan, A., Passchier, C.W., Koehn, D., 2008. Foliation boudinage. *Journal of Structural Geology* 30, 291–309.
- Austrheim, H., 1987. Eclogitization of lower crustal granulites by fluid migration through shear zones. *Earth and Planetary Science Letters* 81, 221–232.
- Austrheim, H., Mørk, M.B.E., 1988. The lower continental crust of the Caledonian mountain chain: evidence from former deep crustal sections in western Norway. *Norge Geologiske Undersøkelse, Special Publications*, 3, pp. 102–113.
- Avigad, D., 1992. Exhumation of coesite-bearing rocks in the Dora Maira massif (western Alps, Italy). *Geology* 20, 947–950.
- Baldwin, S.L., Ireland, T.R., 1995. A tale of two eras: Plio-Pleistocene unroofing of Cenozoic and late Archean zircons from active metamorphic core complexes, Solomon Sea, Papua New Guinea. *Geology* 23, 1023–1026.
- Baldwin, S.L., Lister, G.S., Hill, E.J., Foster, D.A., McDougall, I., 1993. Thermochronologic constraints on the tectonic evolution of active metamorphic core complexes, D'Entrecasteaux Islands, Papua New Guinea. *Tectonics* 12, 611–628.
- Baldwin, S.L., Montealeone, B., Webb, L.E., Fitzgerald, P.G., Grove, M., Hill, J., 2004. Pliocene eclogite exhumation at plate tectonic rates in eastern Papua New Guinea. *Nature*. doi:10.1038/nature02846, 8 pp.
- Baldwin, S.L., Webb, L.E., Montealeone, B.D., 2008. Late Miocene coesite-eclogite exhumed in the Woodlark Rift. *Geology* 36, 735–738.
- Barth, N., Hacker, B.R., Seward, G.G.E., Walsh, E.O., Young, D.J., Johnson, S.E., 2010. Strain within the Ultrahigh-Pressure Western Gneiss Region of Norway Recorded by Quartz CPO's. Geological Society of London Special Publication.
- Beaumont, C., Jamieson, R.A., Nguyen, M.H., Lee, B., 2001. Himalayan tectonics explained by extrusion of a low-viscosity crustal channel coupled to focused surface denudation. *Nature* 414.
- Beaumont, C., Jamieson, R.A., Butler, J.P., Warren, C.J., 2009. Crustal structure: a key constraint on the mechanism of ultra-high pressure rock exhumation. *Earth and Planetary Science Letters* 287, 116–129.
- Bittner, D., Schmeling, H., 1995. Numerical modeling of melting processes and induced diapirism in the lower crust. *Geophysical Journal International* 123, 59–70.
- Blenkinsop, T.G., Treloar, P.J., 1995. Geometry, classification and kinematics of S–C and S–C' fabrics in the Mushandike area, Zimbabwe. *Journal of Structural Geology* 17, 397–408.
- Bobyarchick, A.R., 1986. The eigenvalues of steady state flow in Mohr space. *Tectonophysics* 122, 35–51.
- Bond, C.E., Butler, R.W.H., Dixon, J.E., 2007. Co-axial stretching within extending orogens: the exhumation of HP rocks on Syros (Cyclades) revisited. In: Ries, A.C., Butler, R.W.H., Graham, R.H. (Eds.), Deformation of Continental Crust: The Legacy of Mike Coward. The Geological Society of London, London, pp. 203–222.
- Buck, C.E., Lavier, L.L., 2001. A tale of two kinds of normal fault: the importance of strain weakening in fault development. *Geological Society of London Special Publication* 187, 289–304.
- Burg, J.-P., Kaus, B.J.P., Podlachikov, Y.Y., 2004. Dome structures in collision orogens: mechanical investigation of the gravity/compression interplay. In: Whitney, D.L., Teysier, C., Siddoway, C.S. (Eds.), Gneiss Domes in Orogeny: Geological Society of America, Boulder, Colorado, pp. 47–66.
- Burov, E., Jolivet, L., Pourhiet, L.L., Poliakov, A., 2001. A thermomechanical model of exhumation of high pressure (HP) and ultra-high pressure (UHP) metamorphic rocks in Alpine-type collision belts. *Tectonophysics* 342, 113–136.
- Calvert, A., Gans, P.B., Amato, J.M., 1999. Diapiric ascent and cooling of a sillimanite gneiss dome revealed by ⁴⁰Ar/³⁹Ar thermochronology: the Kigluak Mountains, Seward Peninsula, Alaska. In: Ring, U., T., B.M., Lister, G.S., Willet, S.D. (Eds.), Exhumation Processes: Normal Faulting, Ductile Flow and Erosion, pp. 205–232.
- Carreras, J., Druguet, E., Griera, A., 2005. Shear zone-related folds. *Journal of Structural Geology* 27, 1229–1251.
- Carreras, J., Czeck, D.M., Druguet, E., Hudleston, P.J., 2010. Structure and development of an anastomosing network of ductile shear zones. *Journal of Structural Geology* 32, 656–666.
- Chemenda, A.I., Mattauer, M., Malavielle, J., Bokun, A.N., 1995. A mechanism for syn-collisional rock exhumation and associated normal faulting: results from physical modelling. *Earth and Planetary Science Letters* 132, 225–232.
- Cloos, M., Shreve, R.L., 1988. Subduction-channel model of prism accretion, melange formation, sediment subduction, and subduction erosion at convergent late margins, 2. Implications and Discussion. *Pure and Applied Geophysics* 128, 501–545.
- Cloos, M., Sapiie, B., van Ufford, Q.A., Weiland, R.J., Warren, P.Q., McMahon, T.P., 2005. Collisional delamination in New Guinea: the geotectonics of slab break-off. *Geological Society of America Special Paper* 400 48 pp.
- Cruden, A.R., 1988. Deformation around a rising diapir modeled by creeping flow past a sphere. *Tectonics* 7, 1091–1110.
- Cruden, A.R., 1990. Flow and fabric development during the diapiric rise of magma. *Journal of Geology* 98.
- Daczko, N., Caffi, P., Halpin, J.L., Mann, P., 2009. Exhumation of the Dayman dome metamorphic core complex, eastern Papua New Guinea. *Journal of Metamorphic Geology* 27, 405–422.
- Davies, H.L., 1973. The Geology of Fergusson Island, 1:250,000 Geological Series, SC/56-15. Australia Bureau of Mineral Resources, p. map with explanatory notes.
- Davies, H.L., 1980a. Folded thrust fault and associated metamorphics in the Suckling-Daymon massif, Papua New Guinea. *American Journal of Science* 280A, 171–191.
- Davies, H.L., 1980b. Crustal structure and emplacement of ophiolite in southeastern Papua New Guinea. *Colloques Internationaux du C.N.R.S* 272, pp. 17–33.
- Davies, H.L., 1990. Structure and evolution of the border region of New Guinea. In: Carman, G.J., Carman, Z. (Eds.), Petroleum Exploration in Papua New Guinea: Proceedings of the First PNG Petroleum Convention, Port Moreby, February 12–14, 1990, pp. 249–269.

- Davies, H.L., Ives, D.J., 1965. The geology of Fergusson and Goodenough Islands, Papua. Australian Bureau of Mineral Resources Report, 82.
- Davies, H.L., Jaques, A.L., 1984. Emplacement of ophiolite in Papua New Guinea. Geological Society of London Special Publication 13, 341–350.
- Davies, H., Warren, R.G., 1988. Origin of eclogite-bearing, domed, layered metamorphic complexes ("core complexes") in the D'Entrecasteaux islands, Papua New Guinea. *Tectonics* 7, 1–21.
- Davies, H.L., Warren, R.G., 1992. Eclogites of the D'Entrecasteaux Islands. *Contributions to Mineralogy and Petrology* 112, 463–474.
- Davies, H.L., Williamson, A.N., 1998. Buna, Papua New Guinea, 1:250,000 Geological Series. Geological Survey of Papua New Guinea Explanatory Notes SC/55-3., Port Moresby, Papua New Guinea.
- Davies, H.L., Honza, E., Tiffen, D.L., Lock, J., Okuda, Y., Keene, J.B., Murakami, F., Kisimoto, K., 1987. Regional setting and structure of the western Solomon Sea. *Geo-Marine Letters* 7, 153–160.
- Dewey, J.F., Ryan, P.D., Andersen, T.B., 1993. Orogenic uplift and collapse, crustal thickness, fabrics and metamorphic phase changes: the role of eclogites. In: Prichard, H.M., Alabaster, T., Harris, N.B.W., Neary, C.R. (Eds.), *Magmatic Processes and Plate Tectonics*, pp. 325–343.
- Di Toro, G., Nielson, S., Pennacchioni, G., 2005. Earthquake rupture dynamics frozen in exhumed ancient faults. *Nature* 436, 1009–1012.
- Dixon, J.M., 1975. Finite strain and progressive deformation in models of diapiric structures. *Tectonophysics* 28, 89–124.
- Dow, D.G., 1977. A geological synthesis of Papua New Guinea. Australian Bureau of Mineral Resources. *Geology and Geophysics Bulletin* 201 41 p.
- Engvik, A.K., Andersen, T.B., 2000. Evolution of Caledonian deformation fabrics under eclogite and amphibolite facies at Vårdalsneset, Western Gneiss Region, Norway. *Journal of Metamorphic Geology* 18, 241–257.
- Engvik, A.K., Austrheim, H., Andersen, T.B., 2000. Structural, mineralogical and petrophysical effects on deep crustal rocks of fluid-limited polymetamorphism, Western Gneiss Region, Norway. *Journal of the Geological Society of London* 157, 121–134.
- Epard, J.L., Steck, A., 2008. Structural development of the Tso Moriri ultra-high pressure nappe of the Ladakh Himalaya. *Tectonophysics* 451, 242–264.
- Ernst, W.G., 2001. Subduction, ultrahigh-pressure metamorphism, and regurgitation of buoyant crustal slices — implications for arcs and continental growth. In: Rubie, D., van der Hilst, R. (Eds.), *Processes and Consequences of Deep Subduction*, pp. 253–275.
- Fang, J., 2000. Styles and Distribution of Continental Extension Derived from the Rift Basins of Eastern Papua New Guinea. Columbia University, New York, New York. 223 p.
- Fayon, A.K., Whitney, D.L., Teysier, C., 2004. Exhumation of orogenic crust: diapiric ascent versus low-angle normal faulting. *Geological Society of America Special Paper* 380, 129–140.
- Ferguson, C.C., 1981. A strain reversal technique for extension from fragmented rigid inclusions. *Tectonophysics* 79, T43–T52.
- Ferris, A., Abers, G.A., Zelt, B., Taylor, B., Roecker, S., 2006. Crustal structure across the transition from rifting to spreading: the Woodlark rift system of Papua New Guinea. *Geophysical Journal International* 166, 622–634.
- Fitzgerald, P.G., Baldwin, S.L., Miller, S.L., Perry, S.E., Webb, L.E., Little, T.A., 2008. Low-temperature constraints on the evolution of metamorphic core complexes of the Woodlark rift system. Annual Meeting of the American Geophysical Union, AGU, EOS Transactions, San Francisco, CA.
- Foreman, R., Andersen, T.B., Wheeler, J., 2005. Eclogite-facies polyphase deformation of the Drøsdal eclogite, Western Gneiss Complex, Norway, and implications for exhumation. *Tectonophysics* 398, 1–32.
- Forste, A.M., Bailey, C.M., 2007. Testing the utility of the porphyroblast hyperbolic distribution method of kinematic vorticity analysis. *Journal of Structural Geology* 29, 983–1001.
- Francis, G., Lock, G., Okuda, Y., 1987. Seismic stratigraphy and structure of the area to the southeast of the Trobriand Platform. *Geo-Marine Letters* 7, 121–128.
- Frotzheim, N., Pleuger, J., Roller, S., Nagel, T.J., 2003. Exhumation of high- and ultra-high pressure metamorphic rocks by slab extraction. *Geology* 31, 925–928.
- Gautier, P., Bozkurt, E., Bosse, V., Hallot, E., Dirik, K., 2008. Coeval extensional shearing and lateral underflow during Late Cretaceous core complex development in the Niğde Massif, Central Anatolia, Turkey. *Tectonics* 27, TC1003.
- Gerya, T.V., Stockhert, B., 2006. Two-dimensional numerical modeling of tectonic and metamorphic histories at active continental margins. *International Journal of Earth Sciences* 95, 250–274.
- Gessner, K., Wijns, C., Moresi, L., 2007. Significance of strain localization in the lower crust for structural evolution and thermal history of metamorphic core complexes. *Tectonics* 26, TC2012. doi:10.1029/2004TC001768.
- Glodny, J., Ring, U., Kuhn, A., Gleissner, P., Franz, G., 2005. Crystallization and very rapid exhumation of the youngest Alpine eclogites (Taurin Window, Eastern Alps) from Rb/Sr mineral assemblage analysis. *Contributions to Mineralogy and Petrology* 149, 699–712.
- Goodliffe, A., Taylor, B., Martinez, F., Hey, R., Maeda, K., Ohno, K., 1997. Synchronous reorientation of the Woodlark basin spreading center. *Earth and Planetary Science Letters* 146, 233–242.
- Gordon, S.M., Bowring, S.A., Baldwin, S.L., Little, T.A., Hacker, 2009. Timing of melting associated with HP-UHP exhumation, D'Entrecasteaux Islands, SE Papua New Guinea, American Geophysical Union, Annual Meeting, Eos Trans. AGU, San Francisco, California. pp. Abstract V33B-2036.
- Gordon, S.M., Hacker, B.R., Little, T.A., Baldwin, S.L., Bowring, S.A., 2010. Partial Melting and the Exhumation of a UHP Terrane: CA-TIMS Results from the D'Entrecasteaux Islands, Papua New Guinea. Geological Society of America Abstracts with Programs 42 (5), 659.
- Goscombe, B.D., Passchier, C.W., Hand, M., 2004. Boudinage classification: end-member boudin types and modified boudin structures. *Journal of Structural Geology* 26, 739–763.
- Grasemann, B., Stuwe, K., Vannay, J.-C., 2003. Sense and non-sense of shear in flanking structures. *Journal of Structural Geology* 25, 19–34.
- Griffith, W.A., Rosakis, A., Pollard, D.D., Ko, C.W., 2009. Dynamic rupture experiments elucidate tensile crack development during propagating earthquake ruptures. *Geology* 37, 795–798.
- Hacker, B.R., 2006. Pressures and temperatures of ultrahigh-pressure metamorphism: implications for UHP tectonics and H₂O in subducting slabs. *International Geology Review* 48, 1053–1066.
- Hacker, B., 2007. Ascent of the ultra-high pressure Western Gneiss Region, Norway. *Geological Society of America Special Paper* 419 14 pp.
- Hacker, B.R., Ratschbacher, L., Webb, L.A., McWilliams, M.O., Ireland, T., Calvert, A., Dong, S., Wenk, H.-R., Chateigner, D., 2000. Exhumation of ultrahigh-pressure continental crust in east-central China: late Triassic-Early Jurassic tectonic unroofing. *Journal of Geophysical Research* 105 (B6), 13339–13364.
- Hacker, B.R., Andersen, T.B., Kylander-Clark, A.R.C., Johnston, S.M., Peterman, E., Walsh, E.O., Young, D., 2010. High-temperature deformation during continental-margin subduction and exhumation: the ultrahigh-pressure Western Gneiss Region of Norway. *Tectonophysics* 480, 149–171.
- Hall, R., Spakman, W., 2002. Subducted slabs beneath the eastern Indonesia-Tonga region: insights from tomography. *Earth and Planetary Science Letters* 201, 321–336.
- Hasche, M., Ben-Avraham, Z., 2005. Adakites from collision-modified lithosphere. *Geophysical Research Letters* 32, L15302. doi:10.1029/2005GL023468 022005.
- Hegner, E., Smith, I.E.N., 1992. Isotopic compositions of late Cenozoic volcanics from southeast Papua New Guinea: evidence for multi-component sources in arc and rift environments. *Chemical Geology* 97, 233–250.
- Hill, E.J., 1994. Geometry and kinematics of shear zones formed during continental extension in eastern Papua New Guinea. *Journal of Structural Geology* 16, 1093–1105.
- Hill, E.J., Baldwin, S.L., 1993. Exhumation of high-pressure metamorphic rocks during crustal extension in the D'Entrecasteaux region, Papua New Guinea. *Journal of Metamorphic Geology* 11, 261–277.
- Hill, E.J., Baldwin, S.L., Lister, G.S., 1992. Unroofing of active metamorphic core complexes in the D'Entrecasteaux Islands, Papua New Guinea. *Geology* 20, 907–910.
- Hill, E.J., Baldwin, S.L., Lister, G.S., 1995. Magmatism as an essential driving force for formation of active metamorphic core complexes in eastern Papua New Guinea. *Journal of Geophysical Research* 100, 10441–10451.
- Hirth, G., Tullis, J., 1992. Dislocation creep regimes in quartz aggregates. *Journal of Structural Geology* 14, 145–160.
- Hudleston, P., 1999. Strain compatibility and shear zones: is there a problem? *Journal of Structural Geology* 21, 923–932.
- Jackson, M.P.A., Talbot, C.J., 1989. Anatomy of mushroom-shaped diapirs. *Journal of Structural Geology* 11, 211–230.
- Johnston, S.M., Hacker, B.R., Andersen, T.B., 2007. Exhuming ultrahigh-pressure rocks: overprinting extensional structures and the role of the Nordfjord-Sogn Detachment Zone. *Tectonics* 26, TC5001.
- Kaneko, Y., Maruyama, S., Terabayashi, M., Yamamoto, H., Isikawa, M., Amma, R., Parkinson, C.D., Ota, T., Nakajima, T., Katayama, I., Yamamoto, J., Yamauchi, K., 2000. Geology of the Kochetav UHP-HP metamorphic belt, northern Kazakhstan. *Island Arc* 9, 264–283.
- Kington, J.D., Goodliffe, A.M., 2008. Plate motions and continental extension at the rifting to spreading transition in Woodlark Basin, Papua New Guinea: can oceanic plate kinematics be extended into continental rifts? *Tectonophysics* 458, 82–95.
- Kirchoff-Stein, K.S., 1992. Seismic reflection study of the New Britain and Trobriand subduction systems and their zone of initial contact in the western Solomon Sea. University of California, Santa Cruz, Santa Cruz, California.
- Krabbendam, M., Wain, A., Andersen, T.B., 2000. Pre-Caledonian granulite and gabbro enclaves in the Western Gneiss Region, Norway: indications of incomplete transition at high pressure. *Geological Magazine* 137, 235–255.
- Kruckenberger, S.C., Vanderhaeghe, O., Ferre, E.C., Teysier, C., Whitney, D.L., 2011. Flow of partially molten crust and the internal dynamics of a migmatite dome, Naxos, Greece. *Tectonics* 30, TC3001.
- Kruhl, J.H., 1998. Prism- and basal-plane parallel subgrain boundaries in quartz: a microstructural geothermobarometer. *Journal of Metamorphic Petrology* 16, 142–146.
- Kruhl, J.H., Peternell, M., 2002. The equilibration of high-angle grain boundaries in dynamically recrystallized quartz: the effect of crystallography and temperature. *Journal of Structural Geology* 24, 1125–1137.
- Kruse, R., Stunitz, H., Kunze, K., 2001. Dynamic recrystallization processes in plagioclase porphyroclasts. *Journal of Structural Geology* 23, 1781–1802.
- Kugler, K.A., 1993. Detailed analysis from seismic data of the structure within the Aure fold and thrust belt, Gulf of Papua, Papua New Guinea. In: Carman, G.J., Carman, Z. (Eds.), *Petroleum Exploration and Development in Papua New Guinea*, Proceedings of the Second PNG Petroleum Convention, Port Moresby, May 31–June 2, 1993, pp. 399–411.
- Kurz, G.A., Northrup, C.J., 2008. Structural analysis of mylonitic rocks in the Cougar Creek Complex, Oregon-Idaho using the porphyroblast hyperbolic distribution method, and potential use of SC'-type extensional shear bands as quantitative vorticity indicators. *Journal of Structural Geology* 30, 1005–1012.
- Kylander-Clark, A., Hacker, B., Johnson, C.M., Beard, B.L., Mahlen, N.J., 2009. Slow subduction of a thick ultrahigh-pressure terrane. *Tectonics* 28, TC2003.
- Labrosse, L., Jolivet, L., Andersen, T.B., Agard, P., Hebert, R., Maluski, H., Schärer, U., 2004. Pressure-temperature-time deformation history of the exhumation of ultra-high pressure rocks in the Western Gneiss Region, Norway. In: Whitney, D.L., Teysier, C.,

- Siddoway, C.S. (Eds.), *Gneiss Domes in Orogeny*. Geological Society of America, Boulder, Colorado, pp. 155–183.
- Labrousse, L., Jolivet, L., Agard, R., Hebert, R., Andersen, T.B., 2002. Crustal-scale boudinage and migmatization of gneiss during their exhumation in the UHP Province of western Norway. *Terra Nova* 14, 263–270.
- Lackschewitz, K.S., Mertz, D.F., Devey, C.W., Garbe-Schonberg, 2003. Late Cenozoic volcanism in the western Woodlark Basin area, SW Pacific: the sources of marine volcanic ash layers based on their elemental and Sr-Nd isotope compositions. *Bulletin of Volcanology* 65, 182–200.
- Lee, J., Hacker, B., Wang, Y., 2004. Evolution of the North Himalayan gneiss domes: structural and metamorphic studies in Mabja Dome, southern Tibet. *Journal of Structural Geology* 26, 2297–2316.
- Little, T.A., Baldwin, S.L., Fitzgerald, P.G., Monteleone, B., 2007. Continental rifting and metamorphic core complex formation ahead of the Woodlark Spreading Ridge, D'Entrecasteaux Islands, Papua New Guinea. *Tectonics* 26, TC1002. doi:10.1029/2005TC001911.
- Little, T.A., Hacker, B.R., Gordon, S.M., Baldwin, S.L., Fitzgerald, P.G., 2010. Partial melting a key agent in exhumation of the world's youngest eclogite-facies (and UHP) rocks in the D'Entrecasteaux Islands, Papua New Guinea, American Geophysical Union, Fall Meeting. American Geophysical Union, EOS Transactions, San Francisco California.
- Lus, W.Y., McDougall, I., Davies, H.L., 2004. Age of the metamorphic sole of the Papuan Ultramafic Belt ophiolite, Papua New Guinea. *Tectonophysics* 392, 85–101.
- Mancktelow, N.S., 2002. Finite-element modelling of shear zone development in viscoelastic materials and its implications for localisation of partial melts. *Journal of Structural Geology* 24, 1045–1053.
- Mandal, N., Dhar, R., Misra, S., Chakraborty, C., 2007. Use of boudinaged rigid objects as a strain gauge: insights from analogue and numerical models. *Journal of Structural Geology* 29, 759–773.
- Mann, P., Horton, B.K., Taylor, F.W., Shen, C., Lin, K., Renema, W., 2009. Uplift patterns of reef terraces and sedimentary rocks constrain tectonic models for metamorphic core complexes in eastern Papua New Guinea, American Geophysical Union, Annual Meeting, Eos Trans. AGU, San Francisco, California, pp. G33B–G0642B.
- Marques, F.O., Schmid, D.W., Andersen, T.B., 2007. Applications of inclusion behaviour models to a major shear zone system: the Nordfjord-Sogn Detachment Zone in western Norway. *Journal of Structural Geology* 29, 1622–1631.
- Martinez, F., Goodliffe, A., Taylor, B., 2001. Metamorphic core complex formation by density inversion and lower crustal extrusion. *Nature* 411, 930–933.
- McKenzie, D.P., Nimmo, F., Jackson, J.A., Gans, P.B., Miller, E.L., 2000. Characteristics and consequences of flow in the lower crust. *Journal of Geophysical Research* 105 (B5) 11,029–11,046.
- Miller, E.L., Calvert, A.T., Little, T.A., 1992. Strain-collapsed metamorphic isograds in a strain-collapsed sillimanite gneiss dome, Seward Peninsula, Alaska. *Geology* 20, 487–490.
- Monteleone, B., Baldwin, S.L., Ireland, T.R., Fitzgerald, P.G., 2001. Thermochronometric constraints for the evolution of the Moresby Seamount, Woodlark Basin, Papua New Guinea. In: Huchon, P., Taylor, B., Klaus, A. (Eds.), *Proceedings of the Ocean Drilling Program, Scientific Results, Volume 180*, pp. 1–34.
- Monteleone, B., Baldwin, S.L., Fitzgerald, P.G., Little, T.A., 2006. Thermochronologic constraints for metamorphic core complex formation on Normanby Island, south-eastern Papua New Guinea. *Geological Society of America Abstracts with Programs* 8 (2) Abstract 100960.
- Monteleone, B.D., Baldwin, S.L., Webb, L.E., Fitzgerald, P.G., Grove, M., Schmitt, A.K., 2007. Late Miocene-Pliocene eclogite-facies metamorphism, D'Entrecasteaux Islands, SE Papua New Guinea. *Journal of Metamorphic Geology* 25, 245–265.
- Mutter, J.C., Mutter, C.Z., Fang, J., 1996. Analogies to oceanic behaviour in the continental breakup of the western Woodlark basin. *Nature* 380, 333–336.
- Ollier, C.D., Pain, C.F., 1980. Active rising surficial gneiss domes in Papua New Guinea. *Geological Society of Australia Journal* 27, 33–44.
- Ota, T., Koneko, Y., 2010. Blueschists, eclogites, and subduction zone tectonics: insights from a review of Late Miocene blueschists and eclogites, and related young high-pressure metamorphic rocks. *Gondwana Research* 18, 167–188.
- Ott, B., Mann, P., Campos Aguiniga, H., 2009. Late Miocene to Recent inversion of the Aure rift, eastern Papua New Guinea: a consequence of transpression along the Owen Stanley fault zone, American Geophysical Union, Annual Meeting, Eos Trans. AGU, San Francisco, California, pp. Abstract T23-07.
- Parrish, R.R., Gough, S.J., Searle, M.P., Waters, D.J., 2006. Plate velocity exhumation of ultrahigh-pressure eclogites in the Pakistan Himalaya. *Geology* 34, 989–992.
- Passchier, C.W., 1986. Mylonites in the continental crust and their role as seismic reflectors. *Geologie en Mijnbouw* 65, 167–176.
- Passchier, C.W., 1987. Stable positions of rigid objects in non-coaxial flow: a study in vorticity analysis. *Journal of Structural Geology* 9, 679–690.
- Pennacchioni, G., 1996. Progressive eclogitization under fluid-present conditions of pre-Alpine mafic granulites in the Austroalpine Mt Emilius Klippe (Italian western Alps). *Journal of Structural Geology* 18, 549–561.
- Peterman, E.M., Hacker, B.R., Baxter, E.F., 2009. Phase transformations of continental crust during subduction and exhumation: the Western Gneiss Region, Norway. *European Journal of Mineralogy*. doi:10.1127/0935-1221/2009/0021-1988.
- Pigram, C., Davies, P.J., Feary, D.A., Symonds, P.A., 1989. Tectonic controls on carbonate platform evolution in southern Papua New Guinea: passive margin to foreland basin. *Geology* 17, 199–202.
- Ramberg, H., 1972. Theoretical models of density stratification and diapirism in the earth. *Journal of Geophysical Research* 77.
- Ramberg, H., 1980. Diapirism and the gravity collapse of the Scandinavian Caledonides. *Journal of the Geological Society of London* 137, 261–270.
- Ramberg, H., 1981. The role of gravity in tectonics. *Geological Society of London Special Publication* 9, 125–140.
- Rey, P.F., Teyssier, C., Whitney, D.L., 2009. Extension rates, crustal melting, and core complex dynamics. *Geology* 37, 391–394.
- Ring, U., Glodney, J., 2010. No need for lithospheric extension for exhuming (U)HP rocks by normal faulting. *Journal of the Geological Society of London* 167, 1–4.
- Ring, U., Brandon, M.T., Willet, S.D., Lister, G.S., 1999. Exhumational processes. In: Ring, U., Brandon, M.T., Lister, G.S., Willet, S.D. (Eds.), *Exhumational Processes: Normal Faulting Ductile Flow and Erosion*, pp. 1–28.
- Ring, U., Will, T., Glodney, J., Kumerics, C., Gessner, K., Thomson, S., Gungor, T., Monie, P., Okrusch, M., Druppel, K., 2007. Early exhumation of high-pressure rocks in extrusion wedges: cycladic blueschist unit in the eastern Aegean, Greece, and Turkey. *Tectonics* 26, TC2001.
- Rogerson, R., et al., 1987. The geology and mineral resources of the Sepik headwaters region, Papua New Guinea. Papua New Guinea Geological Surveys Memoir, 12.
- Root, D.B., Hacker, B.R., Gans, P.B., Ducea, M.N., Eide, E.A., Mosenfelder, J.L., 2005. Discrete ultrahigh-pressure domains in the Western Gneiss Region, Norway: implications for formation and exhumation. *Journal of Metamorphic Geology* 23, 45–61.
- Rosenberg, C.L., Handy, M.R., 2005. Experimental deformation of partially melted granite revisited: Implications for the continental crust. *Journal of Metamorphic Geology* 23, 19–28.
- Rosenberg, C.L., Stunitz, H., 2003. Deformation and recrystallization of plagioclase along a temperature gradient: an example from the Bergell tonalite. *Journal of Structural Geology* 25, 389–408.
- Rubatto, D., Hermann, J., 2001. Exhumation as fast as subduction? *Geology* 29, 3–6.
- Sawyer, E.W., 2008. Working with migmatites: nomenclature for the constituent parts. In: Sawyer, E.W. (Ed.), *Working with migmatites*. Mineralogical Association of Canada Short Course 38, Quebec City, Quebec, pp. 1–28.
- Seno, T., 2008. Conditions for a crustal block to be sheared off from the subducted continental lithosphere: what is an essential factor to cause features associated with collision? *Journal of Geophysical Research* 113, B04414. doi:10.1029/2007JB005038.
- Shaked, Y., Avigad, D., Garfunkel, Z., 2004. Alpine high-pressure metamorphism at the Almyropotamus window (southern Evia, Greece). *Geological Magazine* 137, 367–380.
- Siddoway, C.S., Richard, S.M., Fanning, C.M., Luyendyk, B.P., 2004. Origin and emplacement of middle Cretaceous gneiss dome, Fosdick Mountains, West Antarctica. In: Whitney, D.L., Teyssier, C., Siddoway, C.S. (Eds.), *Gneiss Domes in Orogeny*. Geological Society of America, Boulder, Colorado, pp. 267–294.
- Simpson, C., De Paor, D.G., 1993. Strain and kinematic analysis in general shear zones. *Journal of Structural Geology* 15, 1–20.
- Slater, A., Alkwill, H.R., Fong, G.U., 1988. Seismic evidence for structural style in the offshore Kerema area, Papua New Guinea: Application to petroleum exploration. Seventh Offshore South East Asia Conference. South East Asia Exploration Society, Singapore, pp. 141–149.
- Smith, I.E.M., 1976. Peralkaline rhyolites of the D'Entrecasteaux Islands, Papua New Guinea. In: Johnson, R.W. (Ed.), *Volcanism in Australasia*. Elsevier, Amsterdam, pp. 275–285.
- Smith, I.E.M., 1982. Volcanic evolution of Eastern Papua. *Tectonophysics* 87, 315–333.
- Smith, I.E.M., Compston, W., 1982. Strontium isotopes in Cenozoic volcanic rocks from southeastern Papua New Guinea. *Lithos* 15, 200–206.
- Smith, I.E.M., Milsom, J.S., 1984. Late Cenozoic volcanism and extension in the eastern Papua. In: Kokelaar, B.P., Howells, M.F. (Eds.), *Marginal Basin Geology*, pp. 163–171.
- Spencer, J.E., 2010. Structural analysis of three extensional detachment faults with data from the 2000 Space-Shuttle Radar Topography Mission. *GSA Today* 20 (8), 1–10.
- Stern, T.A., Housman, G., Evans, L.A., 2010. The role of upper mantle instability for rock uplift, potassic volcanism and crust-mantle thinning within western North Island, New Zealand. *Geological Society of America Abstracts with Programs*, v. 62, no. 5, p. 184.
- Stipp, M., Stunitz, H., Heilbronner, R., Schmid, S.M., 2002. Dynamic recrystallization of quartz: correlation between natural and experimental conditions. In: De Meer, S., Drury, M.R., De Bresser, J.H.P., Pennock, G.M. (Eds.), *Deformation Mechanisms, Rheology, and Tectonics: Current Status and Future Perspectives*. Geological Society of London, pp. 171–190.
- Stockhert, B., Renner, J., 1998. Rheology of crustal rocks at ultrahigh pressure. In: Hacker, B., Liou, J.G. (Eds.), *When Continents Collide: Geodynamics and Geochemistry of Ultrahigh-Pressure Rocks*. Kluwer, Dordrecht, pp. 57–95.
- Stolz, A.J., Davies, G.R., Crawford, A.J., Smith, I.E.M., 1993. Sr, Nd and Pb isotopic compositions of calc-alkaline and peralkaline silicic volcanics from the D'Entrecasteaux Islands, Papua New Guinea, and their tectonic significance. *Mineralogy and Petrology* 47, 103–126.
- Talbot, C.J., Jackson, M.P.A., 1987. Internal kinematics of salt diapirs. *American Association of Petroleum Geologists Bulletin* 71.
- Taylor, B., 1999. Background and regional setting. In: Taylor, B., et al. (Ed.), *Ocean Drilling Program, Texas A & M University, College Station*, pp. 1–20.
- Taylor, B., Huchon, P., 2002. Active continental extension in the western Woodlark basin: a synthesis of Leg 180 results. In: Huchon, P., Taylor, B., Klaus, A. (Eds.), *Proceedings of the Ocean Drilling Program, Scientific Results, Volume 180*. Ocean Drilling Program, Texas A & M University, College Station, Texas, pp. 1–36 (CD ROM).
- Taylor, B., Goodliffe, A.M., Martinez, F., 1999. How Continents break-up: insights from Papua New Guinea. *Journal of Geophysical Research* 104, 7497–7512.
- ten Grotenhuis, S.M., Trouw, R.A.J., Passchier, C.W., 2003. Evolution of mica fish in mylonitic rocks. *Tectonophysics* 372, 1–21.
- Teyssier, C., Whitney, D.L., 2002. Gneiss domes and orogeny. *Geology* 30, 1139–1142.
- Teyssier, C., Ferre, E., Whitney, D.L., Norlander, O., Vanderhaeghe, O., Parkinson, D., 2005. Flow of partially molten crust and origin of detachments during collapse of the Cordilleran orogen. *Geological Society of London Special Publication* 245, 39–64.
- Tikoff, B., Fossen, H., 1995. The limitations of three-dimensional kinematic vorticity analysis. *Journal of Structural Geology* 17, 1771–1784.
- Tikoff, B., Fossen, H., 1999. Three-dimensional reference deformations and strain facies. *Journal of Structural Geology* 21, 1497–1512.

- Tirel, C., Brun, J.-P., Burov, E., 2008. Dynamics and structural development of metamorphic core complexes. *Journal of Geophysical Research* 113, B04403.
- Tjhin, K.T., 1976. Trobriand Basin exploration, Papua New Guinea. *Australian Petroleum Exploration Association Journal* 16.
- Tullis, J., 2002. Deformation of granitic rocks: experimental studies and natural examples. In: Karato, S., Wenk, H.-R. (Eds.), *Plastic Deformation of Minerals and Rocks*. Mineralogical Society of America, Washington, D. C., pp. 51–95.
- Van Ufford, Q.A., Cloos, M., 2005. Cenozoic tectonics of New Guinea. *American Association of Petroleum Geologists Bulletin* 89, 119–140.
- Van Wijk, J.W., Blackman, D.K., 2005. Dynamics of continental rift propagation: the end-member modes. *Earth and Planetary Science Letters* 229, 247–258.
- Vanderhaeghe, O., 2004. Structural development of the Naxos migmatite dome. In: Whitney, D.L., Teyssier, C., Siddoway, C.S. (Eds.), *Gneiss Domes in Orogeny*. Geological Society of America, Boulder, Colorado, pp. 211–228.
- Waggoner, A., Baldwin, S.L., Webb, L.A., Little, T.A., Fitzgerald, P.G., 2008. Temporal constraints on continental rifting and the exhumation of the youngest known HP metamorphic rocks, SE Papua New Guinea, *Eos Trans. AGU*, 89(53), Fall Meet. Suppl., Abstract T41B-1961.
- Wallace, L.M., Stevens, C., Silver, E., McCaffrey, R., Lorantung, W., Hasiata, S., Stanaway, R., Curley, R., Rosa, R., Taugaloidei, J., 2004. GPS and seismological constraints on active tectonics and arc-continent collision in Papua New Guinea: implications for mechanics of microplate rotations in a plate boundary zone. *Journal of Geophysical Research* 109. doi:10.1029/2003JB002481.
- Walsh, E.O., Hacker, B., 2004. The fate of subducted continental margins: Two-stage exhumation of the high-pressure to ultra-high pressure Western Gneiss Complex, Norway. *Journal of Metamorphic Geology* 22, 671–689.
- Warren, C.J., Beaumont, C., Jamieson, R.A., 2008. Deep subduction and rapid exhumation: role of crustal strength and strain weakening in continental subduction and ultrahigh-pressure rock exhumation. *Tectonics* 27, TC6002.
- Webb, L.E., Baldwin, S.L., Little, T.A., Fitzgerald, P.G., 2008. Can microplate rotation drive subduction inversion? *Geology* 36, 823–826.
- Weinberg, R.F., Regenauer-Lieb, K., 2010. Ductile fractures and magma migration from source. *Geology* 38, 363–366.
- Weissel, J.K., Taylor, B., Karner, G.D., 1982. The opening of the Woodlark Basin, subduction of the Woodlark spreading system, and the evolution of northern Melanesia since mid-Pliocene time. *Tectonophysics* 87, 253–277.
- Wernicke, B., 1992. Cenozoic extensional tectonics of the U. S. Cordillera. In: Burchfiel, B.C., et al. (Ed.), *The Cordilleran Orogen: Coterminal United States*. Geological Society of America, Boulder, CO, pp. 553–582.
- Westaway, R., 2005. Active low-angle normal faulting in the Woodlark extensional province, Papua New Guinea: a physical model. *Tectonics* 24, TC6003. doi:10.1029/2004TC001744.
- Westaway, R., 2007. Correction to "Active low-angle normal faulting in the Woodlark extensional province, Papua New Guinea: a physical model. *Tectonics* 26, TC1003.
- Whitney, D.L., Dilek, Y., 1997a. Core complex development in central Anatolia. *Geology* 25, 1023–1026.
- Whitney, D.L., Dilek, Y., 1997b. Metamorphism during Alpine crustal thickening and extension in central Anatolia, Turkey: the Nigde metamorphic core complex. *Journal of Petrology* 39, 1385–1403.
- Whitney, D.L., Teyssier, C., Vanderhaeghe, O., 2004. Gneiss domes and crustal flow. In: Whitney, D.L., Teyssier, C., Siddoway, C.S. (Eds.), *Gneiss Domes in Orogeny*. Geological Society of America, Boulder, Colorado, pp. 15–33.
- Yin, A., 2004. Gneiss domes and gneiss dome systems. In: Whitney, D.L., Teyssier, C., Siddoway, C.S. (Eds.), *Gneiss Domes in Orogeny*. Geological Society of America, Boulder, Colorado, pp. 1–14.
- Zeitler, P.K., Meltzer, A.S., Koons, P.O., Craw, D., Hallet, B., Chamberlain, C.P., Kidd, W.S.F., Park, S.K., Seeber, L., Bishop, M., Shroder, J., 2001. Erosion, Himalayan geodynamics, and the geomorphology of metamorphism. *GSA Today* 11 (1), 4–8.
- Zhang, R.Y., Liou, J.G., 1997. Partial transformation of gabbro to coesite-bearing eclogite from Yankhou, Sulu terrane, eastern China. *Journal of Metamorphic Geology* 15, 183–202.
- Zhang, L., Ellis, D.J., Arculus, R.J., Jiang, W., W., C., 2003. Forbidden subduction of sediments to 150 km depth – the reaction of dolomite to magnesite + aragonite in the UHPM metapelites from western Tianshan, China. *Journal of Metamorphic Geology* 21, 523–529.
- Zheng, Y., Wang, T., Ma, M., Davis, G.A., 2004. Maximum effective moment criterion and the origin of low-angle normal faults. *Journal of Structural Geology* 26, 271–286.
- Zheng, Y., Wang, T., Zhang, J., 2009. Comment on Structural analysis of mylonitic rocks in the Cougar Creek Complex, Oregon-Idaho using porphyroclast hyperbolic distribution method. and potential use of SC'-type extensional shear bands as quantitative vorticity indicators. *Journal of Structural Geology* 31, 541–543.
- Zirakparvar, N.A., Baldwin, S., Vervoort, J.D., Fitzgerald, P.G., 2009. Lu-Hf dating of garnet from MCC's in the Woodlark Rift of southeastern Papua New Guinea, Abstract V43D-2291 presented at 2009 Fall Meeting. AGU, San Francisco, Calif. 14–18 Dec.
- Zirakparvar, N.A., Baldwin, S., Fitzgerald, P.G., Vervoort, J.G., 2010. Piecing together the eastern Australia margin in Gondwana: origin of metamorphic rocks in the Woodlark Rift, SE Papua New Guinea. Abstract T13C-2220 presented at 2010 Fall Meeting. AGU, San Francisco, Calif. 13–17 Dec.